Genome wide search for glycine metabolism genes

Alain R Bataille

A Thesis

in

The Department

of

Biology

Presented in Partial Fulfillment of the Requirements
For the Degree of Master of Science at
Concordia University
Montreal, Quebec, Canada

September 2003

Your file Votre référence
ISBN: 0-612-83846-3
Our file Notre référence
ISBN: 0-612-83846-3

ABSTRACT

Genome wide search for glycine metabolism genes

Alain R Bataille

The yeast *Saccharomyces cerevisiae* uses glycine for the synthesis of activated one-carbon units and nitrogen metabolism. The homozygous diploid set of deletion strains includes strains deleted from all the *S. cerevisiae* non-essential genes (about 4700). This deletion set was screened for strains exhibiting a growth phenotype when glycine was used as the sole nitrogen source (Gmin medium). This screen identified a total of 321 strains. Within the 321 strains, 250 showed a growth defect on Gmin (G- phenotype) whereas 71 exhibited better growth on Gmin (G+ phenotype). Further high-density colony-array analyses established the growth profile for each of the 321 strains on ten different media. These growth profiling experiments identified genes important for various aspects of glycine metabolism. For example vesicular transport from the plasma membrane to the multivesicular body compartment was important for growth in media containing high concentrations of glycine. This suggests that the general amino acid permease (Gap1p) must be targeted to the vacuole for degradation to prevent glycine toxicity. Growth profiling also confirmed the importance of the mitochondrial compartment for glycine metabolism and defined the functional role of *CEM1* and *YJL046W* for lipoate metabolism. This study therefore validated the use of growth profiling data generated using high density colony assays for the study of eukaryotic gene function.

ACKNOLEDGEMENTS

I wish to thank Dr. Storms for providing me with the opportunity to work in his laboratory. I am grateful to Dr. Tsang and Dr. Varin for being my committee members. I also would like to thank Dr. Peter Ulycznyj and Alex Spurmanis for their help with computers and equipment and Dr. Ian Ferguson for his help with statistic. A special thanks to my colleagues, past and present, Barbara Decelle, Edith Munro, Arsal Shahabuddin, Yun Zheng and Rosa Zito for their assistance, support and friendship. I would like to thank my fellow graduate students and friends in the departments of Biology and Chemistry. Last but not least I must thank my family for its never-ending support.

TABLE OF CONTENTS

Page

LIST OF FIGURES

LIST OF TABLES

ABBREVIATIONS

AAP	amino acid permease
bp	base pair
CH+-THF	5,10-N-methynyl tetrahydrofolate
CH2-THF	5,10-N-methylene tetrahydrofolate
CH3-THF	5-N methyl-tetrahydrofolate
CHO-THF	formyl-tetrahydrofolate
DNA	deoxyribonucleic acids
GOGAT	glutamate synthase
GS	glutamine synthase
L	liter
M	molar
mg	milligram
MIPS	Munich information center for protein sequences
mL	milliliter
mM	millimolar
mRNA	messenger ribonucleic acids
MVB	multivesicular body
NAD	nicotinamide adenine dinucleotide
NADP	nicotinamide adenine dinucleotide phosphate
NCR	nitrogen catabolite repression
NKHG	non-ketotic hyperglycinaemia

OGDH	2-oxoglutarate dehydrogenase
ORF	open reading frame
PCR	polymerase chain reaction
PDH	pyruvate dehydrogenase
RNA	ribonucleic acids
SAM	S-adenosyl methionine
SGD	*Saccharomyces* genome Database
SHMT	serine hydroxymethyl transferase
THF	tetrahydrofolate
THS	tetrahydrofolate synthase

1 Introduction

Saccharomyces cerevisiae is a simple unicellular eukaryote that can be easily used for genetic studies due to its genetic tractability. The remarkable degree of conservation among eukaryotes in protein sequence and regulation mechanisms make this yeast an excellent model organism for the study of eukaryotic gene function (for example, 30% of the identified human genes linked to a genetic disease possess a yeast homologue) (Bassett *et al.*, 1997).

The complete sequencing of its genome (14 million bp per haploid genome) revealed 6335 putative open reading frames (ORFs) that could, in theory, encode proteins longer than 99 amino acids in length. However, 470 of the ORFs have been found unlikely to encode proteins (questionable ORF) (Mewes *et al.*, 2002). The next step in the comprehension of eukaryotic genomes entails identifying the function of these genes.

S. cerevisiae is the most extensively used organism in studies of basic eukaryotic cellular function. About 3573 genes have been biochemically or genetically characterized (classified as proteins of known function on MIPS: Munich information center for protein sequences). However the cellular function of about 2000 of the 6275 yeast genes remains unidentified (30%) (Mewes *et al.*, 2002). These two-thousand genes are classified as encoding for proteins of unknown function. Whole genome approaches such as microarray and parallel phenotypic analyses are therefore required to methodically determine the function of these uncharacterized genes and their interactions.

The complete sequence of the *S. cerevisiae* genome and efficient gene replacement cassettes strategy were used to systematically delete all 6275 putative ORFs.

The international gene deletion effort coordinated by W. Johnston (Giaever *et al.*, 2002; Winzeler *et al.*, 1999) produced four different deletion libraries: a set of haploids corresponding to the two mating types MATa and MATα, homozygous diploids containing the non-essential genes and heterozygous diploids containing both essential and non-essential genes. These sets can be used in systematic phenotype searches to determine gene function.

1.1 The yeast deletion sets

A two-step PCR strategy was used allowing the systematic replacement of nearly all the ORFs from the start to stop codon with a kanamycin module flanked by two unique 20 mer sequences called tags or barcodes (Baudin *et al.*, 1993). The kanamycin module confers resistance to the antibiotic G418 (an aminoglycoside related to gentamicin), whereas the two molecular barcodes permit unique identification of each deletion strain, as well as fitness assays via hybridization to high-density oligonucleotide arrays (Winzeler *et al.*, 1999).

1.1.1 Deletion strategy

The first step of the deletion strategy is the PCR amplification of the KanMX gene from pFA6-KanMX4 using two ORF-specific 74 bp oligonucleotides. These two oligos are called the UPTAG and DOWNTAG primers (Fig.1). Each one of these primers consists of: 18 bp of genomic sequence flanking the start and the stop codon of the target

Figure 1. Deletion Strategy. Figure adapted from the yeast deletion web page. The systematic replacement of the identified ORFs, from start to stop codon, was accomplished via a two-step PCR strategy. The first set of primers (74 mer) contain the TAG region (or molecular barcode) unique for each strain and a short region of homology. The second set of primers (45 mer) is used to extend the specific homology to 45 bp with the flanking region of the target ORF.

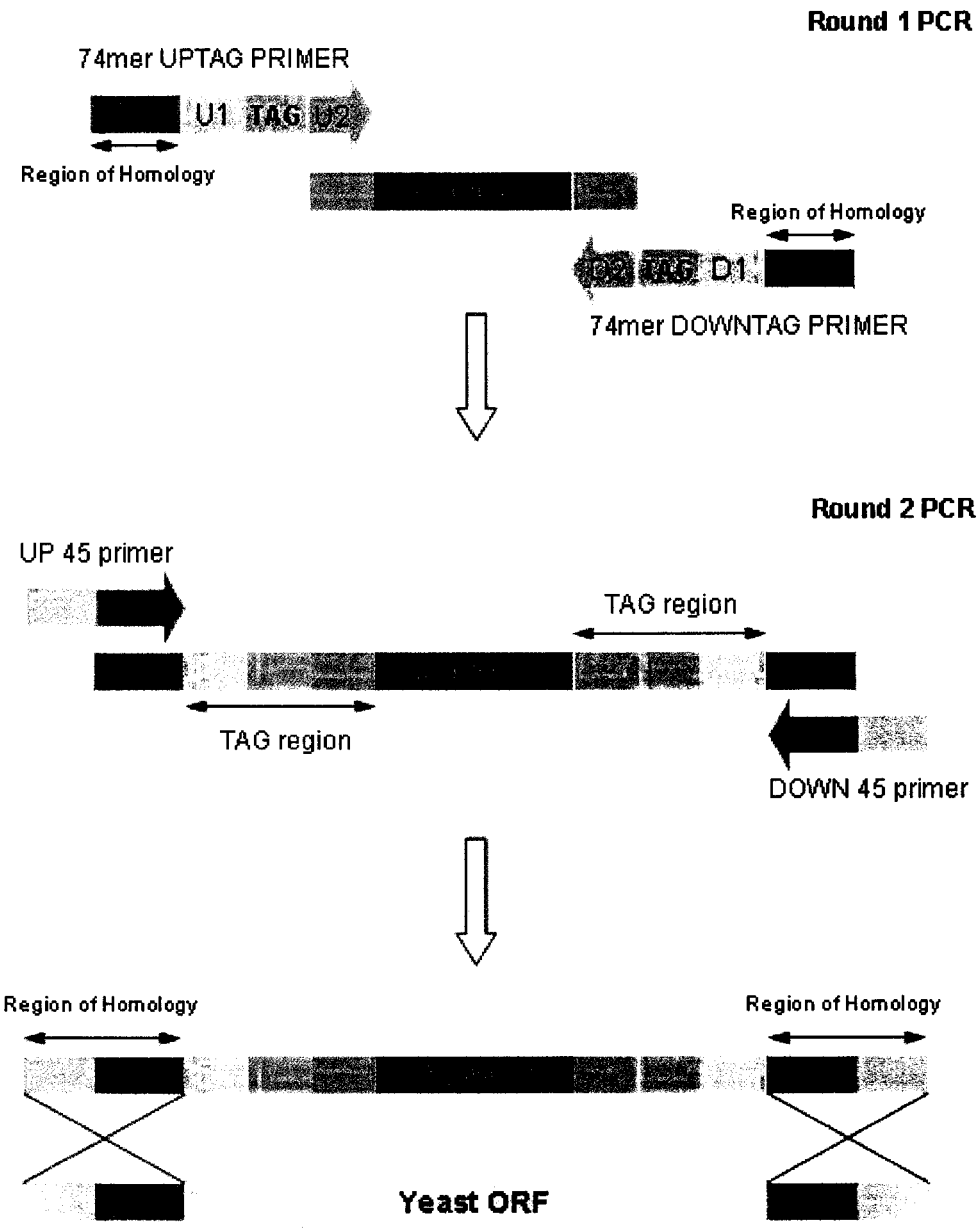
Round 1 PCR
74mer UPTAG PRIMER
U1
TAG
U2
Region of Homology
Region of Homology
D2
TAG
D1
74mer DOWNTAG PRIMER
Round 2 PCR
UP 45 primer
TAG region
TAG region
DOWN 45 primer
Region of Homology
Region of Homology
Yeast ORF

ORF, 18 or 17 bp of sequence common to all gene disruptions (U1 or D1), 20 bp of unique sequence called TAG1 and TAG2 respectively, and 18 or 19 bp of sequence homologous to the KanMX4 cassette, U2 or D2 respectively.

The second step used 45-mer primers homologous to the ORF flanking region designated UP45 and DOWN45. The primers extend the ORF-specific homology to 45 bp increasing the efficiency of targeted mitotic recombination.

PCR amplification of molecular barcodes for identification or oligo-assay can be performed using the sequence common to all deletion strains. The redundancy of the UPTAG and DOWNTAG barcodes (2 distinct and unique sequences for each strain) thereby greatly increases the hybridization reliability of PCR amplified barcodes derived from the disruption strains. However, approximately 3% of the strains constructed early in the project contain the same UPTAG sequence.

1.1.2. Mutant construction

Diploid yeast cells BY4743 were transformed, selected on G418 containing agar plates and sporulated. Haploid spores of the two mating types MATa and MATα were recovered from the tetrads. The homozygous diploid set was obtained by mating the confirmed haploids. About 30% of the gene disruptions were obtained by direct transformation of the two mating types and successive mating of the independently constructed haploid mutants (Yeast Deletion Web Page).

Unsuccessful deletions were attempted a second time using a pair of longer 63-mer primers in order to extend the sequence flanking the target ORF. The success rate of

this method was greater than 97%. All the strains where confirmed by PCR using primers specific to the flanking region of each of the ORF. Knowing that the DNA transformation procedure (a standard lithium-acetate) is itself mutagenic; every tetrad with a lethal or slow growth phenotype, not segregating with G418 resistance was discarded. Haploid strains that contained a wild type copy as well as the kanamycin disruption cassette (after confirmation procedure) were discarded, since this is likely due to aneuploidy (duplication of all or part of the targeted genes chromosome).

1.2 Nitrogen sources

Saccharomyces cerevisiae evolved the ability to use a large number of nitrogen sources encountered in its environment. This does not mean, however, that all nitrogen sources are equally valuable. Yeast has developed mechanisms to adapt to environmental variation and thereby select among available nitrogen sources. Nitrogen sources can be arbitrarily categorized as good or poor based on their ability to sustain growth. Ammonia (NH_4^+), glutamate and glutamine are good nitrogen sources whereas proline, glycine, and urea are considered to be poor nitrogen sources (Sinclair and Dawes, 1995).

Utilization of nitrogen sources depends on two-steps: the first step is the detection and the uptake of the nitrogen source available. The second is the degradation of the compound and the incorporation of nitrogen groups into glutamate and glutamine (ter Shure *et al.*, 2000). Yeast has been shown to possess multiple amino acid transport systems that allow a single amino acid to be transported by diverse transporters with different kinetic properties, specificities and regulations (Forsberg and Ljungdahl, 2001).

It is interesting to note that during starvation, an important part of the cell's nitrogen can be obtained by the degradation of proteins inside the cell. This degradation is localized in two distinct cellular organelles: the proteasome and the vacuole (Coffman and Cooper, 1997).

1.2.1. Detection and transport

1.2.1.1. Ammonia

Ammonia is a preferred nitrogen source and is widely used in the preparation of laboratory media. Three distinct yet highly similar transmembrane transporters mediate its detection and uptake (Marini *et al.*, 1997). The *MEP1* gene encodes a high-capacity, high-affinity ammonia transporter; *MEP2* encodes a high-affinity ammonia transporter, whereas the *MEP3* gene encodes a lower-affinity ammonia transporter. However, the fact that the triple mutant, *mep1Δ*, *mep2Δ*, *mep3Δ*, retains the ability to grow on a buffered media with a high concentration of ammonia as the sole nitrogen source suggests the existence of at least one additional ammonium transporter unrelated to this family (as no other homologous sequence has been found in the *S. cerevisiae* genome) (Marini *et al.*, 1997). In addition to its role in ammonia transport, Mep2p has been suggested to act as an ammonium sensor able to generate signals for induction of diploid-specific pseudohypheal growth on media that contains limiting amounts of ammonium (Lorenz and Heitman, 1998).

1.2.1.2 Glycine

Yeast scavenges amino acids from the immediate environment in order to use them either directly in protein synthesis or as a nitrogen supply. This active transport process is driven by a proton gradient, via a variety of more or less specific amino-acid permeases (Horak, 1997).

Glycine is a poor nitrogen source. When a preferred nitrogen source is unavaible *S. cerevisiae* can use glycine as an alternative nitrogen source (Sinclair and Dawes, 1995). Five of the eighteen members of the Amino Acid Permease (AAP) family are assumed to be responsible for glycine uptake (Regenberg *et al.*, 1999). The first and probably the most important member of the AAP family is *GAP1* (general amino acid permease), a high-capacity amino acid permease with broad specificity, that it can transport all of the naturally occurring L-amino acids, several D-amino acids and related compounds. Gap1p activity appear to be tightly regulated, nitrogen starvation and growth on a poor source of nitrogen results in high level of Gap1p activity (Regenberg *et al.*, 1999). Put4p (a proline permease that also seems to act as a glycine permease) Agp1p, Dip5p and to a smaller extent Tat2p (usually considered as tryptophan cysteine permease) participate in glycine importation (Regenberg *et al.*, 1999).

1.3. Catabolism of Glycine

1.3.1. General reaction

Unlike ammonia, which can be directly used and incorporated into glutamate and glutamine, the amino acid glycine needs to be oxidized by the glycine cleavage system in order to supply nitrogen to the cell (Sinclair and Dawes, 1995). The glycine cleavage system, also called the glycine decarboxylase system or glycine synthase, is a multienzyme complex located in the mitochondria. This complex is formed by four protein subunits named protein-T, protein-P, protein-H and protein-L. It catalyses the oxidative decarboxylation of glycine, resulting in the production of N^5-N^{10}-methylene tetrahydroxyfolate, CO_2, NADH, and NH_3.

Ammonia produced by the glycine cleavage system can be used as a nitrogen source by the cell and directly incorporated into glutamate and glutamine by the enzymes glutamate dehydrogenase and glutamine synthetase respectively. NADH will be subsequently reduced by the electron transport chain giving an electron to the NADH reductase complex found in the inner membrane of the mitochondria. CO_2 does not play an important role in the metabolism of yeast. However, in C3 plants, CO_2 generated from the glycine cleavage system will be used for the fixation of carbon in the Calvin Cycle to form carbohydrates. This reaction is catalyzed by the enzyme Ribulose Biphosphate Carboxylase, also called RuBisCo (Douce *et al.*, 2001). The mitochondria of plant leaves will oxidize glycine at an extremely high rate requiring the glycine cleavage system to be present at an exceptionally high concentration within the mitochondrial matrix. It can therefore account for up to one third of the total soluble enzymes of the matrix (Olivier

and Douce, 1990). N^5-N^{10}-methylene tetrahydrofolate serves as a source of one carbon units (C1-units) in a wide range of cellular reactions such as the synthesis of purine nucleotides, thymidylate and amino acids like histidine, serine, methionine and formylmethionine.

1.3.2. Glycine Cleavage System (GCV)

The yeast genome harbors four genes that encode subunits of the glycine cleavage system. *GCV1*, *GCV2*, *GCV3* encode the T-protein, P-protein and H-protein respectively, while *LPD1* encodes the L-protein (Sinclair *et al.*, 1996; Sinclair and Dawes, 1995). Lipoic acid, a sulfur containing cofactor of the glycine cleavage system, is attached to the H-protein by an amine linkage to carbon six of a specific lysine side chain.

The L protein is a homodimer that participates in two other multienzymatic complexes: pyruvate dehydrogenase (PDH) catalyzing the conversion of pyruvate to acetyl coenzyme A (acetyl CoA) and therefore the entry of pyruvate into the citric acid cycle and 2-oxoglutarate dehydrogenase (OGDH) catalyzing the oxidative decarboxylation of 2-oxoglutarate to succinyl-Coenzyme A (succinyl CoA) (Dickinson *et al.*, 1986; Sinclair and Dawes, 1995).

In humans, an inborn metabolic defect is linked to mutations in one of the subunits of the glycine cleavage system. The autosomal recessive disease non-ketotic hyperglycinaemia (NKHG) demonstrates the important role of glycine as a neuromediator in the central nervous system. NKHG causes an accumulation of glycine

in plasma and cephalo-spinal fluid leading to irreversible brain damage (Tada and Hayasaka, 1987).

1.3.3. Biochemical reactions

The oxidation reaction catalyzed by the glycine cleavage system is a three step reaction using the H-subunit as a pivot (Fig.2). During this process, the lipoic arm of the H subunit commutes between the active sites of the others subunits. Such reactions have been mainly studied in plants because of their critical role in C3-plant metabolism (Oliver *et al.*, 1990; Douce *et al.*, 2001).

The first reaction is the decarboxylation of glycine catalyzed by the P-protein. The pyridoxal phosphate of the protein forms a shift base with the amino group of glycine leading to the release of carbon dioxide from glycine. The reaction catalyzed by the P-protein also transfers the methylamine moiety to the lipoic arm of the H-protein. The second reaction is catalyzed by the T-protein. This reaction releases ammonia and transfers a one carbon group from the lipoic residue of the H-protein to tetrahydrofolate. Finally the L-protein catalyzes the oxidation of the H-protein with the concomitant reduction of NAD, regenerating the H protein. During this process the lipoid arm of the H-protein has been successively methylamined reduced and oxidized, while holding the reaction intermediates (Douce *et al.*, 2001).

The Glycine Cleavage System is closely linked to the mitochondrial enzyme serine hydroxymetyltransferase (SHMT) that catalyzes the production of serine from glycine and N^5-N^{10} tetrahydrofolate, via a pool of tetrahydrofolates.

Figure 2. Biochemical reactions for glycine degradation. Figure adapted from Olivier and Douce (1990). During the reaction the lipoic arm of the H-protein commutes between the active sites of the other subunits, holding the reaction intermediates. The first reaction is the decarboxylation of glycine catalyzed by the P-protein (*GCV2)*. The second reaction is catalyzed by the T-protein leading to the release of ammonia and to the transfer of one carbon from the lipoic residue to tetrahydrofolate. The third reaction is catalyzed by the L-protein regenerating the H-protein with the concomitant reduction of NAD. In one cycle, the lipoic arm has been successively methylamined (Hmet), oxidized (Hox) and reduced (Hred).

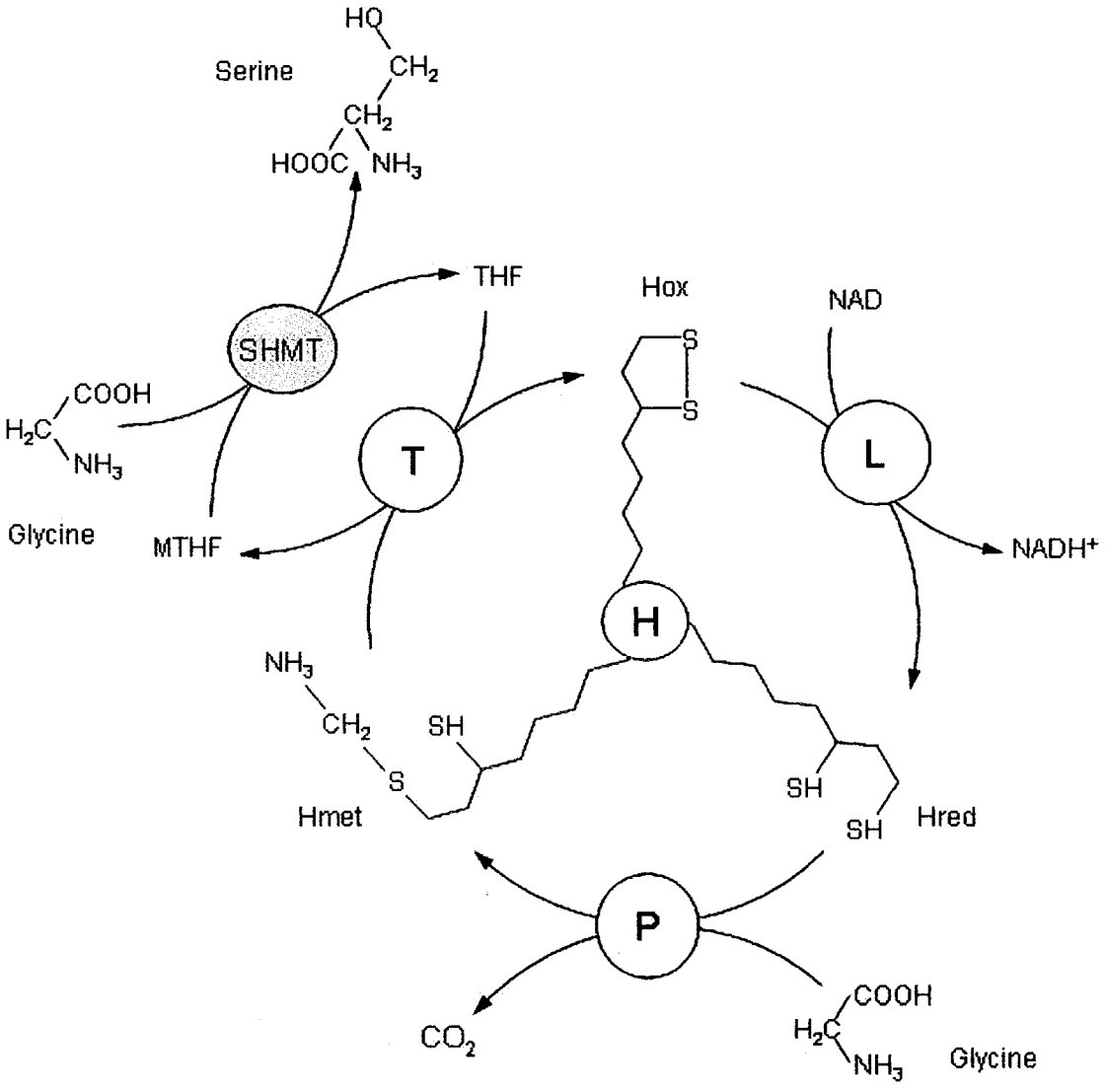
HO
Serine
CH2
CH2
HOOC
NH3
THF
Hox
NAD
SHMT
S
S
COOH
H2C
NH3
T
L
Glycine
MTHF
NADH+
H
NH3
CH2
SH
S
SH
SH
Hmet
Hred
P
CO2
COOH
H2C
NH3
Glycine

1.4. Nitrogen metabolism

Nitrogen assimilation occurs via incorporation of ammonia into glutamate and glutamine (ter Schure *et al.*, 2000). Glutamate and glutamine can serve as nitrogen sources and can be interconverted by glutamine synthase (GS), and glutamate synthase (GOGAT) (Fig.3 and 4). Consequently, they are playing a central role in nitrogen metabolism (ter Schure *et al.*, 2000). Glutamate generated by ammonia incorporation can be used as an amine group donor in the synthesis of purines and most of the 20 major amino acids used for protein synthesis by transamination reaction with α-Keto acids (ter Shure *et al.*, 2000).

1.5. One-carbon unit metabolism

One-carbon unit metabolism is a set of reactions that lead to the formation of 5,10-N methylene tetrahydrofolate (CH2-THF) and its derivatives, which are used to synthesize compounds like amino acids and purines (Fig.5).

Serine is the primary contributor to the pool of C1 units. It can be synthesized from the conversion of the glycolytic intermediate 3-phosphoglycerate or alternatively via the cytoplasmic serine hydroxymethyl transferase (SHMT) from glycine and CH2-THF (Sinclair and Dawes, 1995). Glycine can also entirely act as a substitute for serine. Under non-limiting serine conditions, 25% of C1 carbon units are produced in the mitochondria by the oxidation of glycine. These enter the cytoplasm C1 unit pool in the

Figure 3. Interconversion of α-ketoglutarate, ammonia, glutamate and glutamine in central nitrogen metabolism. Figure by ter Shure *et al.*, 2000. Ammonia (NH_4^+) can be incorporated directly into glutamate at the expense of one NADPH or into glutamine at the expense of one ATP. Glutamine and α-ketoglutarate can give two glutamates via the GOGAT reaction consuming one NADH. Glutamate can be converted to α-ketoglutarate with the release of NH_4^+.

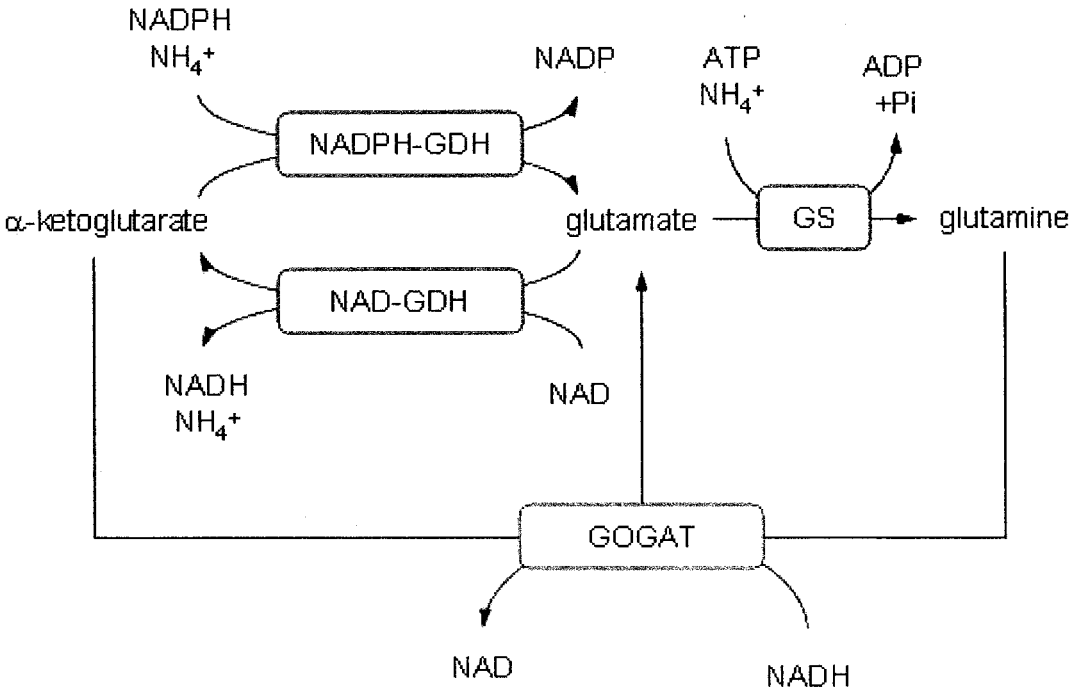
NADPH
NH4+
NADP
ATP
NH4+
ADP
+Pi
NADPH-GDH
α-ketoglutarate
glutamate
GS
glutamine
NAD-GDH
NADH
NH4+
NAD
GOGAT
NAD
NADH

Figure 4. Chemical reaction associated with the central nitrogen metabolism. Glutamate dehydrogenase catalyzes the reversible incorporation of ammonia into glutamate using NADPH as a cofactor. Glutamine synthase catalyzes the two-step reaction that incorporates NH_3 into glutamine with the consumption of one ATP. Glutamate synthase (GOGAT) catalyzes the conversion of one glutamine and one α-ketoglutarate into two glutamates at the expense of one $NADPH+H^+$. Transaminase enzymes catalyzed the transfer of amino groups from glutamate to convert α-keto acid into α-amino acids.

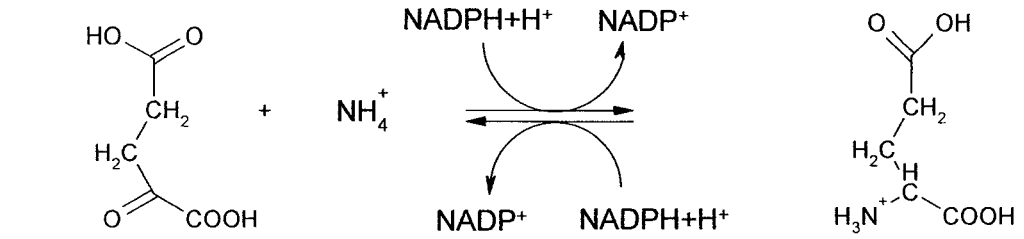

α-Ketoglutarate *Glutamate dehydrogenase* Glutamate

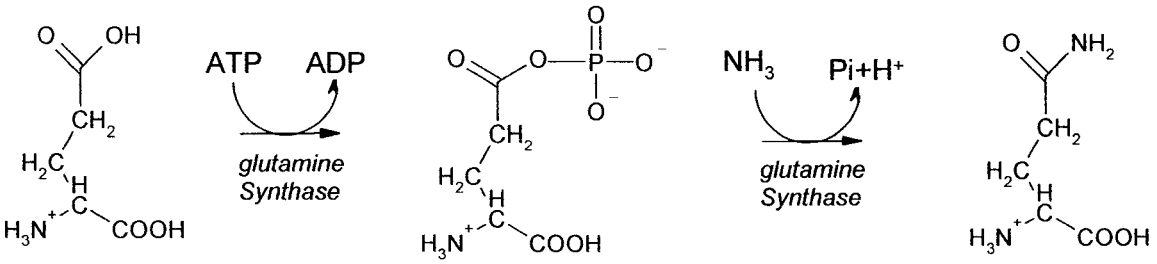

Glutamate Glutamine

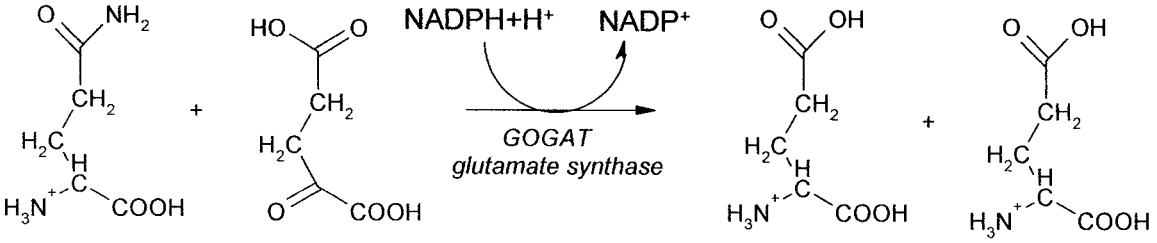

Glutamine α-Ketoglutarate Glutamate Glutamate

TRANSAMINATION

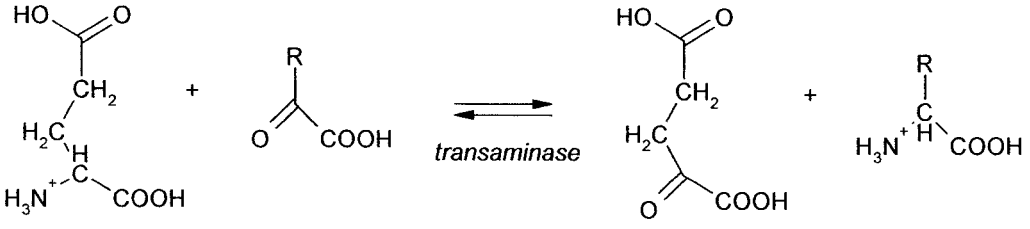

Glutamate α–keto acid α-Ketoglutarate α-Amino acid

Figure 5. One-carbon unit metabolism. Figure adapted from Pasternack *et al.* 1994; Denis and Daignan-Fornier, 1998. One-carbon unit metabolism is a set of reactions that lead to the formation of 5,10-N-methylene tetrahydrofolate and its derivatives.

PRPP: 5'-Phosphoribosyl-1-pyrophosphate, PS: Phosphatidylserine,

PE: Phosphatidylethanolamine, PC: Phosphatidylcholine.

Enzyme or complex catalyzing reaction indicated by numbers:

(1) glycine cleavage system (GCV), (2) mitochondrial C1-THF synthase (Mis1p), (3) mitochondrial serine hydroxymethyl transferase (Shm1p), (4) cytoplasmic serine hydroxymethyl transferase (Shm2p), (5) cytoplasmic C1-THF synthase (Ade3p), (6) CH2-THF reductase, (7) NAD-dependent CH2-THF dehydrogenase (Mtd1p), (8) Glutamine synthase (Gln1p)

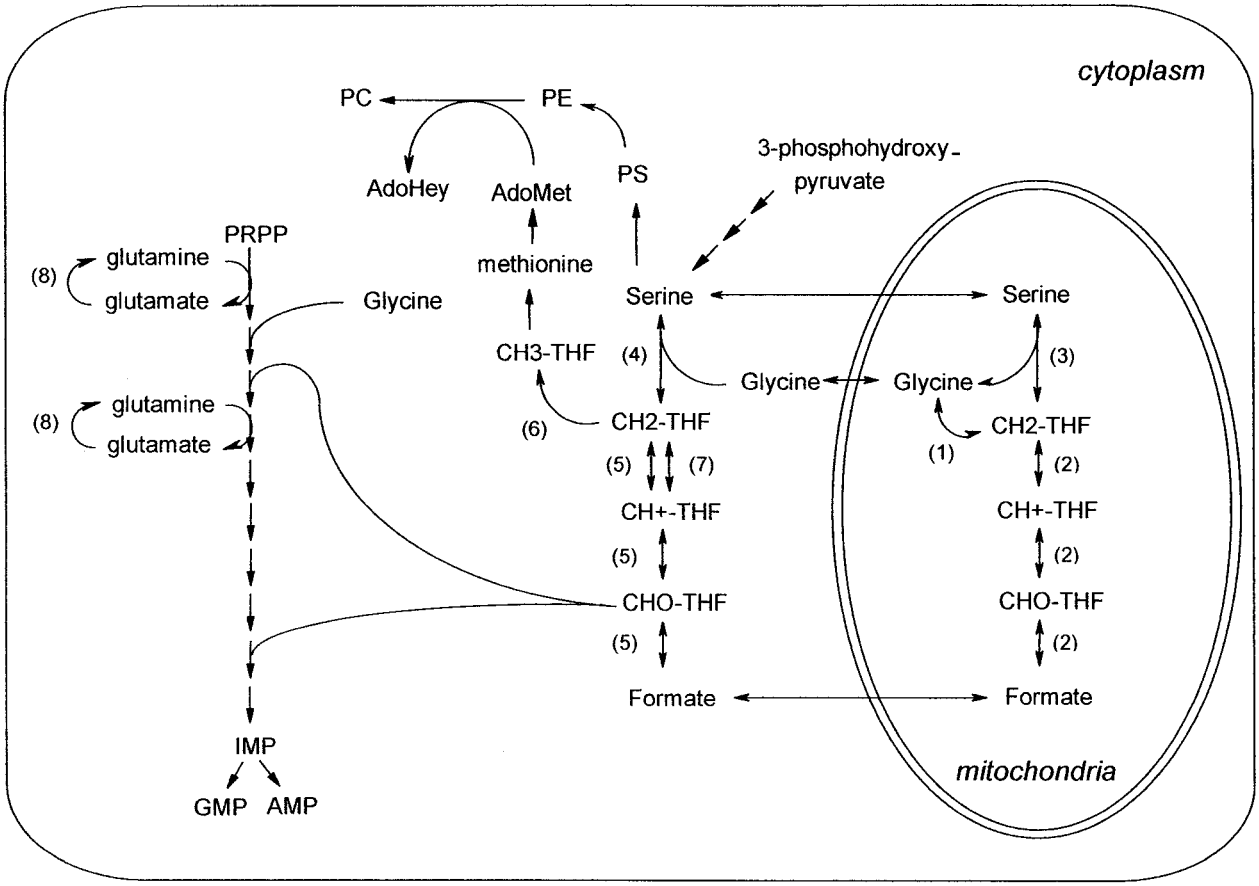
cytoplasm
PC
PE
AdoHey
AdoMet
PS
3-phosphohydroxy-
pyruvate
PRPP
(8)
glutamine
glutamate
methionine
Serine
Serine
Glycine
CH3-THF
(4)
Glycine
Glycine
(3)
(8)
glutamine
glutamate
(6)
CH2-THF
(1)
CH2-THF
(5)
(7)
(2)
CH+-THF
CH+-THF
(5)
(2)
CHO-THF
CHO-THF
(5)
(2)
Formate
Formate
IMP
GMP
AMP
mitochondria

Figure 6. Interconvertion of one-carbon units. One carbon units can be interconverted in the mitochondria and in the cytoplasm via a duplicated set of enzymes composed of the trifunctional C1-tetrahydrofolate synthase (*ADE3* cytoplasmic and *MIS1* mitochondrial isoenzyme) and the two isoforms of serine hydroxymethyl transferase (*SHM1*, *SHM2*).

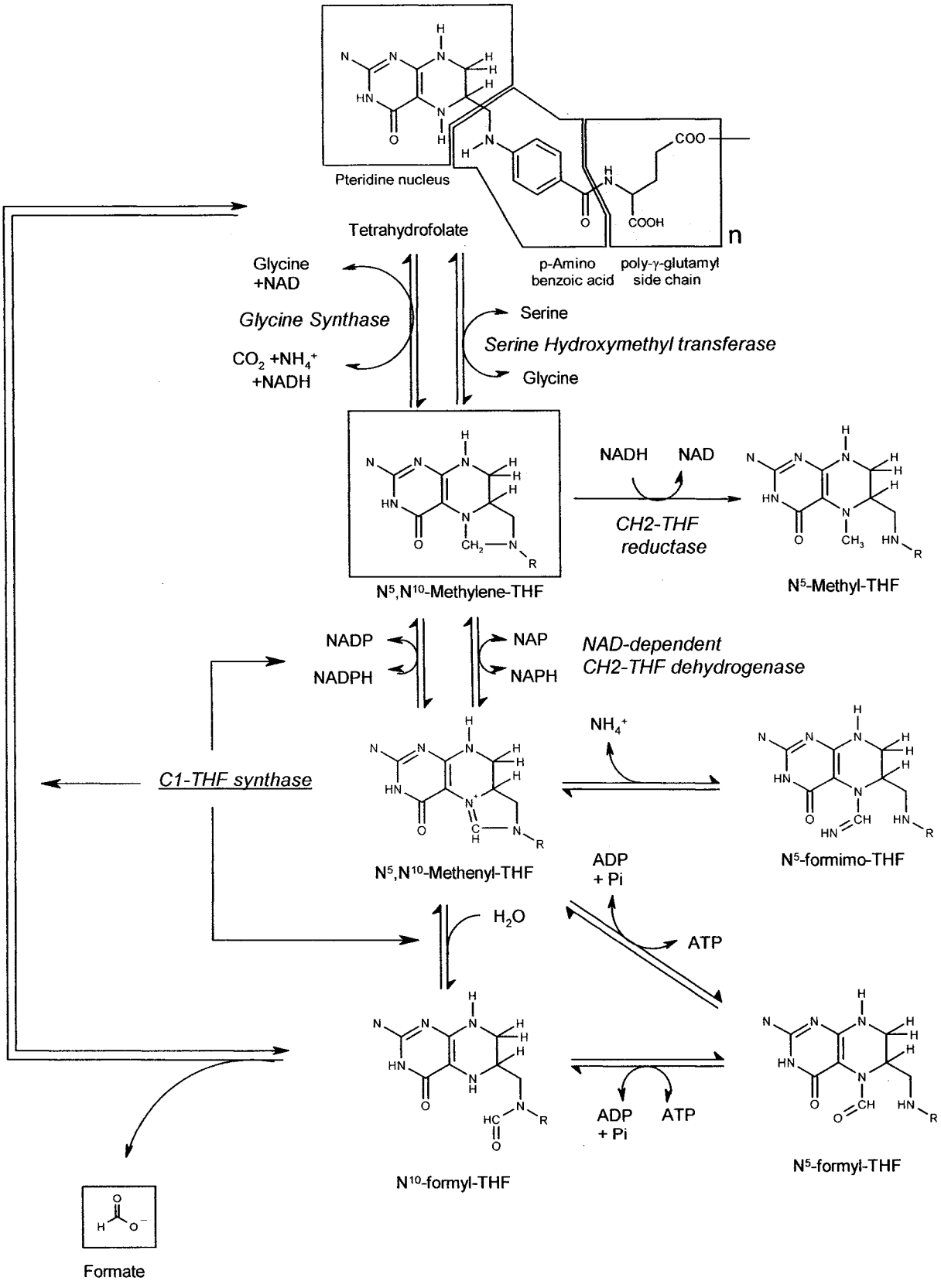
Pteridine nucleus
p-Amino benzoic acid
poly-γ-glutamyl side chain
n
Tetrahydrofolate
Glycine +NAD
Glycine Synthase
CO2 +NH4+ +NADH
Serine
Serine Hydroxymethyl transferase
Glycine
N5,N10-Methylene-THF
NADH
NAD
CH2-THF reductase
N5-Methyl-THF
NADP
NADPH
NAP
NAPH
NAD-dependent CH2-THF dehydrogenase
C1-THF synthase
NH4+
N5,N10-Methenyl-THF
N5-formimo-THF
ADP + Pi
ATP
H2O
N10-formyl-THF
N5-formyl-THF
Formate

formate form. Only three one-carbon metabolism products: glycine, serine and formate will flow between the cytoplasm and the mitochondria. Furthermore, formate synthesis is dependent on methyl-tetrahydrofolate thus it is suspected that formate shuttles between these two compartments as a carbon unit carrier. In both the mitochondria and the cytoplasm, C1-derivatives can be interconverted via the trifunctional C1-tetrahydroxyfolate synthase (*ADE3* encodes the cytoplasmic isoenzyme and *MIS1* the mitochondrial one) and the two isoforms of SHMT. The oxidation of glycine, however, remains exclusively mitochondrial (Zelikson and Luzzati, 1977) (Fig.6).

Once in the cytoplasm, folate will be converted to formyl-tetrahydrofolate (CHO-THF) by the C1-tetrahydroxyfolate synthase and mainly used for purine synthesis, leaving only a small portion to be converted to CH2-THF. Purine synthesis will then use a mix of one-carbon metabolites of both mitochondrial and cytoplasmic origins.

Under glycine growth conditions, SHMT uses glycine and CH2-THF for the synthesis of serine that can then be used for protein synthesis or synthesis of phosphatidyl choline.

Cytosolic CH2-THF can be converted to methyl-tetrahydrofolate (CH3-THF) by methylene tetrahydrofolate reductase (MTHFR). Methyl-tetrahydrofolate will subsequently be used for the formation of methionine and S-Adenosyl methionine (SAM), which is a much stronger methyl group donor than methylene-tetrahydrofolate, and can be used in the synthesis of phophatidyl choline.

1.6. Regulation of glycine metabolism

In the bacteria *Escherichia coli,* glycine and purine levels regulate the gcvTHP operon encoding three subunits of the glycine cleavage system (Wilson *et al.*, 1995). The regulation is mediated by GcvA a LysR family member transcription factor the global transcriptional regulator Lpr and the negative regulator GcvR (Ghrist and Stauffer, 1995). Mechanism of glycine regulation in yeast seems to be far more complex in the number and variety of factors that can influence it. Also, factors involved in amino acid, purine, nitrogen and C1 metabolism have been shown to play a role in the activation or the repression of the glycine cleavage system.

1.6.1. The general amino acid control system

Under conditions of amino acid starvation, the general amino acid control system activates the expression of genes involved in amino acid pathways as well as several other genes for purine biosynthesis (Rolfes and Hinnebusch, 1993). Gcn4p is a leucine zipper transcriptional activator that binds DNA as a homodimer. It acts as a proximal positive regulator of gene expression in the general amino acid control system. Its binding site, the General Control Response Element (GCRE) contains the core sequence 5'-TGACTC-3' (Arndt and Fink, 1986; Tice-Baldwin *et al.*, 1989). Gcn4p-mediated regulation extends much farther than simply the direct pathways for amino acid and purine biosynthesis. It has been reported to regulate the expression of at least two of the genes encoding for glycine cleavage system subunits: *LPD1* and *GCV3* (Zaman *et al.*,

1999). Furthermore the genes for the two other units possess copies of the GCRE sequence in their promoter (Nagarajan and Storms, 1997).

Since the two main products of glycine catabolism, ammonia and methylene tetrahydrofolate, are used in amino acid synthesis, it is therefore not surprising that the general amino acid control system plays a role in its regulation.

1.6.2. Bas1p and Bas2p regulation

The synthesis of several substrates used during *de novo* biosynthesis of purines (such as glutamine, CHO-THF and glycine) have been shown to be coregulated with the synthesis of the purine biosynthetic pathway enzymes. *SHM2* (serine hydroxyymethyl transferase), *GLN1* (glutamine synthetase) and *MTD1* (NAD-dependent 5-10 methylene tetrahydrofolate dehydrogenase) are repressed by adenine and require Bas1p and Bas2p for maximal transcription (Denis *et al.*, 1998; Denis and Daignan-Fornier, 1998).

Bas1p is required for the expression of all genes repressed by adenine (Daignan-Fornier and Fink, 1992; Rolfes *et al.*, 1997; Denis *et al.*, 1998). Bas1p has an amino terminal Myb motif domain that binds to a core sequence identical to GCRE (5'-TGACTC-3'). The flanking nucleotides, however, affect differently the binding affinity of these two proteins (Tice Baldwin *et al.*, 1989; Rolfes *et al.*, 1997). *ADE3*, *SER1*, *GCV1* and *LPD1* possess the BAS1 consensus sequence in their promoters. However they have not been shown to be regulated by adenine (Denis and Daignan-Fornier, 1998). This differs from the *E. coli* regulation mechanism in which purine availability regulates

expression of the gcv operon encoding the three subunits of the glycine cleavage system (Wilson *et al.*, 1993).

Bas1p seems to be specialized in the activation of genes involved in the biosynthesis of purines in the absence of external sources, whereas Bas2p (previously identified as PHOS2) seems to have a broader stimulating activity, being able to stimulate other pathways. DNA footprinting analyses on the HIS4 promoter suggests that Bas2p binds to AT-rich DNA sequences via its N-terminal homeodomain, but unlike Bas1p, no clear sequence has been derived (Tice Baldwin *et al.*, 1989). Repression by adenine is thought to be due to the inhibition of the formation of an activating complex between Bas1p and Bas2p in the presence of adenine (Zhang *et al.*, 1997). However a study by Yun Zheng shows that glycine induction and repression by C1 end product was dependant from Bas1p with little involment of Bas2p (Zheng, 1995).

1.6.3. Nitrogen catabolite repression (NCR)

Selectivity between good and poor nitrogen sources is accomplished by nitrogen catabolite repression (NCR). In the presence of preferred nitrogen sources, the NCR ensures a low level of transcriptional expression of genes encoding transport and enzyme proteins needed for the utilization of poor nitrogen sources (Cunningham *et al.*, 2000).

The expression of nearly all genes whose products participate in the uptake and catabolism of nitrogenous compounds are NCR-sensitive. NCR is mediated by GATA family factors: two positively acting regulators, Gln3p and Nil1p/Gat1p and two negatively acting regulators, Dal80p and Deh1p (Coffman *et al.*, 1997; Stanbrough *et al.*,

1995; ter Schure *et al.*, 2000). In addition to these factors, Ure2p (and possibly other proteins acting on a similar mechanism) acts as a negative regulator of the NCR-sensitive gene expression (Coffman *et al.*, 1994). In the presence of a good nitrogen source, Ure2p seems to bind to the Gln3p and Gat1p factors excluding them from the nucleus, and leaving GATA sites unoccupied (Coffman *et al.*, 1994; ter Schure *et al.*, 2000)

DAL80p has been shown to bind the same sequence as Gln3p, The competition of the two proteins for the same binding site results in the down-regulation of GLN3p-mediated transcription (Cunningham *et al.*, 2000).

Almost all of the transport systems associated with poor nitrogen source uptake are regulated by the NCR. In the absence of preferred nitrogen sources or after preferred souces of nitrogen are used up, the production of poor nitrogen-source transport systems is derepressed. The poor nitrogen source transporters operate at full capacity allowing the cell to scavenge for all nitrogen sources present. However, enzymes required for the degradation of a given compound are not expressed at a high level until the compound accumulates in the cell (ter Schure *et al.*, 2000).

Interestingly, the GATA factors seem to regulate the transcription of some vacuolar proteases (Coffman and Cooper, 1997). This suggests that the vacuolar degradation of proteins supplies the cell with a source of nitrogen in the presence of less favorable sources of nitrogen.

1.6.4. Regulation of the one-carbon unit metabolism

The cell needs to regulate the balance of one-carbon metabolism between cytoplasm and mitochondrion in order to supply one-carbon units for the important biosynthesis pathways. Studies on the flow of C1 compounds between the different cellular compartments (Piper *et al.*, 2000; Pasternack *et al.*, 1994) have partially uncovered the regulation of C-1 metabolism.

The cytoplasmic CH2-THF level acts as an indicator of the C-1 unit state of the cell. By monitoring the level of CH2-THF, the cell can upregulate the glycine cleavage system in response to one-carbon starvation or glycine excess. Under normal growth conditions CH2-THF is converted to CH3-THF for the synthesis of methionine and secondly for the formation of more oxidized C1-THF derivatives for the synthesis of purines. In excess glycine or one-carbon depletion, CHO-THF accumulation inhibits SHMT causing a decrease in the level of CH2-THF. The SHMT inhibition results from a side reaction of the SHMT: hydrolysis of 5,10-methenyl-tetrahydrofolate (CH+-THF) to 5-formyl-tetrahydrofolate (CHO-THF) (Fig.7) (Piper *and al.*, 2000; Stover and Schirch, 1990). CHO-THF or CH3-THF binds SHMT in conjunction with glycine forming a dead end complex that drastically inhibits the activity of this enzyme (Piper *et al.*, 2000). The resulting reduction in CH2-THF triggers the switch to glycine for the production of one-carbon units, increasing GCV genes transcription. A decrease in CH2-THF signals the need for the cell to synthesize one-carbon units from glycine (Fig.7). Transcriptional regulation is assumed to be mediated by protein binding to a Glycine Response Sequence

Figure 7. Model of how cells regulate one-carbon metabolism and gene transcription via the activity of cytoplasmic SHMT. Figure by Piper *et al.*, 2000. Regulation of SHMT activaty by a side reaction dictate cytoplasmic CH2-THF levels, which mediate transcription of genes involved in generation of one-carbon units from glycine. Solid black arrows indicate enzyme-catalyszed reactions; gray lines indicate control of enzyme activity; and the dashed line indicates regulation of gene expression.

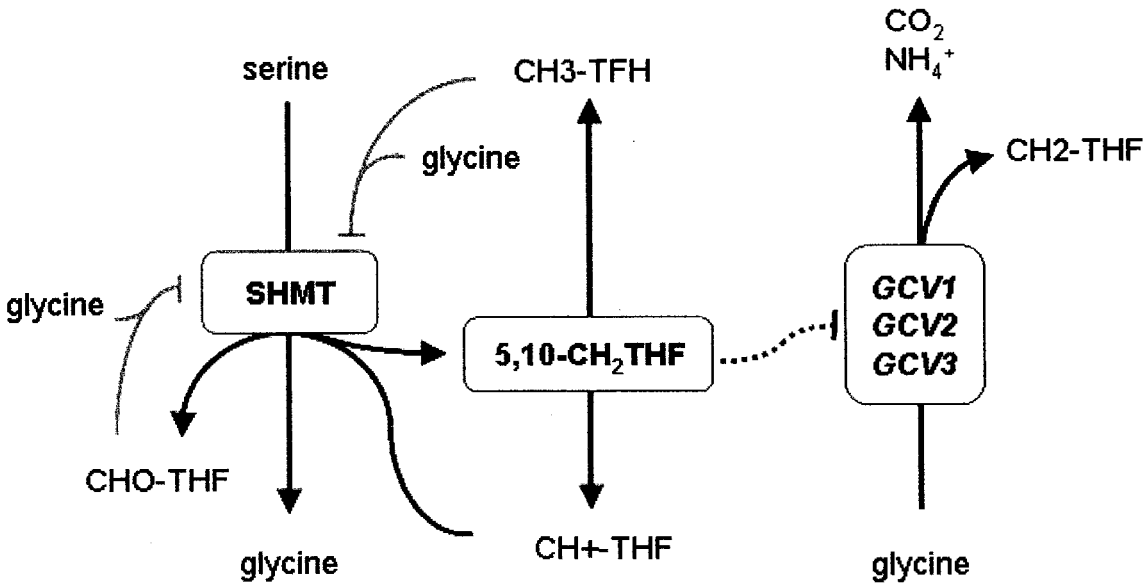
serine
CH3-TFH
glycine
CO_2
NH_4^+
CH2-THF
glycine
SHMT
5,10-CH_2THF
GCV1
GCV2
GCV3
CHO-THF
glycine
CH+-THF
glycine

(GRS) containing a core 5'-CTTCTT-3' (Hong *et al.*, 1999). The affinity of the protein for the GRS sequence is decreased in the presence of CH2-THF (Piper *et al.*, 2000).

1.7. Rationale of the thesis

Despite the fact that activated one-carbon metabolism and nitrogen metabolism have been studied for decades, the unique role of glycine is not yet completely understood. The yeast *Saccharomyces cerevisiae* can use glycine as a sole nitrogen source as well as activated one-carbon units. Previous results from our laboratory showed that glycine at high concentration is toxic for yeast. Glycine metabolism should therefore be regulated so that the amount of glycine does not reach toxic levels. This study focuses on developing a high throughput method to screen the library of deletion strains in order to identify genes that are associated with altered growth phenotypes when glycine is the sole nitrogen source. Selected strains from preliminary screening with glycine as a sole nitrogen source will be further characterized on media with alternative poor or good nitrogen sources, supplementation in various C1 metabolism products, different glycine concentrations or glycerol as carbon source. Clustering analyses of the results may help us gain insight into the regulatory mechanism controlling nitrogen source utilization and activated one-carbon units. This approach is complementary to transcriptional gene profiling since a significant proportion of the genes necessary for survival or optimal growth in a given condition does not exhibit a significant increase in messenger RNA expression (Giaever *et al.*, 2002). Thus looking directly at the phenotype resulting from the deletion can help us understand the function and interaction of genes.

2 Material and Methods

2.1 Strains and media

2.1.1 Strains

The strains used in this study are the homozygous diploid yeast deletion mutants generated by the *Saccharomyces* genome deletion project and distributed by Research Genetics. ORFs have been systematically deleted and replaced by a Kanamycin cassette. Strains are provided in 96-well plates containing 200µl YPD/15% glycerol media with G418 at a concentration of 200mg/L. The fifty-four plates are "footprinted" by leaving two wells blank; the first sequentially identifies the plate number, and the second indicates the strain background (always in row H). Two working copies of the set have been made and stored at -80°C.

The strains' background is BY4743 (MATa/α his3Δ1/his3Δ1 leu2Δ0/leu2Δ0 lys2Δ0/LYS2 MET15/met15Δ0 ura3Δ0/ura3Δ0) (4741/4742). Additional information about the *Saccharomyces* Genome Deletion Project can be found at the following link: http://www-sequence.stanford.edu/group/yeast_deletion_project/deletions3.html

2.1.2 Media

Rich media (YPD) consisted of 1% Bacto-Yeast extract, 2% Bacto-peptone, and 2% dextrose.

Minimum media (Dmin) consisted of 0.175% yeast nitrogen base without amino acids and without ammonium sulfate (DIFCO), 2% dextrose, and 0.5% ammonium sulfate. For all minimum media leucine, histidine and uracil were added to a final concentration of 40mg/L (as required by the strain background).

In Gmin, Pmin and Emin, ammonium sulfate have been replaced by 1.5% glycine, proline or sodium glutamate, respectively.

Dmin0.5mM, Dmin10mM and Dmin200mM are minimum media supplemented with glycine to a final concentration of 0.5mM, 10mM and 200mM respectively (Sinclair and Dawes, 1995; Piper *et al.*, 2000).

GminF and GminS are glycine minimum media supplemented with sodium formate at a final concentration of 44mM (stock solution 2.2M, pH7) or serine at a final concentration of 400mg/L respectively (Sinclair and Dawes, 1995). GminC1 is glycine minimum media supplemented with adenine 40mg/L, methionine 20mg/L, serine 400mg/L, and sodium formate at a final concentration of 10mM.

In Golmin glucose has been replaced by glycerol, 30ml/liter, as sole carbon source.

2.2 Screen for strains that showed a growth phenotype on Gmin compared to Dmin

2.2.1 Plating

The complete homozygous diploid set was replicated using the MULTI-BLOT™ VP408FS replicator and LIBRARY COPIER™ from V&P Scientific, Inc. San Diego CA. at a density of 864 colonies per Omnitray uniwell agar plate. Using this format three 96-well plates were spotted in triplicate to each uniwell plate. The replicator (with 96 floating slot pins), which delivers 1µl, was cleaned by bathing the pins twice in distillated water, once in 70% ethanol followed by 95% ethanol and sterilized by flame between each replication. The format of the assay plate for the primary screen is illustrated in Figure 8. All plates were incubated at 30°C, until the spots were ready to be scored. The complete set of diploid deletion strains were replicated onto YPD, Dmin and Gmin media.

2.2.2 Analyses

Following incubation on plates the growth of each strain was evaluated by digital imaging. Images of each plate were generated with the Gene Genius™ Bio Imaging system. The brightness of each spot was evaluated using the Gene tools™ software from Syngene®. The spot blot analysis function was used to generate a grid that overlapped the plate image. The brightness of each spot was assigned relative to a reference spot (blank) with a designated value of 1. Automatic correction of the background was also performed.

Figure 8. Plating format of the Preliminary screen. The complete homozygous diploid set has been replicated manually at a density of 864 colonies per plate. Three 96-well plates from the set were assayed in triplicate on each uniwell plate. Spots corresponding to wells left empty for microtiter plate footprinting appear as white circles (row A and H)

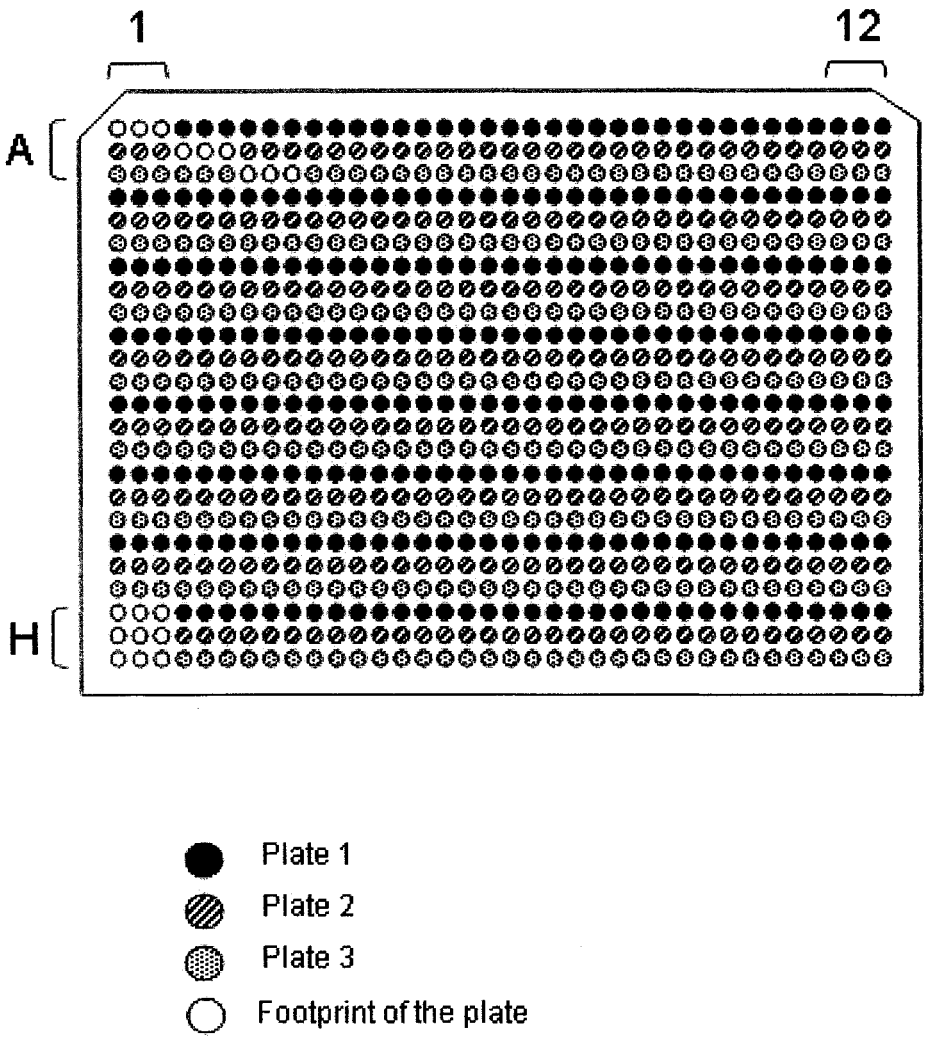
1
12
A
H
Plate 1
Plate 2
Plate 3
Footprint of the plate

In order to compare the relative amount of growth, the relative brightness of each spot was normalized by expressing it as a fraction of the mean intensity of all the spots on the plate. The relative growth of each spot was then used to calculate the relative Gmin/Dmin ratio (relative growth on Gmin/relative growth on Dmin). The mean of the three ratio values was calculated and transformed to log base 2. Based on the set of data, strains showing a log base 2 ratio greater than 1 or lower than -1, were arbitrarily selected for further analysis.

2.3 High-density colony array

2.3.1 Assay

Following the screening for strains with growth phenotype on Gmin, strains showing a growth phenotype were selected for high density colony array analysis to compare growth rate on Gm, GminF, GminS, GminC1, Dmin0.5mM, Dmin10mM, Dmin250mM, Pmin, Emin and Golmin media with Dmin.

In order to do this, colony arrays were generated using a VIRTEK® colony arrayer equipped with a 96 or 384 pin replicator head. The script design allowed the precise positioning of each strain at a maximum density of 9216 colonies per 245 mm, square bioassay plate.

Strains displaying a growth phenotype were grown in YPD in 96 well plates. 96 well microtiter plates containing strains to be assayed were first transferred using the V&P replicator to YPD agar plates and allowed to grow for two days. The colony arrayer (with the 96 pin replicator head) was used to transfer the strains to YPD agar

plates in the format of 384 spots per omnitray plate. Depending on the plates, this was done either by combining 3 different plates or by replicating the same plate 3 times, (using 288 of the 384 positions available in that format) (Fig.9). Each plate was subsequently replicated several times onto fresh YPD agar using the colony arrayer (with the 384 pin replicator head) in order to obtain several sets of copied master plates of arrayed colonies that could be subject to further analysis.

The strains exhibiting a phenotype on Gmin were arrayed onto 245mm, square bio assay dishes (Fig.10). Cells were transferred from the master plate (384 colonies format) to one of the four positions on an intermediate YPD plate (1536 colonies format). The replicator head was cleaned to remove remaining cells and sterilized. One position on the intermediate plate served as the source plate for printing one block before the head returned to the master plate to transfer cells to the next position on the intermediate plate (Fig.11). To minimize differences in the number of cells deposited between replicates, the robot was programmed to contact the source plate colonies at four distinct locations, offset by 0.2 mm. Blocks were alternately spotted on two bioassay plates processed simultaneously to reduce differences between them (Fig.11). One set of master plates was used for each run.

The washing protocol used in this program was the following: 2 min. in water (1 min repeat with refill), 2 min. sonication in 70% ethanol, 30 sec. in 95% ethanol, followed by 30 sec. of vent drying (personal communication C. Boone).

After replication, all plates were incubated at 30°C for a period of at least one week and scanned every 24 hours on a Hewlett-Packard scanner at a resolution of 600dpi.

Figure 9. High-density colony array. Three 96-spot plates were combined to obtain a 384-spot plate. Only 288 of the 384 positions available were used. The 384-spot plate was replicated onto bioassay dishes in the 9212-spot format. Each bioassay plate contained 6 blocks of 1536 spot.

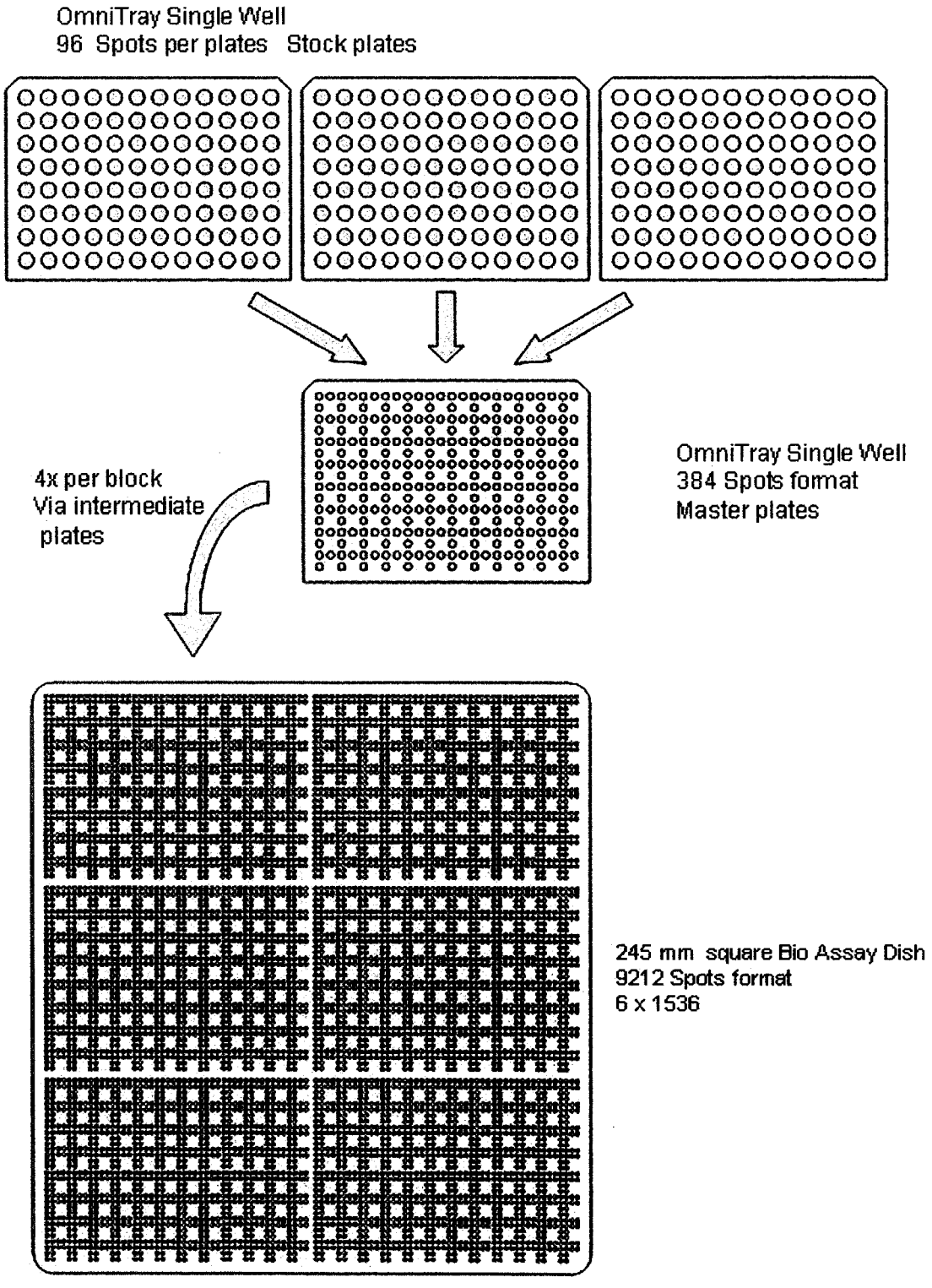
OmniTray Single Well
96 Spots per plates Stock plates
4x per block
Via intermediate
plates
OmniTray Single Well
384 Spots format
Master plates
245 mm square Bio Assay Dish
9212 Spots format
6 x 1536

Figure 10. Organization of the Virtek® Colony arrayer workstation. The workstation platform can accommodate up to 2 bioassay dishes and 8 omnitray plates. Each master plate was replicated in quadruplicate in 2 of the 6 blocks (0 through 5) of the bioassay dish. Each strain selected in the primary screen is therefore replicated a minimum of 8 times on each bioassay dish.

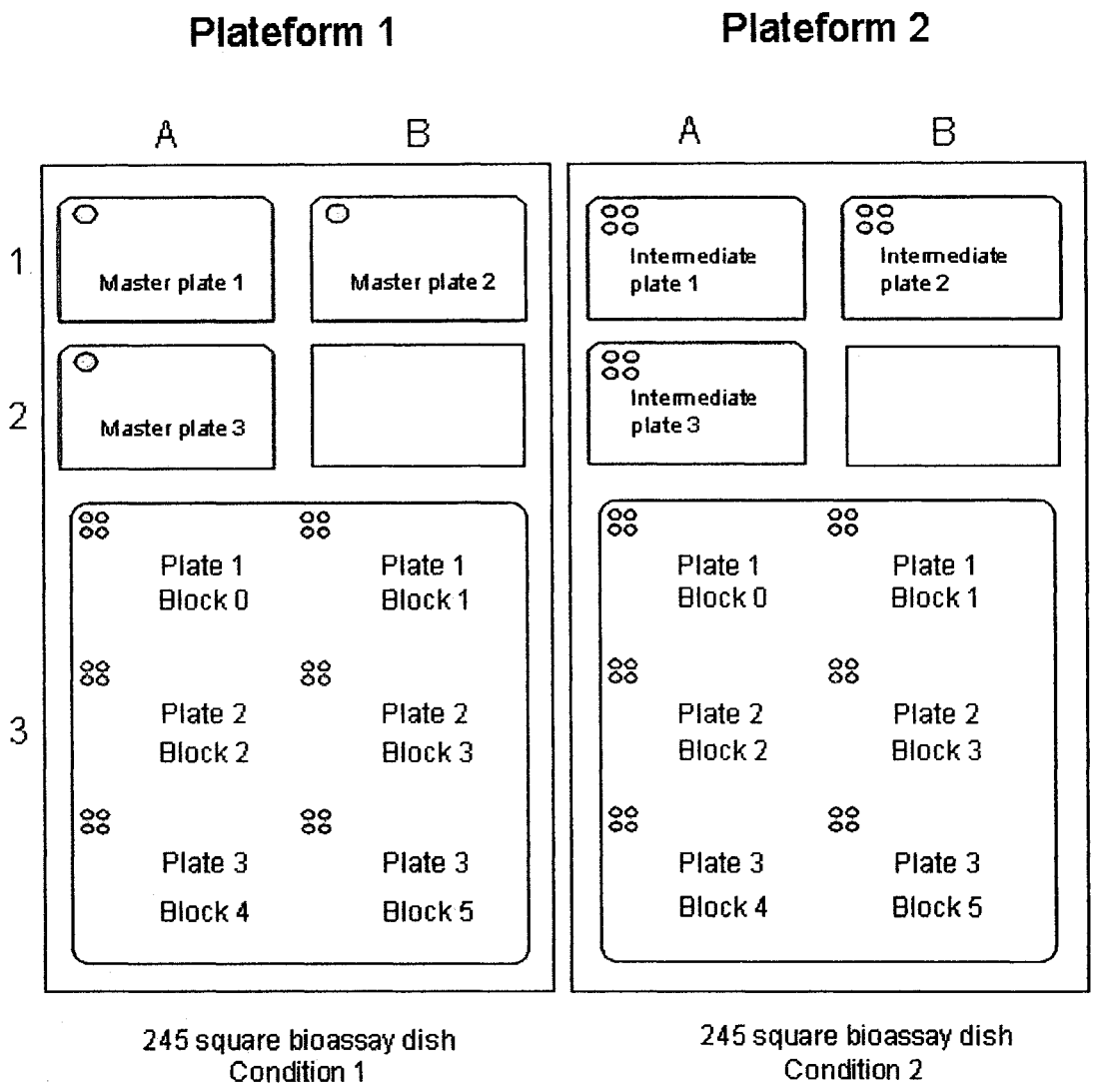
Plateform 1
Plateform 2
A
B
A
B
1
2
3
Master plate 1
Master plate 2
Master plate 3
Intermediate plate 1
Intermediate plate 2
Intermediate plate 3
Plate 1 Block 0
Plate 1 Block 1
Plate 2 Block 2
Plate 2 Block 3
Plate 3 Block 4
Plate 3 Block 5
Plate 1 Block 0
Plate 1 Block 1
Plate 2 Block 2
Plate 2 Block 3
Plate 3 Block 4
Plate 3 Block 5
245 square bioassay dish Condition 1
245 square bioassay dish Condition 2

Figure 11. Printing the block on a bioassay dish. In order to limit the number of cells spotted on the bioassay dish, intermediate plates were generated to serve as source plate for printing the blocks on the two assay plates. Blocks were alternately spotted on bioassay plate 1 and 2 to reduce possible differences between bioassay plates.

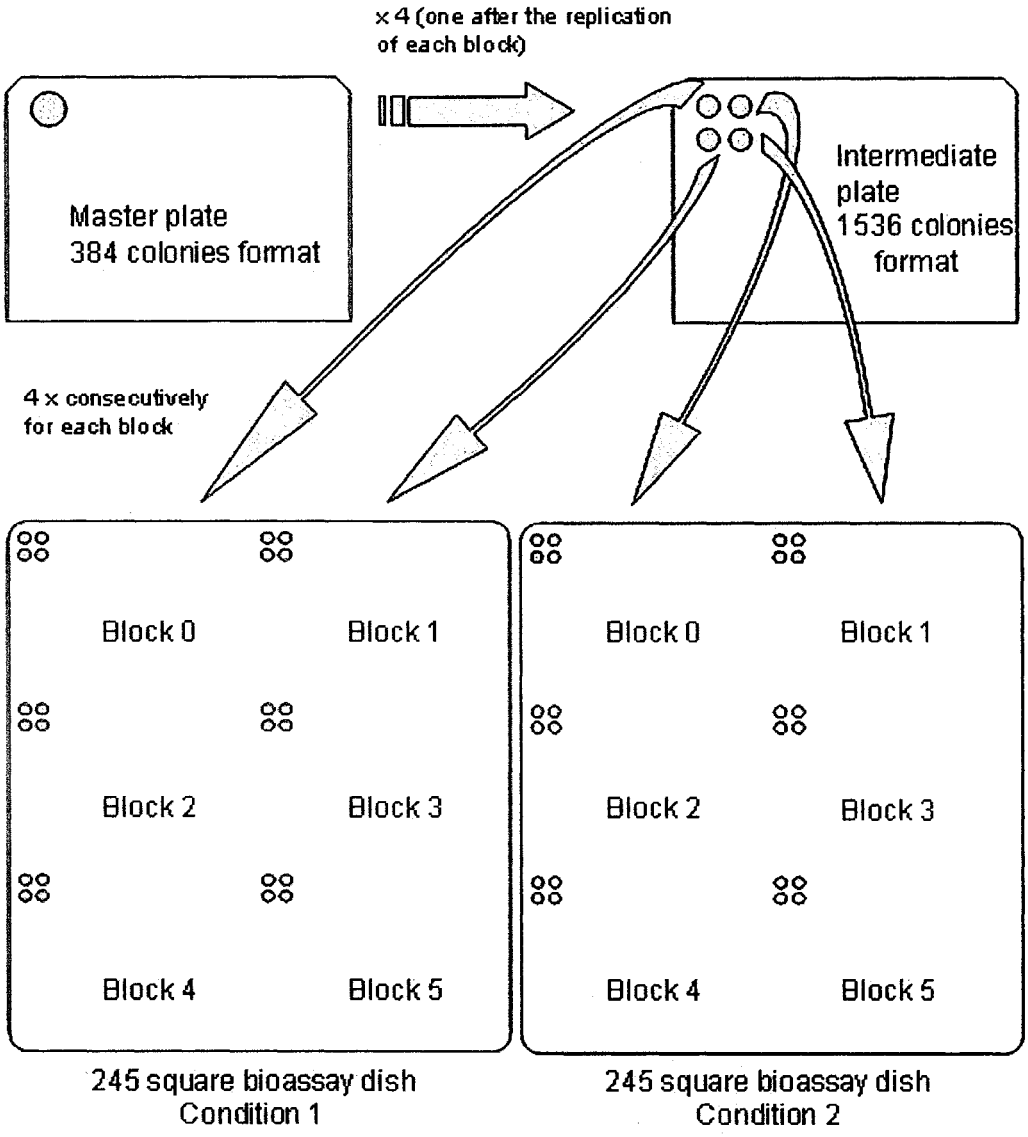
× 4 (one after the replication of each block)
Master plate
384 colonies format
Intermediate plate
1536 colonies format
4 × consecutively for each block
Block 0
Block 1
Block 2
Block 3
Block 4
Block 5
Block 0
Block 1
Block 2
Block 3
Block 4
Block 5
245 square bioassay dish
Condition 1
245 square bioassay dish
Condition 2

2.3.2 Software analysis

Bioassay plate images selected on the basis of colony size were processed using the microarray GenePix™ Pro 4.0 array, acquisition and analysis software (from Axon instruments, Inc.). False colors, typically red and green, representing colony brightness, were assigned to the control and test media condition, respectively, to facilitate visual comparison. Colony brightness was calculated by the following method. First the software generates an analysis array that defines the location and dimensions of each spot or feature. The intensity of the pixels within the circular area defined by each feature was measured and averaged for both media. The local background subtraction method was employed to subtract the amount of feature brightness contributed by the background. This was done by computing a different background for each individual feature as indicated in Figure 12. The data collected (brightness values) for each feature corresponds to the mean pixel intensity of the feature area minus the median pixel intensity of the local background (Fig.11).

2.3.3 Statistical analysis

Feature intensity readings generated by GenePix™ were matched to the corresponding strains in Microsoft Excel® using dynamic spreadsheets designed to keep track of strains arrayed in both the 96 and the 9216 spots formats (Fig.13).

Figure 12. Feature and background pixels. Each colony is included in a circular area call feature. The pixels neighboring the feature border are excluded from the calculation (light gray). The area containing the pixels compute for the background (black region) is three times the diameter of the feature (dark gray).

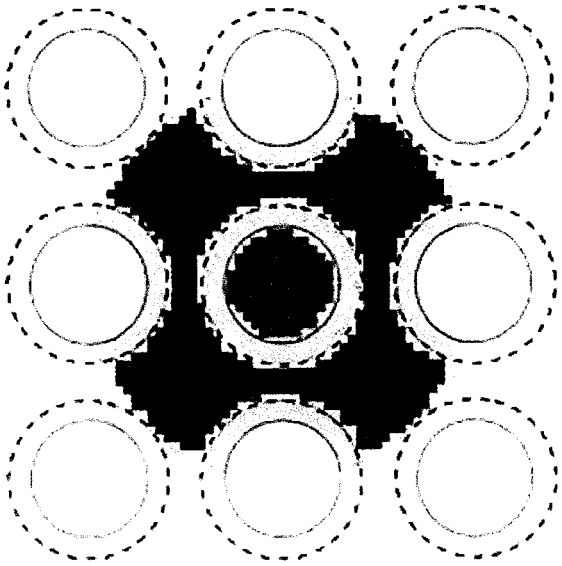

Feature pixels
Background pixels
2-pixel exclusion region

Figure 13. Organization chart of high density colony array. Inputs files are represented as white boxes, the software used are circled and the treatment of the data appears in light gray boxes. Three tests were run to assess the quality of the data for each quadruplicate. First the strains that did not grow were filtered out using the median quadruplicate intensity. Then the remaining strains (each quadruplicate) had to pass one of the 2 following test: (1) the mean of the difference is greater than 2 times the standard deviation in the quadruplicate, or (2) the mean intensity for each media is greater than 3 times the standard deviation in the quadruplicate. If both quadruplicates passed, ratios were calculated in log 2, averaged and the resulting value standardized for clustering.

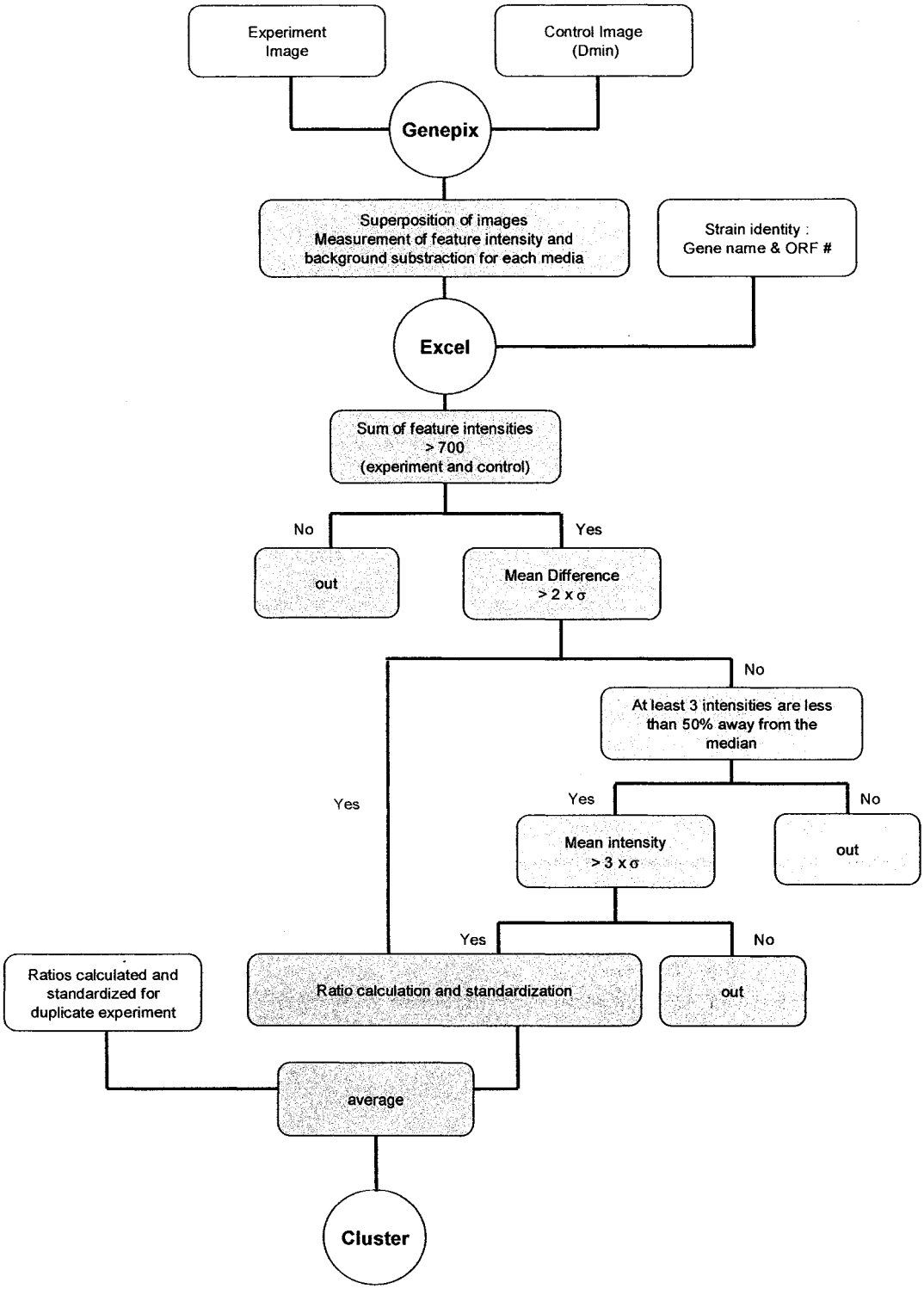
Experiment Image
Control Image (Dmin)
Genepix
Superposition of images
Measurement of feature intensity and background substraction for each media
Strain identity : Gene name & ORF #
Excel
Sum of feature intensities > 700 (experiment and control)
No
Yes
out
Mean Difference > 2 x σ
No
At least 3 intensities are less than 50% away from the median
Yes
No
Yes
Mean intensity > 3 x σ
out
Yes
No
Ratios calculated and standardized for duplicate experiment
Ratio calculation and standardization
out
average
Cluster

Since each strain was replicated a minimum of 8 times per assay plate, Microsoft Excel® was used to calculate the final ratio of each strain as well as the parameters allowing the selection of the strains.

In order to increase the confidence in the results obtained, three tests were run to access the quality of the data for each quadruplicate (Fig.11). First the strains that did not grow on both media were filtered out using the intensity of the quadruplicate. Based on the intensity values and histogram distribution of the blanks (where no cells were spotted) the strains that produced median brightness values not significantly above background brightness (sum of the median intensity lower than 700) were not used for further analysis.

The remaining quadruplicates had to pass one of the 2 following test: (1) the mean of the difference was greater than 2 times the standard deviation in the quadruplicate, or (2) the mean intensity for each media was greater than 3 times the standard deviation in the quadruplicate. Just prior to the second test each feature was controlled for the two intensities (red and green) to check if the values were more than 50% apart from the median intensities of the quadruplicate. Only one feature per quadruplicate was allowed to fall in that category, and was not taken into account to run the test. When more than one feature was in that case the second test was not run. Finally the test results for the quadruplicate corresponding to the same strain were compared. The ratios were calculated only if more than half the quadruplicates were retained for the same strain (2 on 2, or 4 on 6).

In order to calculate the ratio, features with negative brightness intensities, due to background subtraction, were removed from the data set. The intensity ratios of the

control versus experimental conditions were calculated and converted to log base 2 for each quadruplicate spots. The median ratio of the selected quadruplicate was then averaged for each strain.

A control sample composed of 10 strains that did not show a phenotype in the first screening, was treated identically and used to standardize the brightness ratios obtained. The standardization method allowed growth comparisons of each strain to the control strains under each condition tested. It was then also possible to compare the ratios obtained from the different conditions tested. The distribution of the ratio values of the control strains was checked for normality, and the mean and standard deviations were then used to standardize the other ratios obtained in the experiment.

The following formula was applied:

$$t = \frac{x_o - \overline{x_s}}{s_s}$$

where t is the standardized ratio

x_o is the observed ratio

$\overline{x_s}$ is the mean of the control sample

s_s is the standard deviation of the control sample

Finally the standardized ratios of each strain were averaged between the two bioassay plates printed for each of the 10 media included in this study.

Based on the set of data obtained the values greater than +3 or lower than -3 were considered as significant, that is, ratios that is more than 3 standard deviations from the average of the control strains.

2.4 Databases

The function of a gene was assigned according to the SGD (*Saccharomyces* Genome Database) (Issel-Tarver *et al.*, 2002), and MIPS (Mewes *et al.*, 2002) databases. A gene belonging to more than one functional category was arbitrarily assigned to a simple functional category based on published articles.

2.5 Clustering

Hierarcherical clustering analysis was done on strains with standardized ratio greater +3 or lower than -3. The ratios that did not pass the test were omitted (Fig.12). This was done using Cluster and Tree View created by Michael Eisen at the University of Stanford, California, U.S.A. (Eisen *et al.*, 1998) and freely available to download at the following web link:

http://rana.lbl.gov/EinsenSoftware.htm

Hierarchical clustering is produced using a pair-wise distance matrix. The algorithm searches the distance matrix for strain pairs that have the smallest distance between them and then merges these two genes into a cluster. The distance matrix is then recalculated to take into account the new cluster as well as the strains not clustered. The hierarchical average linkage algorithm operates by iteratively merging the genes or gene clusters with the smallest distance between them followed by an updating of the pair-wise matrix. In average linkage, when two genes are clustered, the distance of the other genes and gene clusters to this new cluster is based on the midpoint of the new cluster.

3. Results

3.1. Screen for strains that showed a growth phenotype on Gmin.

I wanted to identify the set of yeast genes that were important for growth with glycine as the sole nitrogen source. For this, the complete set of homozygous diploid deletion strains was screened to identify mutants that had a growth phenotype on Gmin medium. Figure 14 shows the corresponding Dmin and Gmin omnitray plates where a subset of the arrayed strains was replicated. Included within this subset are, five strains, the Δ*gcv3*, Δ*pep12*, Δ*hfa1*, and Δ*snf2* strains, that produced a visible growth defect phenotype on Gmin medium but not on Dmin (G- phenotype). In Figure 15, the $\log_2$ ratio (Y axis) for all the 4700 strains (X axis) was plotted where each strain was ranked in order from the lowest to the highest $\log_2$ ratio. These results show that the $\log_2$ ratio exhibited by the vast majority of the strains did not differ significantly from zero, indicating that most of the strains in the yeast homozygous deletion set did not display a growth phenotype on Gmin media compare to Dmin. Therefore most yeast genes were equally important for growth on Gmin and Dmin media. Since $\log_2$ ratios of +1 and -1 coincided with the inflexion points at the extremities of the curve in Figure 15, and these ratios correspond to a two-fold growth difference between the two media, strains with $\log_2$ ratios less than -1 and greater than +1 were selected for more detailed analysis. Using these cutoffs 321 strains were retained from the primary screen for further analysis. Of these, 250 strains exhibited a growth defect on Gmin compared to Dmin (G- phenotype) (Annex 1) and 71 strains showed a growth defect on Dmin compared to Gmin or/and improved growth on Gmin (G+ phenotype) (Annex 2).

Figure 14. Screening for growth phenotypes associated with the use of glycine as the sole nitrogen source. **a)** Each strain of the homozygous diploid deletion set (4700 strains in total) was spotted three times side by side on Dmin and Gmin agar media. In most cases the strains grow on both media. Some strains, for example, Δgcv2, Δpep12, Δhfa1 and Δsnf2, as seen by comparing their growth under the control and the test condition, exhibited obvious growth defects on G min media (boxed in dashed lines). The empty spots corresponding to the footprint of each plate of the deletion set are boxed in by continuous lines. The spot that was used as a reference by the software for the measurement of brightness is encircled at the left bottom. **b)** Enlarged image of the region where Δgcv2 strain was replicated.

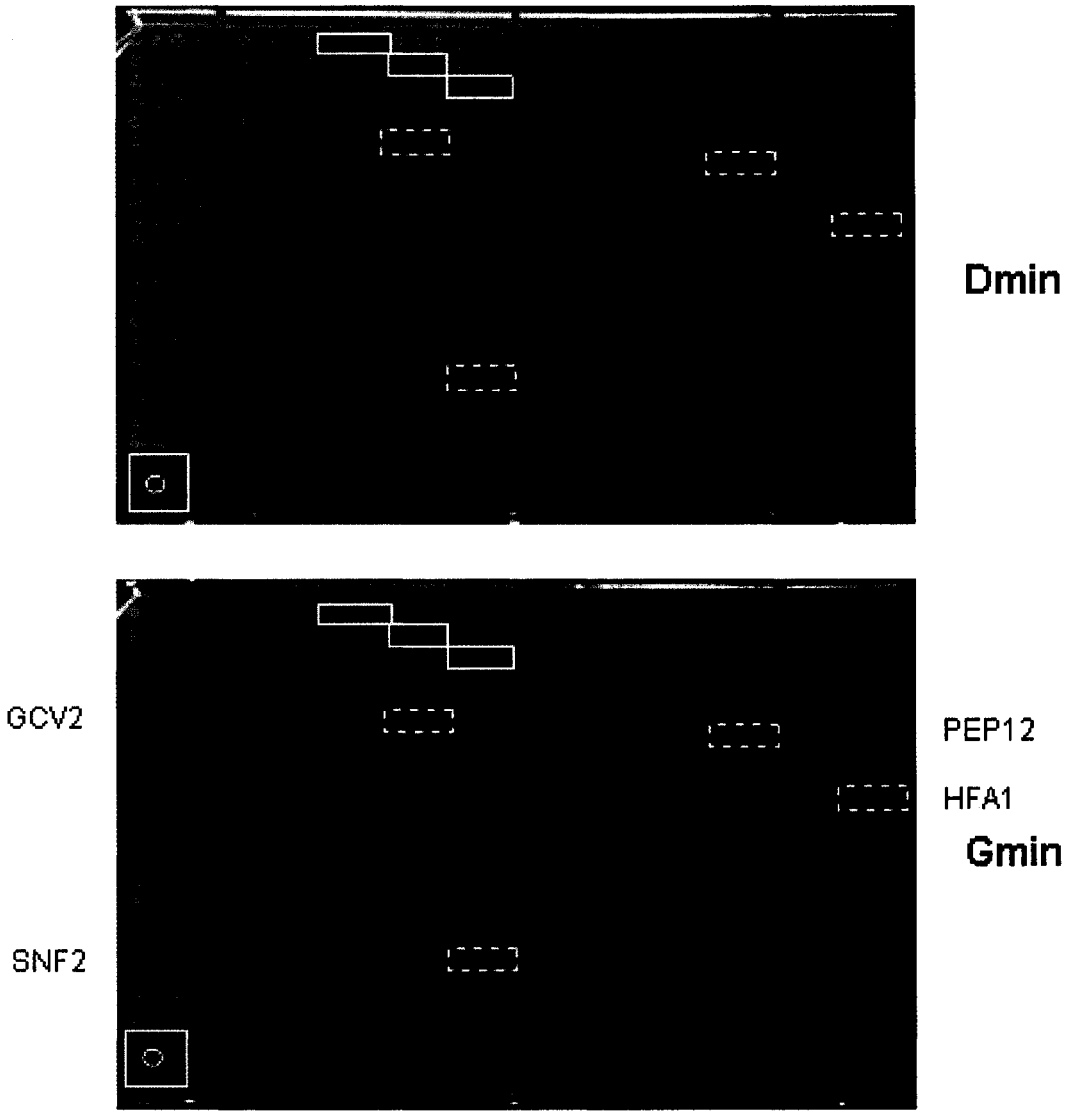

a)

b)

Figure 15. Gm/Dm ratios for the complete diploid deletion set, expressed in $\log_2$. The strains (X axis) are ranked in ascending order of their ratios in $\log_2$ (Y axis). Strains showing a $\log_2$ ratio lower than -1 (250 strains at the left of the graph) or greater than +1 (71 strains at the right of the graph) were arbitrarily selected for further analysis.

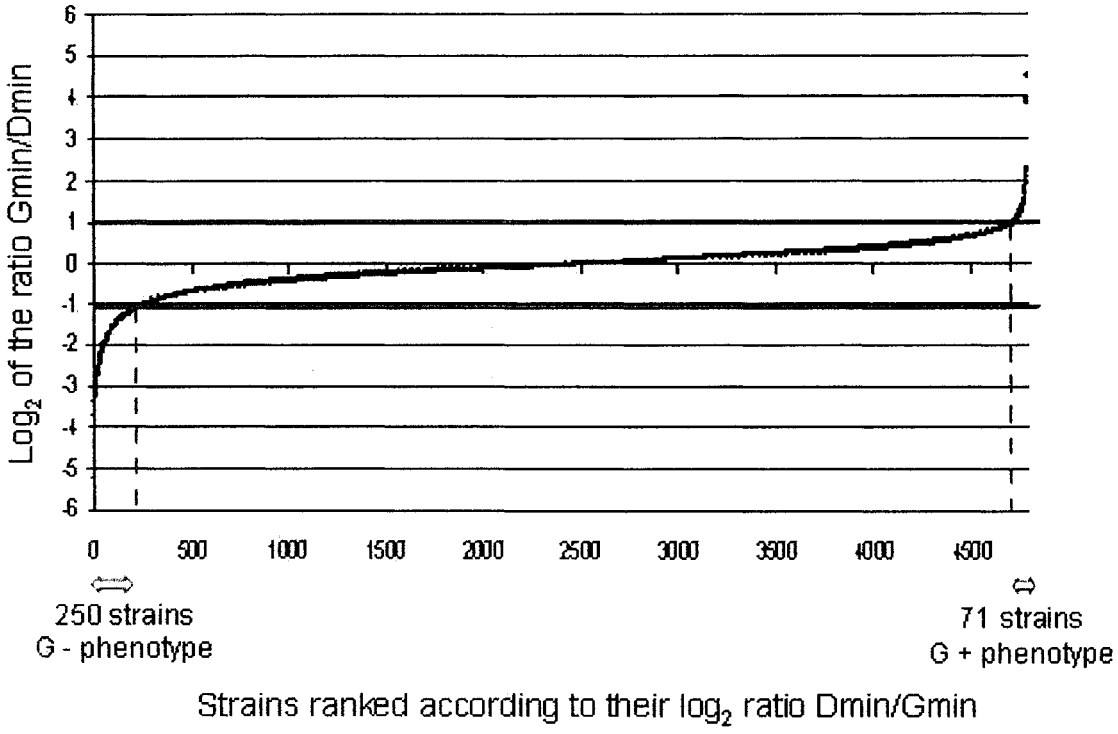
6
5
4
3
2
1
0
-1
-2
-3
-4
-5
-6
Log2 of the ratio Gmin/Dmin
0
500
1000
1500
2000
2500
3000
3500
4000
4500
250 strains
G - phenotype
71 strains
G + phenotype
Strains ranked according to their log2 ratio Dmin/Gmin

The genes encoding subunits of the glycine cleavage system are known to be essential for the catabolism of glycine (Sinclair and Dawes, 1995). In order to perform a preliminary assessment of the primary screen, I checked to see whether the screen identified the four deletion strains unable to encode the four glycine cleavage system subunits. The *Δgcv1*, *Δgcv2*, and *Δgcv3* strains exhibited a G- phenotype. The *Δlpd1* strain however did not show a G- phenotype. The *LPD1* deletion strain was expected to show a G- phenotype but its Gm/Dm $\log_2$ ratio of 0.86 was above the arbitrary threshold used to select strains with a G- phenotype. This may be due to the fact that the *Δlpd1* strain grew poorly on Dmin agar media. The relative growth rate on Dmin media was found to be 0.60 and 0.33 on Gmin media. This more general growth defect is probably due to the participation of Lpd1p in two other multienzymatic complexes, pyruvate dehydrogenase and 2-oxaloacetate dehydrogenase (Sinclair and Dawes, 1995).

Lipoic acid is an essential coenzyme of the glycine cleavage system. The *LIP5* and *LIP2* genes are involved in lipoic acid metabolism (Sulo and Martin, 1993; Marvin *et al.*, 2001). The *LIP5* gene encodes for a lipoic acid synthase specifically involved in lipoic acid synthesis and *LIP2* codes for a lipoic acid ligase responsible for the attachment of this prosthetic group to the H-subunit of the glycine cleavage system and to pyruvate dehydrogenase (Marvin *et al.*, 2001). Therefore, the two genes *LIP5* and *LIP2* are directly linked to glycine catabolism and mutants unable to express functional Lip5p or Lip2p are expected to lack functional glycine cleavage system activity. This was confirmed by the primary screen where the *Δlip2* and *Δlip5* strains produced $\log_2$ ratios of -1.06 and -1.60, respectively.

The transcription factor Bas1p is also important for glycine cleavage activity (Zheng, 1995). The transcription of the *GCV1*, *GCV2* and *GCV3* genes is highly dependent upon Bas1p. However the corresponding deletion strain gave a $\log_2$ ratio of -0.67 and therefore it was not included in the set of G- strains retained from the primary screen. This was also due to the fact that the *Δbas1* strain grew poorly in the control condition (relative growth rate on Dmin: 0.57).

SER1 encodes a phosphoserine transaminase implicated in the synthesis of serine from 3-phosphoglycerate (Mewes *et al.*, 2002). *SER1* deletion mutants have been shown to form heavily grown colonies on Gmin plates after 2 days (Piper *et al.*, 2000). The Δ*gly1* strain is prototrophic for glycine but grows at a reduced rate (MIPS) (Mewes *et al.*, 2002). Therefore *Δser1* and *Δgly1* were expected to exhibit a G+ phenotype in this study. *ADE3* encode the cytoplasmic C1-tetrahydrofolate synthase. The deletion strains was also expected to form a heavily grown colony (Piper *et al.*, 2000) but was not found in this screen.

The gene deleted in each of the 321 strains retained from the primary screen was assigned to a functional category (Fig.16). This was done using the MIPS database and published articles. Among the genes associated with strains displaying a G- phenotype, about 25% do not have an assigned function. About 19% of the strains are involved in metabolism, 4.4% in C-compound metabolism, 4.4% in lipid fatty acid metabolism, 4.4% in amino acid metabolism. About 10% are involved in transcription and, 10% in cellular transport with 8% in vacuolar or vesicular transport. The MIPS database indicated that 15% of the proteins are localized in the nucleus 13% in the mitochondria, and 8% in the vesicular, endosomal or vacuolar membrane for 21, 14 and 2% respectively in the whole

Figure 16. Functional classification of the deleted genes associated with strains that had a growth phenotype. Genes associated with strains displaying a G- phenotype (Panel A) and Genes associated with strains displaying a G+ phenotype (Panel B). The function of the deleted gene was assigned using to the MIPS database. Genes belonging to more than one functional category were arbitrarily assigned to one of them based on published articles.

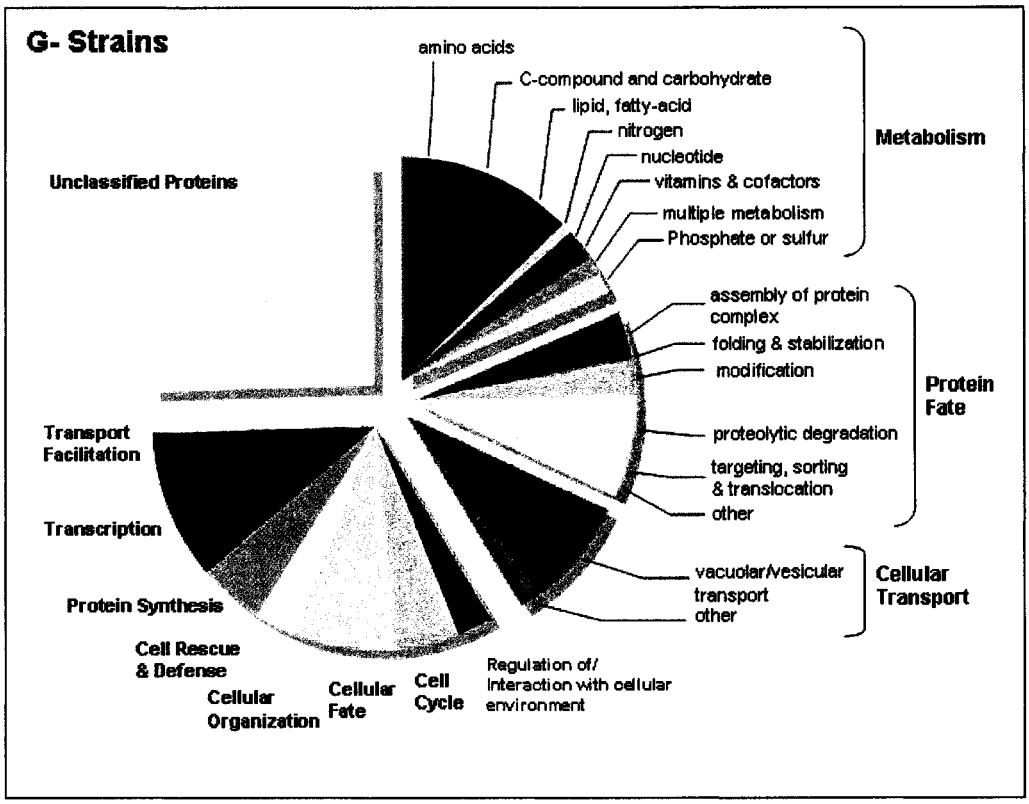
G- Strains
amino acids
C-compound and carbohydrate
lipid, fatty-acid
nitrogen
nucleotide
vitamins & cofactors
multiple metabolism
Phosphate or sulfur
Metabolism
Unclassified Proteins
assembly of protein complex
folding & stabilization
modification
proteolytic degradation
targeting, sorting & translocation
other
Protein Fate
Transport Facilitation
Transcription
vacuolar/vesicular transport
other
Cellular Transport
Protein Synthesis
Cell Rescue & Defense
Cellular Organization
Cellular Fate
Cell Cycle
Regulation of/ interaction with cellular environment

a)

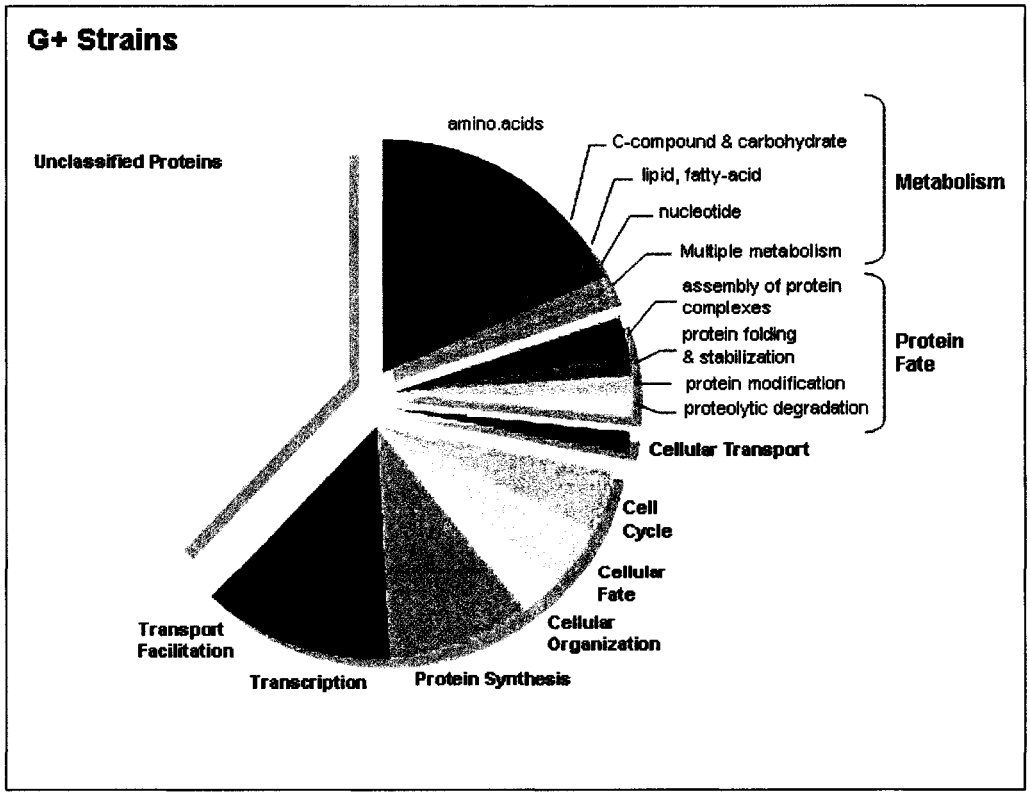
G+ Strains
amino.acids
C-compound & carbohydrate
lipid, fatty-acid
nucleotide
Multiple metabolism
Metabolism
Unclassified Proteins
assembly of protein complexes
protein folding & stabilization
protein modification
proteolytic degradation
Protein Fate
Cellular Transport
Cell Cycle
Cellular Fate
Cellular Organization
Transport Facilitation
Transcription
Protein Synthesis

b)

yeast genome. For the genes associated with strains that displayed a G+ phenotype, about 38% do not have an assigned function, about 20% are involved in metabolism with 14% involved in amino acid metabolism and 10% are involved in protein synthesis with 7% located in the mitochondria. In addition about 14% of the genes encode proteins that are localized to the mitochondria which represent a similar proportion than for the G- strains.

3.2. Detailed phenotypic characterization

The G+ and G- strains, identified in the primary screen, were further characterized using a high density colony array. In order to accomplish this task five master plates were assembled. Three of the 96-well master plates contained the 250 G- strains (1.a.1, 2, 3), one plate contained the G+ strains (1.b.1) and a fifth plate contained the 10 growth control strains (1.c.1) (Table 1). In the master plate containing the control strains, each strain was present either eight or sixteen times. To facilitate identification of the plates, some wells were left empty in each plate, with the exception of the control plate. Two criteria were used to select the ten control strains: first the control strains did not display a growth phenotype in the primary screen (*ie*: all ten strains had an average relative growth rate between 0.96 and 1.04 for both media and their Gm/Dm $\log_2$ ratios were between -0.02 and +0,02), and secondly, the deleted, ORF had to be an ORF without an assigned MIPS function or a known phenotype.

Table 1. Control strains for high density colony array

position in the original yeast deletion library							
Plate	**Row**	**Column**	**ORF**	**relative growth on Gm**	**relative growth on Dm**	**ratio Gm/Dm**	**Log2 Gm/Dm**
324	H	3	YBL055C	0.97	0.96	1.00	0.01
309	E	1	YBR174C	0.98	0.98	1.00	0.00
321	E	9	YDR222W	1.13	1.13	0.99	-0.01
319	C	9	YJL178C	1.02	1.03	1.00	-0.01
321	G	2	YJR030C	1.04	1.03	1.01	0.01
317	G	4	YKL171W	1.04	1.04	1.00	0.00
316	A	9	YLR171W	1.06	1.06	1.00	0.01
331	B	8	YMR103C	1.00	0.99	1.01	0.01
344	F	2	YPR022C	1.03	1.03	1.00	0.00
344	F	10	YPR064W	0.98	0.98	1.00	0.00

3.2.1. Verification of the method

The 321 strains, determined to have a growth phenotype on Gmin, were subjected to further phenotypic analysis using high density colony arrays. For these arrays, the strains were spotted on various bioassay plates and after growth for different lengths of time, the plates were scanned and the images obtained were analyzed with GenePix software. This microarray software allows one to work with scanned images of the plates, giving the mean of the brightness intensity of the feature subtracted by the median of the local background. Each plate was organized in 6 blocks, with the G- strains in the upper 2 blocks, the G+ strains in the lower two blocks and the control strains in the middle 2 blocks (Fig.17). Each experimental condition plate was compared with a Dmin plate. The relative pixel intensity of each feature was converted to false color images, where red was assigned to features from the control condition plates and green was assigned to features on the various experimental condition plates.

The mean brightness intensity obtained for each feature (before background subtraction) was about 22,000 whereas background intensity was approximately 20,000. The background represented a large portion of the signal. Therefore it was important to assess if the local subtraction carried out by the software resulted in values that were accurately subtracted. The distributions of the intensity values for the blanks and for the spotted control strains on a Dmin plate were compared. After background subtraction the mean of the blanks was 200 and the mean of the control population was about 1200 (Fig.18). More importantly, the two distributions did not overlap and were separated by about 600 intensity units. The software subtracts the median background-pixel intensity

Figure 17. Overlapped false color images of bioassay dishes. This image was generated using GenePix microarray software. Strains selected in the first screening for altered growth on Gmin compared to Dmin (G- and G+) were arrayed in quadruplicate in a square pattern. **a)** 6 blocks were spotted on each bioassay plate with a vertical symmetry. The G- strains were located on the two upper blocks (1 and 2), the control strains in the middle blocks (3 and 4) and the G+ strains on the lower blocks (5 and 6). Red was assigned to the control media (Dmin) and green to the experimental media (Gm). As expected, the majority of the G- strains appear red, the control strains appear yellow and the G+ strains appear green. **b)** Enlarged image of G-, control and G+ groups of strains.

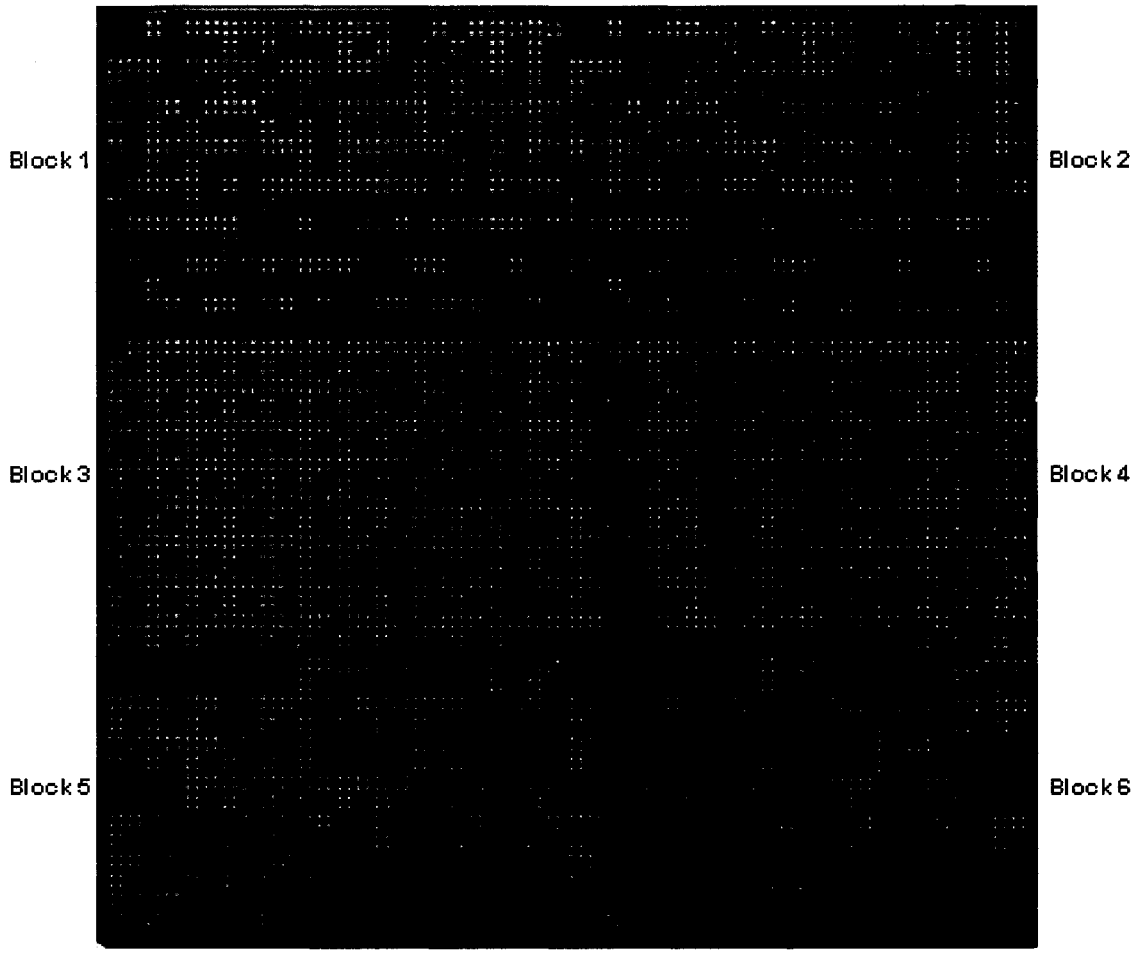
Block 1
Block 2
Block 3
Block 4
Block 5
Block 6

a)

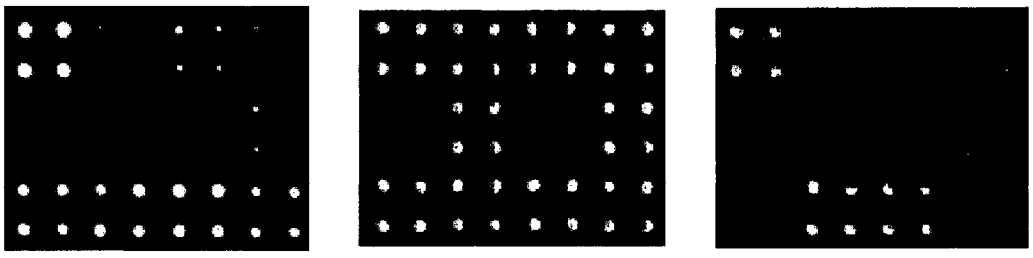
G- phenotype
control
G+ phenotype

b)

Figure 18. Histogram of the intensity signals associated with the blank features (no cells spotted) and the control strain features for one of the Gmin bioassay plates. The intensity signal for each feature was determined by taking the mean of the pixel intensities within each feature and substracting the median intensity of the background surrounding each feature. The two distributions did not overlap, they were separated by a region of about 600 intensity units and their means are separated by 2000 intensity units.

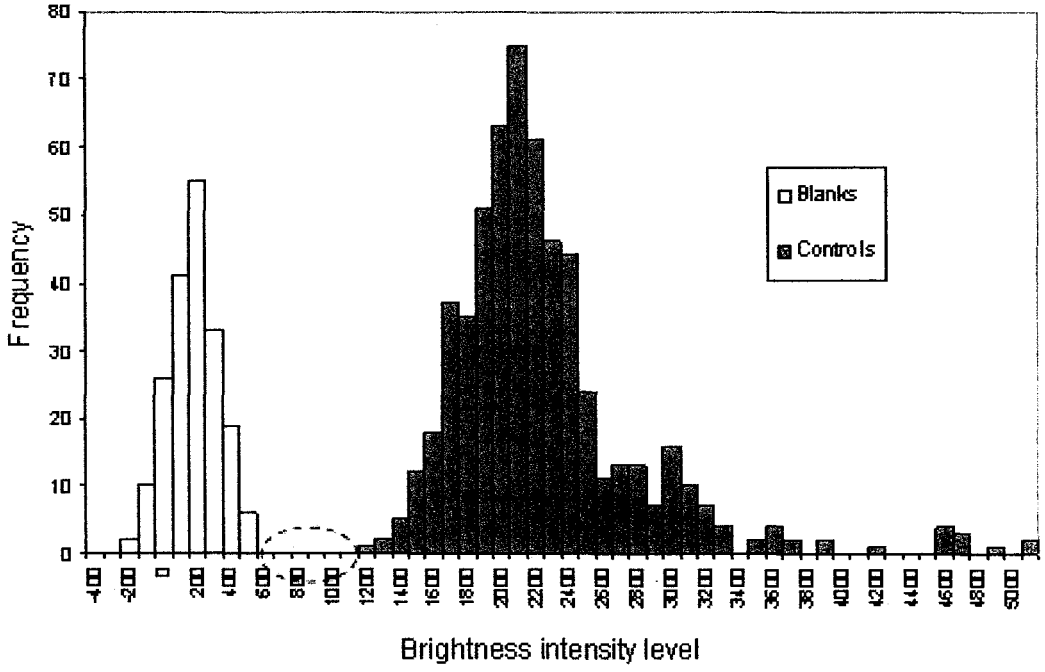
Frequency
Brightness intensity level
Blanks
Controls

from the mean feature-pixel intensity. This background-subtraction method tends to slightly increase the intensity values for both blank and experimental features. This explains why the histogram showing the distribution of feature intensities for the blanks is not centered upon 0 (Fig.18). For consistency it might be expected to use the mean background intensity instead of the median background intensity when using the mean feature intensity. However, the median is less affected by extremely low and high values, therefore it is a more reliable value for the background. The few intensity values that laid on the right of the control strains intensity distribution correspond to colonies located on the edge of the blocks where there was less competition for nutrients. Yet this effect was corrected for by the fact that each strain was always replicated to the same relative positions on all the bioassay plates. Therefore, nutrient competition effects should be similar on both the test condition and control condition bioassay plates.

It was important to know how reproducible the measurements of relative growth rates were. To accomplish this, the average growth intensities of all the G-, G+ and control strains on two Dmin plates spotted in the same experiment from a single set of master plates were compared. A correlation plot (Fig.19) was generated using the average intensity values obtained for all the spots coming from the same colony in the 384-master plate. Regression analysis gave a trend-line with a slope of 0.99 which was very close to the theoretical value of 1 and the regression coefficient of 0.92 was acceptable.

Figure 19. Correlation graph using two Dmin Bioassay dishes. Plotted data corresponds to the intensity calculated by averaging the median of 2 corresponding quadruplicates (spotted from the same colony on the master plate). The slope obtained was 0.99, which is very close to the expected theoretical value of 1. The correlation coefficient was equal to 0.92 which was acceptable. This confirmed that the two plates of arrayed strains were similar in their printing and thus suitable for comparison.

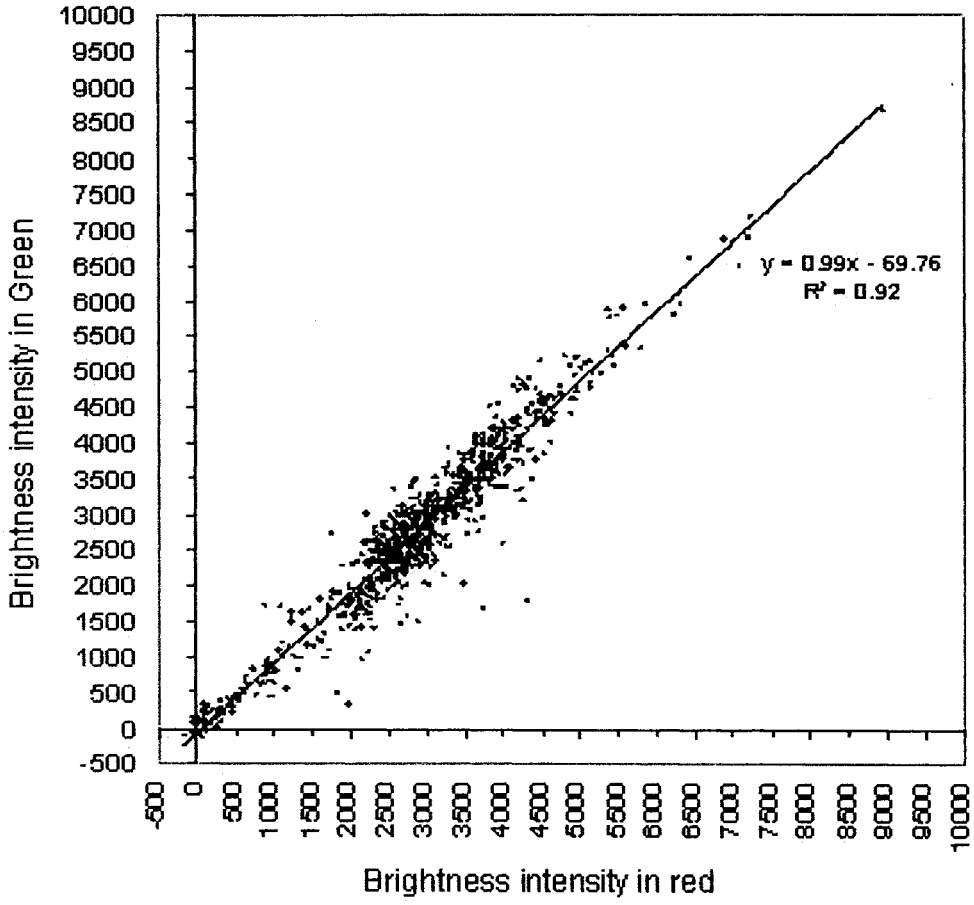
Brightness intensity in Green
Brightness intensity in red
y = 0.99x - 69.76
R² = 0.92
10000
9500
9000
8500
8000
7500
7000
6500
6000
5500
5000
4500
4000
3500
3000
2500
2000
1500
1000
500
0
-500
-500
0
500
1000
1500
2000
2500
3000
3500
4000
4500
5000
5500
6000
6500
7000
7500
8000
8500
9000
9500
10000

It was also important to show that regardless of the growth condition used, all the control strains grew equally well. To test this, the control blocks present on all the assay plates were submitted to the following analysis. The $\log_2$ ratio averages and standard deviations were determined for each control strain in each media (Fig.20). To facilitate the comparison between the different conditions the average of each strain was subtracted by the average of all the strains. The standard deviations indicate that there was no significant difference between the control strains. In order to apply the standardization the normality of the distribution of the average $\log_2$ ratio obtained for each quadrupliquet of the control strains was also verified (Fig.21).

3.2.2. Selection of the strains

The 321 strains identified as having a growth phenotype in the primary screen were subjected to further analysis using the high density colony array method. For this the phenotype of each strain was assessed by comparing its growth on Dmin control media with its growth on each of the ten test media. Media composition in the experimental conditions differs from the control condition with regard to, the supplements added, the concentration of glycine, the nitrogen source or the carbon source. Strains with a standardized values greater than +3 or less than -3 on Gmin compared to Dmin were retained and subjected to clustering analysis. That is, strains with a $\log_2$ ratio more than three standard deviations from the average $\log_2$ ratio of the control strains.

Figure 20. Control strains average growth for the 10 conditions tested. The average $\log_2$ ratio (Y axis) of the 10 control strains is represented for each condition tested (X axes). For each strain the data were filtered in the same manner as the experimental data. In order to facilitate the comparison between the media tested the average of each strain was subtracted by the average of all the strains in the condition tested. The vertical bars represent the standard deviation calculate for the strain in this condition. The deletion strains are represented in the same order for each media: *Δybl055c*, *Δybr174c*, *Δydr222w*, *Δyjl178c*, *Δyjr030c*, *Δykl171w*, *Δylr171w*, *Δymr103c*, *Δypr022c*, *Δypr064w*.

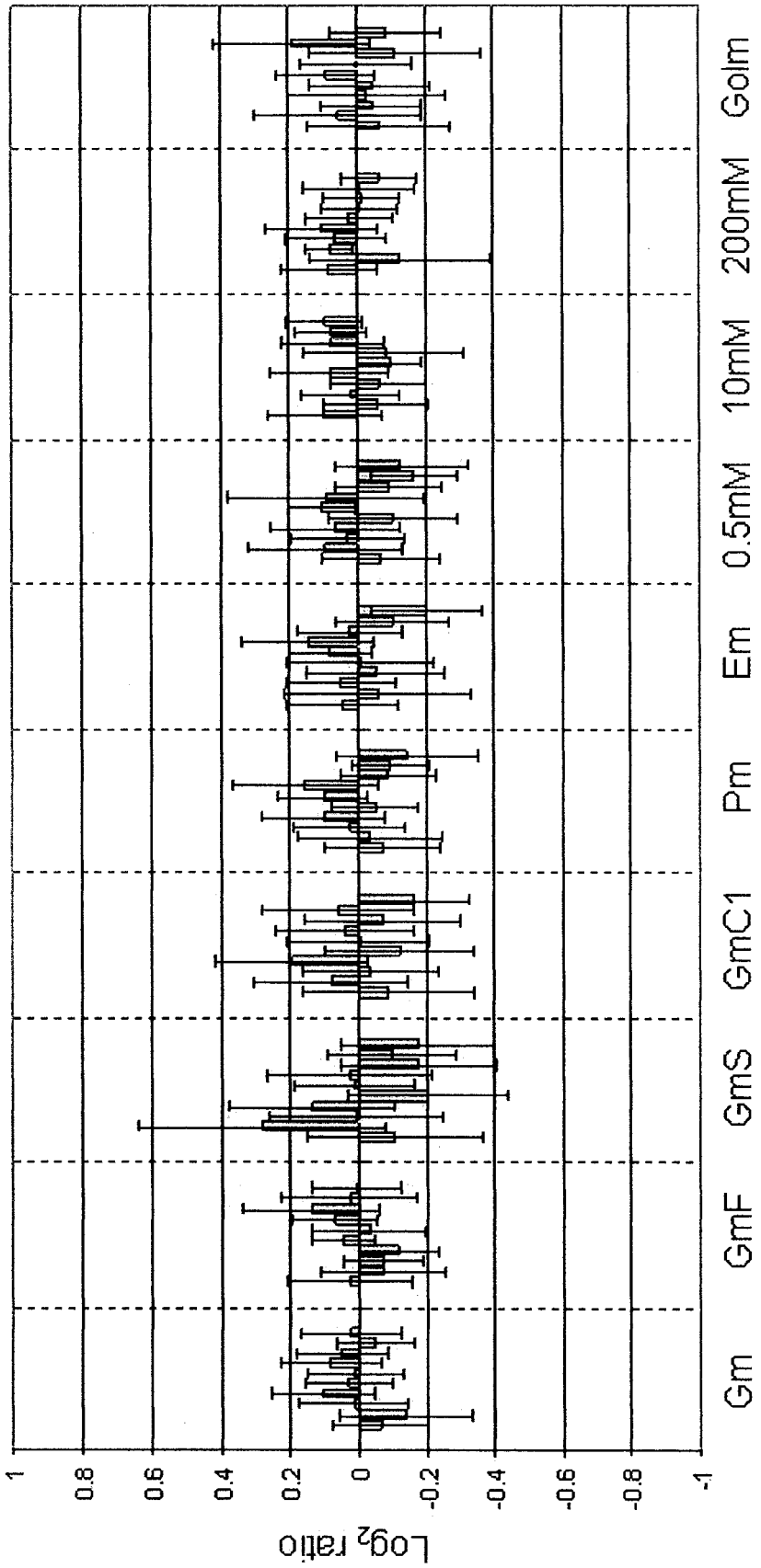
Log2 ratio
1
0.8
0.6
0.4
0.2
0
-0.2
-0.4
-0.6
-0.8
-1
Gm
GmF
GmS
GmC1
Pm
Em
0.5mM
10mM
200mM
Golm

Figure 21. Histogram distribution of the $\log_2$ ratios obtained for the control strains. The distribution obtained for the control strains was a normal distribution: thus it could be used for the standardization of the experimental ratios. Similar results were obtained for the other experimental conditions tested.

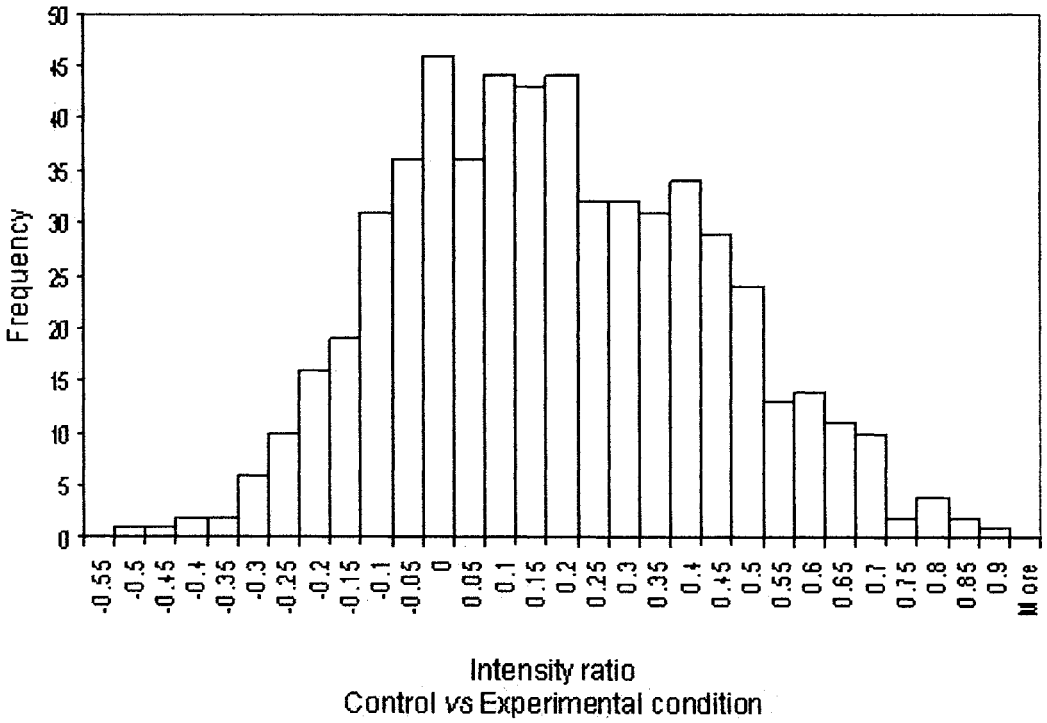
Frequency
50
45
40
35
30
25
20
15
10
5
0
-0.55
-0.5
-0.45
-0.4
-0.35
-0.3
-0.25
-0.2
-0.15
-0.1
-0.05
0
0.05
0.1
0.15
0.2
0.25
0.3
0.35
0.4
0.45
0.5
0.55
0.6
0.65
0.7
0.75
0.8
0.85
0.9
More
Intensity ratio
Control vs Experimental condition

3.2.3. Clustering analysis of the media

The horizontal dendrogram depicting relationships between the 10 test media (Fig.22) shows that the five media with high concentrations of glycine (the four Gmin based media and the Dmin + 200mM glycine media) form one group. The next clustering level shows that the Dmin +10mM glycine media clusters most closely to this group. Indeed the glycine concentration of 10mM has been shown to elicit a glycine response (Dawes et al., 1995; Zheng master thesis). The two media containing either proline or glutamate as the sole nitrogen source form a distinct cluster. Clearly Dmin + 0.5mM, which contains the lowest concentration of glycine, is the media closest to the Dmin reference media. The dendrogram confirmed that, the global effect on the set of genes tested was more similar when the media were related in their compositions.

3.2.4. Strains with G- phenotype

3.2.4.1. Glycine catabolism genes

The genes that were previously used as controls: *GCV1*, *GCV2*, *GCV3*, *LIP2* and *LIP5* were confirmed, presenting a clear glycine catabolism deficient phenotype (Fig.23 panel A). The hypothetical ORF *YAL046C* belong to a cluster close to *GCV1* and *GCV2*. The putative encoded protein does not have strong similarity to any characterized protein, but it is interesting to note that this ORF is adjacent to the *GCV3* ORF and separated from it by less than 600bp. The deletion of this ORF may interfere with the regulation of *GCV3* transcription and therefore, it may result in the observed pattern.

Figure 22. Clustering of strains with a growth phenotype on Gm Media. The 107 strains were hierarchically clustered across all experiments using the program Cluster and visualized in TreeView (http://rana.lbl.gov/EinsenSoftware.htm). Similarity between growth patterns are represented by the vertical dendrogram (left). The horizontal dendrogram (top) represents the similarity between the various experimental conditions. Red color blocks represents strains with relatively better growth in Dm than the condition tested, whereas green blocks represents strains with relatively better growth on the tested condition than on Dm media. Gray corresponds to data that were not retained during the analysis process. Strains are indicated by the name of the deleted gene. The two columns on the far right indicate the function of the genes. Gene functions were assigned according to the MIPS database and from publications. Red and blue color text indicates that the gene product is localized to the mitochondrial or vacuolar compartment respectively. Abbreviations used for the gene functional categories are: CC: Cell cycle, CF: Cell Fate, CR: Cell Rescue defence and virulence, CT: Cellular Transport, MT:Metabolism, PF: Protein Fate, PS: Protein Synthesis, RI: Regulation of/Interaction with cellular environment, TC: Transcription, UP: Unknown Protein. Abbreviation used for the media: 0.5mM: Dmin + 0.5mM glycine, 10mM: Dmin + 10mM glycine, 200mM: Dmin + 200mM glycine, Emin: Glutamate min, Gmin: Glycine min, GminC1: Glycine min + C1 end products, GminF: Glycine min + Formate, Golmin: Glycerol min, GminS: Glycine min + Serine, Pm: Proline min.

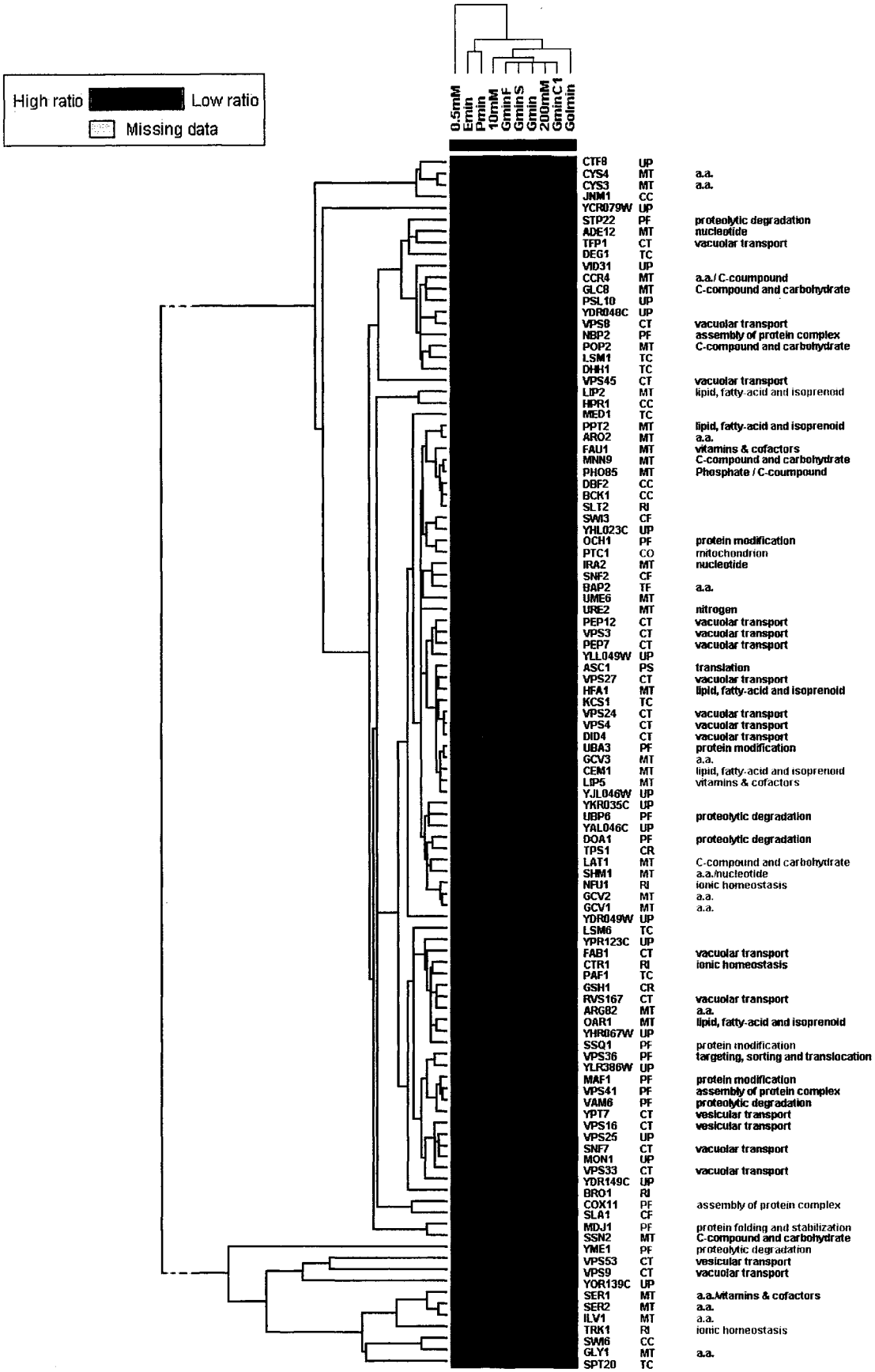
High ratio
Low ratio
Missing data
0.5mM
Emin
Pmin
10mM
GminF
GminS
Gmin
200mM
GminC1
Golmin
CTF8 UP
CYS4 MT a.a.
CYS3 MT a.a.
JNM1 CC
YCR079W UP
STP22 PF proteolytic degradation
ADE12 MT nucleotide
TFP1 CT vacuolar transport
DEG1 TC
VID31 UP
CCR4 MT a.a./ C-coumpound
GLC8 MT C-compound and carbohydrate
PSL10 UP
YDR048C UP
VPS8 CT vacuolar transport
NBP2 PF assembly of protein complex
POP2 MT C-compound and carbohydrate
LSM1 TC
DHH1 TC
VPS45 CT vacuolar transport
LIP2 MT lipid, fatty-acid and isoprenoid
HPR1 CC
MED1 TC
PPT2 MT lipid, fatty-acid and isoprenoid
ARO2 MT a.a.
FAU1 MT vitamins & cofactors
MNN9 MT C-compound and carbohydrate
PHO85 MT Phosphate / C-coumpound
DBF2 CC
BCK1 CC
SLT2 RI
SWI3 CF
YHL023C UP
OCH1 PF protein modification
PTC1 CO mitochondrion
IRA2 MT nucleotide
SNF2 CF
BAP2 TF a.a.
UME6 MT
URE2 MT nitrogen
PEP12 CT vacuolar transport
VPS3 CT vacuolar transport
PEP7 CT vacuolar transport
YLL049W UP
ASC1 PS translation
VPS27 CT vacuolar transport
HFA1 MT lipid, fatty-acid and isoprenoid
KCS1 TC
VPS24 CT vacuolar transport
VPS4 CT vacuolar transport
DID4 CT vacuolar transport
UBA3 PF protein modification
GCV3 MT a.a.
CEM1 MT lipid, fatty-acid and isoprenoid
LIP5 MT vitamins & cofactors
YJL046W UP
YKR035C UP
UBP6 PF proteolytic degradation
YAL046C UP
DOA1 PF proteolytic degradation
TPS1 CR
LAT1 MT C-compound and carbohydrate
SHM1 MT a.a./nucleotide
NFU1 RI ionic homeostasis
GCV2 MT a.a.
GCV1 MT a.a.
YDR049W UP
LSM6 TC
YPR123C UP
FAB1 CT vacuolar transport
CTR1 RI ionic homeostasis
PAF1 TC
GSH1 CR
RVS167 CT vacuolar transport
ARG82 MT a.a.
OAR1 MT lipid, fatty-acid and isoprenoid
YHR067W UP
SSQ1 PF protein modification
VPS36 PF targeting, sorting and translocation
YLR386W UP
MAF1 PF protein modification
VPS41 PF assembly of protein complex
VAM6 PF proteolytic degradation
YPT7 CT vesicular transport
VPS16 CT vesicular transport
VPS25 UP
SNF7 CT vacuolar transport
MON1 UP
VPS33 CT vacuolar transport
YDR149C UP
BRO1 RI
COX11 PF assembly of protein complex
SLA1 CF
MDJ1 PF protein folding and stabilization
SSN2 MT C-compound and carbohydrate
YME1 PF proteolytic degradation
VPS53 CT vesicular transport
VPS9 CT vacuolar transport
YOR139C UP
SER1 MT a.a.Vitamins & cofactors
SER2 MT a.a.
ILV1 MT a.a.
TRK1 RI ionic homeostasis
SWI6 CC
GLY1 MT a.a.
SPT20 TC

Figure 23. Subclusters and gene growth patterns. The subcluster and the genes are organized in panels according to their functions or phenotype: A) Glycine catabolism genes, B) Vacuolar genes, C) Mitochondrial genes, D) Regulation genes and E) Genes associated with G+ phenotype. The subcluster similarity between growth patterns is represented by the vertical dendrogram. Red color represents stain with relatively better growth in Dm than the condition tested, whereas green represents strains with relatively better growth on the tested condition than on Dm media. Gray corresponds to data that were not retained during the analysis process. Strains are indicated by the name of the deleted gene. The two columns on the far right indicate the function of the genes. Gene function was assigned according to the MIPS database and publications. Red and blue color text indicates that the gene product is localized to the mitochondrial and vacuolar compartment respectively. Abbreviations used for the gene functional categories are: CC: Cell cycle, CF: Cell Fate, CR: Cell Rescue defence and virulence, CT: Cellular Transport, MT:Metabolism, PF: Protein Fate, PS: Protein Synthesis, RI: Regulation of/Interaction with cellular environment, TC: Transcription, UP: Unknown Protein. Abbreviation used for the media: 0.5mM: Dmin + 0.5mM glycine, 10mM: Dmin + 10mM glycine, 200mM: Dmin + 200mM glycine, Emin: Glutamate min, Gmin: Glycine min, GminC1: Glycine min + C1 end products, GminF: Glycine min + Formate, Golmin: Glycerol min, GminS: Glycine min + Serine, Pm: Proline min.

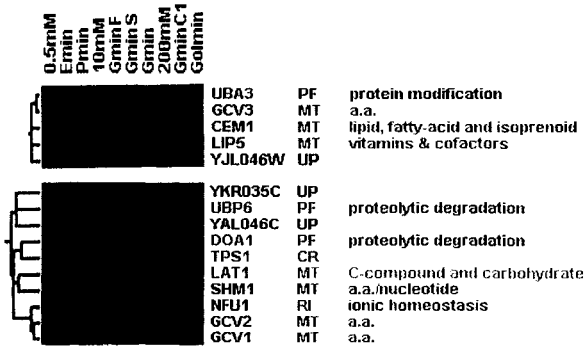

A) Glycine catabolism genes

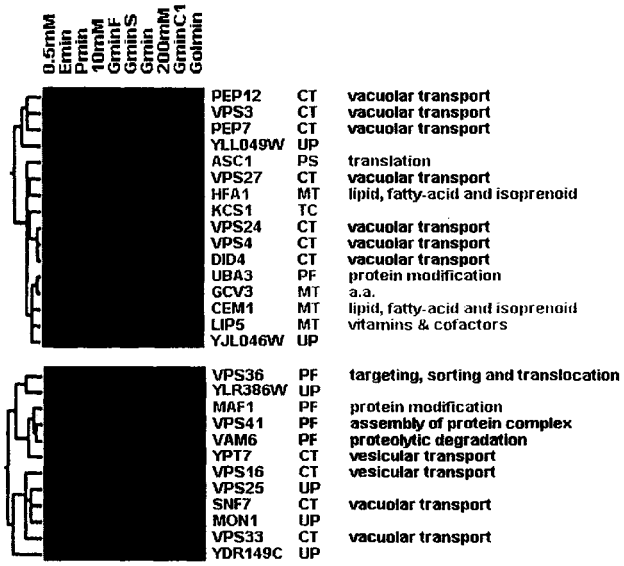

B) Vacuolar genes

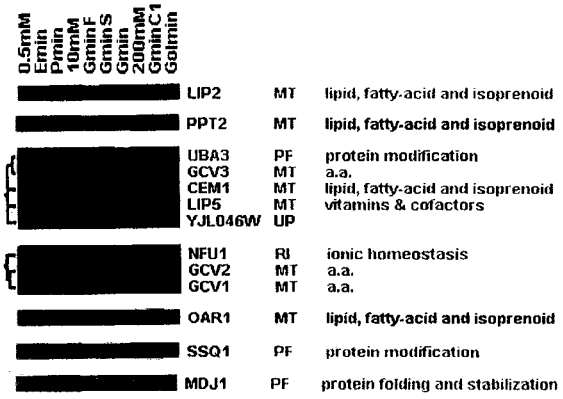

C) Nuclear encoded mitochondrial genes

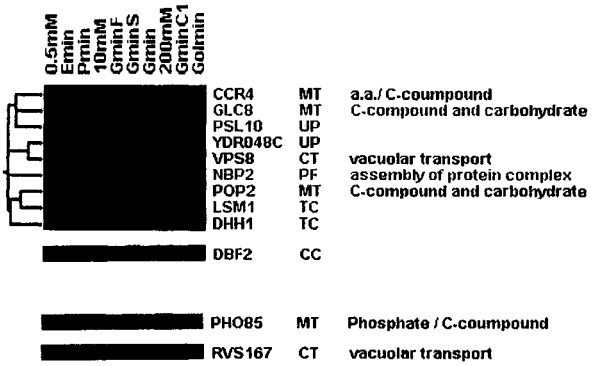

D) Regulatory genes

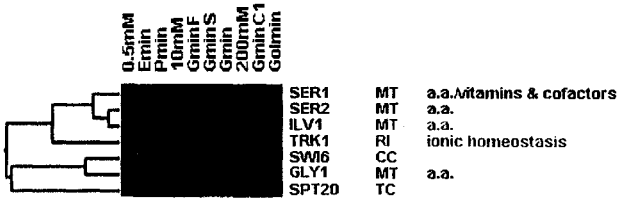

E) Genes associated with G+ phenotype

Another hypothetical ORF *YKR035C* in that group is a dubious ORF but interestingly it overlaps with *DID2* an ORF that encodes a protein with vacuolar function (Fig.23 Panel A). Unlike the Δ*gcv1*and Δ*gcv2* deletion strains, the Δ*gcv3* strain showed a respiratory deficient phenotype and clustered with the Δ*lip5* strain. Interestingly *SHM1* encoding the mitochondrial serine hydroxymethyl transferase clustered close to *GCV1* and *GCV2* genes on the clustering diagram.

3.2.4.2. Gap1p ubiquitination and regulation

GAP1 codes for the general amino acid permease. The absence of the *GAP1* deletion strain in the G- strains identified in the preliminary screen and the presence of *BUL2* and *URE2* (encoding negative regulators of the Gap1p permease) (Stanbrough and Magasanik, 1995) seemed at first problematic. These observations went against the general concept that Gap1p mediates the uptake of amino acids when they are used as primary nitrogen source. However, a study by Chen and Kaiser (2002) demonstrate that in the presence of a high concentration of amino acids, the general amino acid permease Gap1p is directly sorted to the vacuole instead of the plasma membrane. Chen and Kaiser suggest that sorting Gap1p to the vacuole is a control mechanism that evolved to avoid the unchecked import of amino acids into the cell. The necessity of this control seems to result from the toxicity of high intracellular concentrations of most amino acids (Chen and Kaise, 2002). If this is the case, *gap1* deletion strain may not exhibit a growth phenotype on Gmin compare to Dmin and will be more resistant to glycine toxicity. Furthermore, since Gap1p activity is not required for growth on Dmin media, the *Δgap1*

strain will not exhibit a growth phenotype on Dmin. In contrast, strains that cannot reduce the amount of Gap1p localized to the cytoplasmic membrane may be hypersensitive to elevated concentrations of glycine. Consistent with this expectation, deletion of the *URE2*, which prevents transcription of *GAP1* when grown in presence of a preferred nitrogen source (Stanbrough and Magasanik, 1995), resulted in a G- phenotype. The *URE2* deletion strain also showed a growth defect when ammonium sulfate, a preferred nitrogen source, was present if the medium also included high concentrations of glycine. Apparently negative regulation of *GAP1* transcription by Ure2p is required to prevent the accumulation of intracellular glycine from reaching concentrations that are toxic.

Ubiquitination is important in the down regulation of Gap1p. It is a signal required for its sorting to the vacuole and degradation. Mutations in genes required for Gap1p polyubiquitination (*NPI1/RSP5*, *DOA4/NPI2*, *BUL1* and *BUL2*) cause Gap1p to be sorted to the plasma membrane more efficiently (Amerik *et al.*, 2000; Spingael *et al.*, 2002; Spingael *et al.*, 1999; Spingael and Andre, 1999; Soetens *et al.*, 2001). *NPI1* is an essential gene and therefore, it was not present in the screen. *DOA4* and *BUL2* were retained in the preliminary screening but not in the clustering. *BRO1* was selected for cluster analysis. Bro1p is an endosome-associated protein functioning in the multivesicular body (MVB) pathway (Odorizzi *et al.*, 2003) that play a role in the ubiquitin-dependent control of membrane protein trafficking (Spingael *et al.*, 2002).

3.2.4.3. Vacuolar genes

GAP1 is inactivated by being targeted to the vacuole where it is degraded. Hence it is not surprising that an important portion of the genes involved in vacuolar transport were found to exhibit a G- phenotype. Interestingly, the vacuolar genes clustered in two main groups (Fig.22). One cluster of sixteen genes contains seven vacuolar genes (*PEP12, VPS3, PEP7, VPS27, VPS24, VPS4* and *DID4*) that are involved in the endocytosis of cargo from the plasma membrane to the multivesicular body (MVB); a prevacuolar compartment (Fig.23 panelB) (Conibear and Stevens, 1998; Bryant and Stevens, 1998; Gerrard *et al.*, 2000; Kucharczyk and Rytka, 2001). The associated deletion strains grew poorly in presence of elevated glycine concentrations (200mM) even when ammonium sulfate was present. The growth profiles of the deletion strains missing these vacuolar genes corroborate the need for yeast to down regulate the amount of Gap1p when growth is in presence of a high concentration of glycine.

Somewhat unexpectedly, it was found that these same strains were unaffected when proline or glutamate were used as the sole nitrogen source. In this study, proline and glutamate were included at a lower molar concentration when used as sole nitrogen source (1.5% weight/volume). Therefore it is possible that neither proline nor glutamate accumulates at toxic levels under the condition tested. It is even possible that in these strains the reduced degradation of Gap1p causes a more efficient uptake of these amino acids when they are present as sole nitrogen sources and thus explains the phenotypes observed on Pmin and/or Emin for *Δure2*, *Δpep12*, *Δvps3* and *Δpep7* strains (Fig.23 panel B). Among the vacuolar genes in this cluster, the *YLL049W* ORF encodes an

hypoyhetical protein that may be involved in vacuolar transport. However, the intensity of the phenotype displayed by this deletion strains was less pronounced than the neighboring strains in this cluster.

A second cluster of 12 genes contains nine vacuolar genes (*VPS36, VPS41, VAM6, YPT7, VPS16, VPS25, SNF7, MON1* and *VPS33*) (Fig.23 panel B). This cluster is more heterogeneous: 3 genes are involved in early endosome to MVB transport and 6 in MVB to vacuole, with *VPS33*, *VPS16*, *VPS41* and *VAM6* localized at the vacuolar membrane (Conibear and Stevens, 1998; Bryant and Stevens, 1998; Price *et al.*, 2000; Kucharczyk and Rytka, 2001). Unlike the first cluster, they seemed to only be important for growth on Gmin media and when glycerol is used as sole carbon source. The deletion strains belonging to this cluster did not display a reduced growth phenotype on the Dmin+200mM glycine and when formate serine or a mix of C1 end product was added to Gmin. In consequence, this growth profile does not appear to be linked to glycine toxicity. This cluster also includes two ORFs, *YLR386W* and *YDR149C*, encoding unclassified proteins that may be involved in vesicular trafficking to the vacuole or homovacuolar fusion.

3.2.4.4. Nuclear-encoded mitochondrial genes

In addition to identifiying a number of vacuolar localized proteins that were important for growth on glycine, several proteins localized to the mitochondrial compartment were also found to be important. Selected nuclear genome encoded mitochondrial genes can be subdivided in three major groups based on their functional

roles. One group includes proteins that are important for fatty acid synthesis, specifically gene products involved in the synthesis of lipoic acid. The second group includes proteins involved in maintaining iron homeostasis and the formation of iron sulfur (Fe/S) clusters. The last group includes chaperonin proteins involved in the import of mitochondrial proteins. Unlike the vacuolar gene deletion strains, the strains with mitochondrial gene deletions exhibited growth patterns that did not cluster in a tight group. *CEM1* and *OAR1* present in the clustering diagram are two of the four genes (*ACP1, CEM1, OAR1* and *MCT1*) known to encode components of the mitochondrial fatty acid synthesis complex FASII (Shneider *et al.*, 1997). *ACP1* is essential and thus its deletion strain is not present in the homozygous deletion set. The deletion of *CEM1* or *OAR1* genes resulted in a respiratory deficient phenotype as observed when grown on glycerol minimum media (Harington *et al.* 1993, Schneider *et al.* 1997). Analysis of mitochondrial fatty acids of *CEM1* deleted strains by Harington *et al.* (1993) shows no significant difference in comparison to the wild type. It was proposed that the β-Ketoacyl-ACP synthase encoded by *CEM1* participates in the synthesis of a specific fatty acid and not to bulk fatty acids synthesis. The proximity of the *CEM1* and *LIP5* deletion strains within the clustering diagram (Fig.23 panel C) and the growth pattern of the *LIP5* and *CEM1* deletion strains in this experiment suggest that Harington *et al.*'s hypothesis is correct. Furthermore, these results suggest that Cem1p is involved in the synthesis of lipoic acid. Just below *LIP5* on the clustering diagram is the hypothetical ORF *YJL046W* (Fig.23 panel C). *YJL046W* encodes for an unclassified protein which shows similarity to the *Escherichia.coli* lipoate-protein Ligase A (LplA). The *YJL046W* deletion strain has a respiratory deficiency phenotype (MIPS), which was confirmed here (Fig.23 panel C).

Marcus *et al.* (2001) propose that there might be additional enzymes with function similar to Lip2p in *S. cerevisiae*, since growth of *lip2*-null mutants is detected in both glycerol and glycine medium after prolonged incubation. This indicates that Yjl046wp and Lip2p may have overlapping activity and that both can attach lipoic acid to the H-subunit of the glycine cleavage system encoded by *GCV3*. *PPT2* encodes a phosphopantetheine protein transferase. Its disruption leads to a loss of pantetheinylation of the mitochondrial acyl carrier protein (ACP). Cellular lipoic acid synthesis is also abolished in the Δ*ppt2* strain (Stuible *et al.*, 1998). Although the *PPT2* deletion strain did show a defect in growth on almost all the Gmin related media, it did not exhibit the respiratory deficiency expected from a lipoic acid deficient strains.

Ssq1p is a mitochondrial Hsp70-like chaperone protein (Schmidt *et al.*, 2001; Lutz *et al.*, 2001). This protein is thought to be involved in the mitochondrial biosynthesis and repair of Fe/S clusters in the mitochondrion (Strain *et al.*, 1998; Schilke *et al.*, 1999). Indeed mutants in *SSQ1* are compromised in the assembly of the Fe/S cluster containing mitochondrial enzymes (Lutz *et al.*, 2001). Fe/S clusters are used as sulfur atom donors for the lipoic arm and therefore, they are important for the efficiency of the glycine cleavage system (Ollagnier-De Choudens *et al.*, 2000). Ssq1p is a partner for the essential J-type chaperone Jac1p also involved in biogenesis of Fe/S clusters (Voisine *et al.*, 2001). *NFU1* was first identified in a synthetic lethal screen with the mitochondrial heat shock protein *SSQ1* (Schilke *et al.*, 1999). A study from Schilke *et al.* (1999) suggests that it is directly involved in the mobilization of iron for insertion into Fe/S cluster containing proteins. The growth profile of the *NFU1* deletion strains across the test conditions used in this study was very similar to that of the *GCV2* and *GCV3*

deletion strains (Fig.23 panel C). MDJ1 also present close to *GCV2* and *GCV3* in the clustering diagram (Fig.23 panel C) encode a DnaJ-type cochaperone that cooperates with the essential chaperone Ssc1p. Cluster analysis of the *Δssq1*, *Δnfu1* and *Δmdj1* strains (Fig.23 panel C) did not group them close together. This data makes linking their function to glycine metabolism more difficult.

3.2.4.5. Regulatory proteins

Several genes involved in deadenylation were present in the collection of 107 strains. Ccr4, Pop2/Caf1 and Dhh1 proteins associate in a deadenylation complex with the product of the essential gene *NOT1* (Tucker *et al.*, 2002; Maillet and Collart, 2002; Hata *et al.*, 1998; Liu *et al.*, 1998; Liu *et al.*, 1997). Deadenylation plays a very important role in the regulation of mRNA half life moreover this complex seems to also affect transcription both positively and negatively (Liu *et al.*, 1998; Tucker *et al.*, 2002). The presence of the *Δccr4*, *Δpop2* and *Δdhh1* strains and their proximity in the clustering diagram suggest a role for this complex in the turnover of mRNA linked to the utilization of glycine. It is interesting to note that the *DBF2* deletion strain, another strain that was identified as having a G- phenotype, has a gene deleted whose protein product can also associate with this complex. However the deletion strain even if present in the set of 107 genes that were clustered did not cluster with *Δccr4*, *Δpop2* and *Δdhh1* strains (Fig.22, Fig.23 panel D). This result possibly reflects its implication in other complexes (Komarnitsky *et al.*, 1998).

Two genes encoding members of the *PHO85* protein kinase complexes were also identified. The *PHO85* gene product is a multifunctional non essential cyclin-dependant kinase that interacts with at least 10 different identified cyclins (Andrews and Measday, 1998). *PHO85* deletion strain exhibits a broad range of phenotypes, including poor growth on nonfermentable carbon sources and reduced endocytosis (Lee *et al.*, 1998; Carroll *et al.*, 2001*)*. The deletion of *RVS167*, known to be involved in the actin cytoskeleton regulation, leads to similar spectrum of phenotypes. The interaction between Pho85p and Rvs167p suggests that a complex including those two proteins may coordinate actin assembly, endocytosis and maybe the response to environmental stress (Lee *et al.*, 1998). The large distance observed between them in the clustering diagram is probably attributable to the missing data points for the *PHO85* deletion strains as well as the multiple function of Pho85p. Yet another protein Rvs161p, associates with Rvs167p (Lee *et al.*, 1998; Breton and Schaeffer, 2001). The *RVS161* deletion strain was retained following the primary screen but not retained for cluster analysis.

3.2.5. Strains with a G+ phenotype

Strains with a G+ phenotype formed a cluster composed of 7 genes (*SER1, SER2, ILV1, TRK1, SWI6, GLY1* and *SPT20*). This cluster appeared at the bottom of the clustering diagram (Fig.21 and Fig.22 panel E). Half of the genes present in this cluster are involved in metabolism of serine or glycine. *GLY1* encode a L-theonine aldolase which catalyzes the cleavage of threonine to glycine and acetaldehyde (liu *et al.*, 1997). This suggests that threonine is a possible source of glycine in this pathway (liu *et al.*,

1997). The Gly1p-dependent pathway rather than Shm1p and Shm2p (encoding alternative serine hydroxymethyltransferase) appears to be the primary source of glycine in yeast when glucose is the carbon source (Mc Neil *et al.*, 1994; Monshau *et al.*, 1997). Like *SER1*, *SER2* is involved in synthesis of serine from 3-phosphoglycerate. *SER2* encodes a phosphoserine phosphatase. *ILV1* encodes an anabolic serine and threonine dehydratase precursor. The growth profiles of these 7 G+ strains showed that the presence of even a low concentration of glycine (0.5 mM) will result in significant or enhance growth, compare to Dmin.

4. Discussion

The products of glycine cleavage are used for the synthesis of activated one-carbon units and nitrogen metabolism. Previous results from our laboratory showed that glycine at high concentrations is toxic for yeast. Furthermore, these earlier studies showed that mutants defective in the regulation of glycine cleavage activity are hypersensitive to glycine. Glycine catabolism should therefore be regulated so that intracellular glycine does not reach toxic levels and adequate amounts of activated one-carbon units, ammonia for nitrogen assimilation and glycine for protein synthesis are maintained. Furthermore, since wild type yeast can grow on minimal media with either ammonia or glycine as the nitrogen source but mutants deficient in glycine cleavage activity can only grow with ammonia, we reasoned that mutants defective in various aspects of glycine metabolism could be identified by comparing relative growth rates on media with ammonia versus glycine as the nitrogen source.

4.1. Screen for strains that showed a growth phenotype on Gmin

The homozygous diploid set of deletion strains contains all the strains that are viable when both copies of a gene are deleted. Therefore, it represents null mutants of all the non-essential genes (about 4700) in the genome of *S. cerevisiae* (about 6000). I screened the entire homozygous diploid deletion set for strains exhibiting a growth phenotype when glycine was used as the sole nitrogen source. This screen identified a total of 321 strains. Within the 321 strains, 250 showed a growth defect on Gmin (G-

phenotype) whereas 71 exhibited better growth on Gmin (G+ phenotype). Asymmetrical partitioning of the strains into these two classes (G- or G+) was expected, since glycine is a poor nitrogen source that is also important as source of C1 units and as a precursor for purine synthesis.

The primary screen identified strains deleted for genes encoding three of the four glycine cleavage system subunits, *GCV1, GCV2* and *GCV3*. *LPD1*, encoding the lipoate dehydrogenase subunit of the glycine cleavage system and *BAS1*, a positive regulator of the glycine cleavage system genes, were also expected to display a G- phenotype. The absence of the *LPD1* and *BAS1* deleted strains in the set of G- strains was due to the relatively poor growth these strains exhibited on both the Gmin test medium and the Dmin medium used as the control growth condition. This indicate that *LPD1* and *BAS1* have pleiotropic effects that include also include functions important for growth on Dmin medium.

The screen also identified a large portion of vacuolar (8%) and mitochondrial genes (13%). This suggested that both vacuolar- and mitochondrial-based functions are important for growth when glycine is the sole nitrogen source. It was not initially clear why a large number of vacuolar proteins were important for growth on Gmin medium. In contrast, some mitochondrial genes would be expected to be important, since the glycine cleavage system is localized within the mitochondrial compartment.

The criterion used to identify G- and G+ strains in the primary screen was the average $\log_2$ ratio obtained when growth on Gmin versus Dmin media was compared for each strain. This criterion did not consider the relative growth rate obtained on each media. The use of the average $\log_2$, ratio without accounting for the relative growth rate,

increased the possibility of identifying false positives because strains grow poorly on both the test and the control media.

4.2. Detailed phenotypic characterization

A more detailed analysis was performed on the 321 strains identified in the primary screen. This more detailed analysis, performed in an attempt to determine how the various deletions affected cell growth, involved monitoring the relative growth each strains on various media. Software developed for the analysis of DNA microarray data was used to analyze the data from this more detailed study of relative growth rates. This analysis also included a data-filtering step. This step, commonly used in the analyses of transcription profiling data, allowed the identification of strains with insufficient growth on both the experimental and the control media and discarded the unreliable data. Including this filtering step should therefore remove false positives obtained from the primary screen.

4.2.1. Vacuolar genes

Results from the detailed phenotypic characterization confirmed that many of the vacuolar genes identified in the primary screen were indeed important for growth when glycine was the sole nitrogen source. Furthermore, even in the presence of the preferred nitrogen source, ammonium sulfate, seven vacuolar genes were important when glycine was present at high concentrations.

The absence of the *GAP1* deletion strain among the strains identified in the primary screen was intriguing given that Gap1p is thought to be important for the uptake of amino acids when they are used as nitrogen sources. It was also surprising that several strains harboring deletions of negative regulators of Gap1p were identified. Together these results suggested, that at the concentration of glycine tested, the optimal growth of wild type yeast requires down regulation of Gap1p.

Chen and Kaiser (2002) show that the direct sorting of Gap1p to the vacuole rather than the plasma membrane occurs when amino acids are present at high concentrations. Moreover, they hypothesized that the uncontrolled uptake of amino acids by Gap1p can be toxic to the cell when amino acids are present at high concentrations.

Based on the clustering results presented here it appeared that a set of genes involved in the transport of vesicles from the plasma membrane to the multivesicular body may be important for the down regulation of Gap1p levels at the plasma membrane. Indeed, high concentrations of glycine, even in presence of ammonium sulfate, caused a set of seven strains harboring deletions in genes involved in plasma membrane to multivesicular body transport to elicit a growth deficiency.

Glycine toxicity is not completely understood. However, the results presented here and by Chen and Kaiser (2002) suggest that glycine toxicity results from a more generalized perturbation of cellular metabolism that can be elicited by several amino acids. It would therefore be interesting to determine which amino acids are toxic and whether their toxic effects are enhanced by inactivating the various mechanisms that down regulate Gap1p. Regardless, the results presented here suggest that amino acid

toxicity is enhanced when the cell's ability to down regulate the amount of Gap1p at the cell surface is impaired.

It would be interesting to test whether Gap1p levels at the cell surface correlate with the toxic effects of other amino acids. Because the toxic concentrations of amino acids can vary between amino acids, it would be informative to test whether the mutants identified in this study also showed increases sensitivity to the toxic effects of other amino acids. This method may work because Gap1p is able to transport all 20 amino acids.

A second cluster enriched in strains harboring genes involved in vacuolar transport was identified. These strains were not as sensitive to high concentrations of glycine if the media also contained one or a mix of the C1 end products or a preferred nitrogen source. The identification of this second cluster of vacuolar genes suggested that an additional vacuolar function, distinct from the vacuole's role in regulating the amount Gap1p at the cell surface, is important for growth under some circumstances when glycine is the sole nitrogen source. Perhaps this second cluster of vacuolar genes is involved in maintaining a balance of C1 units between the cytoplasm and mitochondria.

4.2.2. Nuclear-encoded mitochondrial genes

Given the mitochondrial location of the glycine cleavage system and the essential role lipoic acid, a product of mitochondrial metabolism, plays in reactions carried out by the glycine cleavage system, it was not surprising that several mitochondrial genes were identified in the primary screen. The varied growth patterns elicited by strains deleted for

mitochondrial genes on the various media tested, as reflected by the clustering analysis, suggested these genes have pleiotropic effects. For example, pleiotropic effects would be expected in the case of chaperonin proteins that are involved in the translocation of proteins into the mitochondrial matrix. Chaperonin proteins for example may be important for the import of proteins for glycine metabolism, and one or more additional mitochondrial-based functions metabolism, mitochondrial organization and respiration. It would therefore be interesting to further investigate those mitochondrial proteins identified here in order to better understand their functional importance for, both glycine cleavage and other mitochondrial functions.

This growth profiling experiments identified two genes that may be involved in lipoic acid metabolism. It will be particularly interesting to confirm that *CEM1* plays a role in lipoic acid synthesis and that *YJL046W* codes for a ligase specific for attachement of lipoate to the glycine cleavage system H subunit.

4.2.3. Regulation proteins

Several regulatory genes were important for growth on Gmin medium. These regulatory genes are part of a global regulatory complex, the CCR4 complex, that is involved in a general response to changes in environmental conditions. The *CCR4* complex regulates the transcription and half-life of mRNA. This study suggests that at least some of the genes regulated by the CCR4 complex are important for growth when glycine is the sole nitrogen source.

PHO85 encoding a multifunctional cyclin-dependent kinase, is another interesting gene that was identified. The results suggest that it might be worthwhile to investigate the role of *PHO85* and its signal transduction pathways in glycine metabolism.

4.3. Improvement and future work

It will be interesting to further investigate the ORFs that encode unclassified proteins (Table 2). The implication of some of them can be deduced from their position on the yeast genome relative to other genes, when there is overlap of two ORFs. The ORFs encoding proteins with similarities to proteins from other organism, or that contain putative functional domains, are of a particular interest. *BAS1* and *LPD1*, genes known to play an important role in glycine metabolism, were not identified in the primary screen. These deletion strains could be added to the subset of strains submitted to further characterization in order to confirm their phenotype on Gmin and included them when additional studies are performed. An additional advantage of including these genes would be that they both have a well-defined function that may help interpret the clustering results obtained in further studies.

Using the homozygous diploid deletion library only allowed the non-essential set of yeast genes to be studied. By looking at physical and genetic interactions identified by others, it was possible in some cases to predict that some essential genes would be important for glycine metabolism. For example, ACP1 involved in fatty acid synthesis is probably important for the synthesis of lipoic acid and therefore for glycine catabolism.

Table 2. Unclassified Protein present in the clustering diagram

ORF	Description	comment
YAL046c	weak similarity to hypothetical protein S. pombe	565 bp from *GCV3*
YDR048c	questionable ORF	overlaps YDR049w
YDR049w	similarity to C. elegans K06H7.3 protein	Cys2His2 zinc-finger
YDR149c	questionable ORF	overlapped *NUM1* encoding a nuclear migration protein
YHR067w	weak similarity to hypothetical S. pombe protein	
YJL046w	similarity to E. coli lipoate-protein ligase A	
YKR035c	hypothetical protein	overlapped *DID2* a vacuolar gene 141 bp from *CAF4* encoding a CCR4 associated factor 213 bp from *DAL80* encoding a nitrogen regulation factor
YLL049w	hypothetical protein	75 bp from YBT1 a vacuolar gene
YLR386w	similarity to unknown protein, of S. pombe and C. elegans	
YOR139c	questionable ORF	overlapped *SLF1* encoding a transcription factor
YPR123c	questionable ORF	overlapped *CTR1* involve in ion homeostasis (present in the cluster diagram)
YCR079w	weak similarity to A. thaliana protein phosphatase 2C	

This study proved that it is possible to spot strains at a high density on plates and score their growth using software designed for the analysis of microarray data. However, it would be desirable to use software specifically designed for applications similar to those used in this study. It will also be important to work with biostatisticians in order to improve on the methods used for data normalization, measurement of growth, analysis of the feature intensity and ratio data. This assistance would aid in defining a more rigorous method of analysis and increase confidence in the results before submitting them to cluster analysis.

The eventual effects of strain location and neighboring colonies on strain growth can be tested by randomization of the strain positions, within the high density array and between the replicates.

The high-density colony array system developed for the secondary screening could also be used to perform primary screens. For example, it could be used to redo the primary screen or to test for growth phenotypes associated with other conditions such as induced stress and antimycotic drug resistance.

It would also be possible to increase the number of colonies on one plate from the 6912 used in this study to 9216 (no blanks). Only a minority of the strains is expected to show a growth phenotype in a given condition, therefore, when the complete set is tested, the normalization of the growth data could be done using the median value of all the feature-intensities measured on one plate instead of using control strains. This method of normalization is often used for gene expression analyses.

Further studies could also be done to determine if the genes deleted in the various G- and G+ strains are transcriptionally regulated. This could be performed using DNA

microarray data of the parental strain grown under the control and various test conditions used in this study. Previous comparisons between fitness analysis and DNA microarray data showed little overlap between the functionally important gene set and expression regulated gene set (Glaever *et al* 2002). Transcription profiling could be used to identify potentially interesting genes and then growth profiling could be used to define the subset of transcriptionally regulated genes that is actually functionally important under the conditions tested. Combining of the growth and transcription profiling data may help us understood the complex relations between the regulation mechanisms and the function of the genes in *S. cerevisiae*.

WORK CITED

Andrews, B. and Measday, V. 1998. The cyclin family of budding yeast: abundant use of a good idea. Trends genet. **14**(2): 66-72

Amerik, A.Y., Nowak, J., Swaminathan, S. and Hochstrasser, M. 2000. The Doa4 Deubiquitinating enzyme is functionally linked to the vacuolar protein-sorting and endocytic pathways. Mol. Biol. Cell **11**: 3365-80

Arndt, K. and Fink G.R. 1986. GCN4 protein a positive transcription factor in yeast, binds general control promoters all 5'TGACTC3' sequences. Proc. Natl. Acad. Sci. U.S.A. **83**: 8516-20

Baudin, A., Ozier-Kalogeropoulos, O., Denouel, A., Lacroute, F. and Cullin, C. 1993. A simple and efficient method for direct deletion in *Saccharomyces cerevisiae*. Nucleic Acids Res. **21**(14): 3329-30

Bassett, D.E.jr., Boguski, M.S., Spencer, F., Reeves, R., Kim, S., Weaver, T. and Hieter, P. 1997. Genome cross-referencing and XREFdb: implications for the identification and analysis of genes mutated in human disease. Nat. Genet. **15**(4): 339-44

Breton, A.M., Schaeffer, J. and Aigle, M. 2001. The yeast Rvs161 and Rvs 167 proteins are involved in secretory vesicles targeting the plasma membrane and in cell integrity. Yeast **18**(11): 1053-68

Brody, S., Oh, C., Hoja, U. and Schweizer, E. 1997. Mitochondrial acyl carrier protein is involved in lipoic acid synthesis in *Saccharomyces cerevisiae*. FEBS lett. **408**(2): 217-20

Bryant, N.J. and Stevens, T.H. 1998. Vacuole biogenesis in *Saccharomyces cerevisiae*: Protein transport pathways to the yeast vacuole. Microbiol. Mol. Biol. Rev. **62**(1): 230-47

Carroll, S.A., Bishop, A.C., DeRisi, J.L., Shokat, K.M. and O'Shea, E.K. 2001. Chemical inhibition of the Pho85 cyclin-dependent kinase reveal a role in the environmental stress response. Proc. Natl. Acad. Sci. U.S.A. **98**(22): 12578-83

Chen, E.J. and Kaiser, C.A. 2002. Amino acids regulate the intracellular trafficking of the general amino acid permease of *Saccharomyces cerevisiae*. Proc. Natl. Acad. Sci. U.S.A. **99**(23): 14837-42

Coffman, J.A. and Cooper, T.G. 1997. Nitrogen GATA Factors Participate in Transcriptional Regulation of Vacuolar Protease genes in *Saccharomyces cerevisiae*. J. Bacteriol. **179**: 5609-13

Coffman, J.A., El Berry, H.M. and Copper, T.G. 1994. The URE2 Proteins Regulates Nitrogen Catabolic Gene Expression through the GATAA-Containing UAS_{NTR} Element in *Saccharomyces cerevisiae*. J. Bacteriol. **176**: 7476-83

Coffman, J.A., Rai, R., Cunningham, T.S., Svetlov, V. and Cooper, T.G. 1996. Gat1p, a GATA Family Protein Whose Production Is Sensitive to Nitrogen Catabolite Repression, Participates in Transcriptional Activation of Nitrogen-Catabolic Genes in *Saccharomyces cerevisiae*. Mol. Cell. Biol. **16**: 847-58

Coffman, J.A., Rai, R., Loprete, D.M., Cunningham, T.S., Svetlov, V. and Cooper T.G. 1997. Cross regulation of four GATA factors that control nitrogen catabolic gene expression in *Saccharomyces cerevisiae*. J. Bacteriol. **179**: 3416-29

Conibear, E. and Stevens, T.H. 1998. Multiple sorting pathways between the late Golgi and the vacuole in yeast. Biochim. Biophys. Acta. **1404**: 211-30

Cunningham, T.S., Rai, R. and Cooper, T.G. 2000. The Level of DAL80 Expression Down-Regulates GATA Factors-Mediated Transcription in *Saccharomyces cerevisiae*. J. Bacteriol. **182**: 6584-91

Daignan-Fornier, B. and Fink, G.R. 1992. Coregulation of purine and histidine biosynthesis by the transcriptional activators BAS1 and BAS2. Proc. Natl. Acad. Sci. U.S.A. **89**: 6746-50

Denis, V. and Daignan-Fornier, B. 1998. Synthesis of glutamine, glycine and 10-formyl tetrahydrofolate is coregulated with purine biosynthesis in *Saccharomyces cerevisiae*. Mol. Gen. Genet. **259**: 246-255

Denis, V., Boucherie, H., Monribot, C. and Daignan-Fornier, B. 1998. Role of the Myb-like protein Bas1p in *saccharomyces cerevi*siae: a proteome analysis. Mol. Microbiology **30**: 557-566

Dickinson, J.R., Roy, D.J. and Dawes, I.W. 1986. A mutation affecting lipoamide dehydrogenase, pyruvate dehydrogenase and 2-oxoglutarate dehydrogenase activities in Saccharomyces cerevisiae. Mol. Gen. Genet. **204**(1): 103-7

Douce, R., Bourguignon, J., Neuburger, M. and Rebeille, F. 2001. The glycine decarboxylase system a facinating complex. Trends Plant Sci. Rev. **6**:167-76

Eisen, M.B., Spellman, P.T., Brown, P.O. and Botstein, D. 1998. Cluster Analysis and Display of Genome-Wide Expression Patterns. Proc. Natl. Acad. Sci. U S A. **95**: 14863-8

Forsberg, H. and Ljungdahl, P.O. 2001. Sensor of Extracellular Nutrients in *Saccharomyces cerevisiae*. Curr. Genet. **40**: 91-109

Gerrard, S.R., Bryant, N.J. and Stevens, T.H. 2000. *VPS21* controls entry of endocytosed and biosynthetic proteins into the yeast prevacuolar compartment. Mol. Biol. Cell **11**: 613-26

Gerrard, S.R., Levi, B.P. and Stevens, T.H. 2000. Pep12p is a multifunctional yeast syntaxin that control entry of biosynthetic, endocytic and retrograde traffic into the prevacuolar compartment. Traffic **1**: 259-69

Ghrist, A.C., Heil, G. and Stauffer, G.V. 2001. GcvR interacts with GcvA to inhibits activation of the *Escherichia coli* glycine cleavage operon. Microbiology **147**: 2215-21

Ghrist, A.C. and Stauffer, G.V. 1995. Characterization of the Escherichia coli gcvR gene encoding a negative regulator of gcv expression. J. Bacteriol. **177**(17): 4980-4

Giaever, G., Chu, A.M., Ni, L., Connelly, C., Riles, L., Veronneau, S., Dow, S., Lucau-Danila, A., Anderson, K., Andre, B., Arkin, AP., Astromoff, A., El-Bakkoury, M., Bangham, R., Benito, R., Brachat, S., Campanaro, S., Curtiss, M., Davis, K., Deutschbauer, A., Entian, K.D., Flaherty, P., Foury, F., Garfinkel, D.J., Gerstein, M., Gotte, D., Guldener, U., Hegemann, J.H., Hempel, S., Herman, Z., Jaramillo, D.F., Kelly, D.E., Kelly, S.L., Kotter, P., LaBonte, D., Lamb, D.C., Lan, N., Liang, H., Liao, H., Liu, L., Luo, C., Lussier, M., Mao, R., Menard, P., Ooi, S.L., Revuelta, J.L., Roberts, C.J., Rose, M., Ross-Macdonald, P., Scherens, B., Schimmack, G., Shafer, B., Shoemaker, D.D., Sookhai-Mahadeo, S., Storms, R.K., Strathern, J.N., Valle, G., Voet, M., Volckaert, G., Wang, C.Y., Ward, T.R., Wilhelmy, J., Winzeler, E.A., Yang, Y., Yen, G., Youngman, E., Yu, K., Bussey, H., Boeke, J.D., Snyder, M., Philippsen, P., Davis, R.W. and Johnston, M. 2002. Functional profiling of the Saccharomyces cerevisiae genome. Nature **418**(6896): 387-91

Harington, A., Herbert, C.J., Tung, B., Getz, G.S. and Slonimski, P.P. 1993. Identification of a new nuclear gene (*CEM1*) encoding a protein homologous to a beta-keto-acyl synthase which is essential for mitochondrial respiration in *Saccharomyces cerevisiae*. Mol. Microbiol. **9**(3): 545-55

Hata, H., Mitsui, H., Liu, H., Bai, Y., Denis, C.L., Shimizu, Y. and Sakai, A. 1998. Dhh1p, a putative RNA helicase, associates with the general transcription factors Pop2p and Ccr4p from Saccharomyces cerevisiae. Genetics **148**(2): 571-9

Heil, G., Stauffer, L.T., Strauffer, G.V. 2002. Glycine binds the transcriptional accessory protein GcvR to disrupt a GcvA/GcvR interaction and allow GcvA-mediated activation of the *Escherichia coli* gcvTHP operon. Microbiology **148**: 2203-14

Hong, S.P., Piper, M.D., Sinclair, D.A. and Dawes, I.W. 1999. Control of Expression of One-carbon Metabolism Genes of *Saccharomyces cerevisiae* is Mediated by a Tetrahydrofolate-responsive Protein Binding to a Glycine Regulatory Region Including a Core 5'-CTTCTT-3'. J. Biol. Chem. **274**: 10523-32

Horak, J. 1997. Yeast nutrient transporters. Biochim. Biophys. Acta. **1331**(1): 41-79

Issel-Tarver, L., Christie, K.R., Dolinski, K., Andrada, R., Balakrishnan, R., Ball, C.A., Binkley, G., Dong, S., Dwight, S.S., Fisk, D.G., Harris, M., Schroeder, M., Sethuraman, A., Tse, K., Weng, S., Botstein, D. and Cherry, J.M. 2002. *Saccharomyces* Genome Database. Methods Enzymol. **350**: 329-46

Kastanos, E.K., Woldman, Y.Y., and Appling, D.R. 1997. Role of the mitochondrial and cytoplasmic serine hydroxymethyltransferase isozymes in *de novo* purine synthesis in *Saccharomyces cerevisiae*. Biochemistry **36**: 14956-64

Komarnitsky, S.I., Chiang, Y.C., Luca, F.C., Chen,J., Toyn, J.H., Winey, M., Johnston, L.H. and Denis, C.L. 1998. Dbf2 protein kinase binds to and acts through the cell cycle-regulated Mob1 protein. Mol. Cell. Biol. **18**(4): 2100-7

Kurcharczyk, R. and Rytka, J. 2001. *Saccharomyces cerevisiae* – a model organism for the studies on vacuolar transport. Acta Biochimica Polonica **48**(4): 1025-42

Lee, J., Colwill, K., Aneliunas, V., Tennyson, C., moore, L., Ho, y. and Andrews, B. 1998. Interaction of yeast RVS 167 and Pho85 cyclin-dependent kinase complexes may link the cell cycle to the actin cytoskeleton. Curr. Biol. **8**: 1310-21

Lemmon, S.K. and Traub, L.M. 2000. Sorting in the endosomal system yeast and animal cells. Curr. Opin. Cell Biol. **12**: 457-66

Liu, H.Y., Badarinarayana, V., Audino, D.C., Rappsilber, J., Mann, M. and Denis, C.L. 1998. The NOT proteins are part of the CCR4 transcriptional complex and affect gene expression both positively and negatively. EMBO. J. **17**(4): 1096-106

Liu, J.Q., Nagata, S., Dairi, T., Misono, H., Shimizu, S. and Yamada, H. 1997. The GLY1 gene of *Saccharomyces cerevisiae* encodes a low-specific L-threonine aldolase that catalyzes cleavage of L-allo-threonine and L-threonine to glycine--expression of the gene in Escherichia coli and purification and characterization of the enzyme. Eur. J. Biochem. **245**(2): 289-93

Lorenz, M.C. and Heitman, J. 1998. The MEP2 ammonium permease regulates pseudohyphal differentiation in *Saccharomyces cerevisiae*. EMBO J. **17**: 1236-47

Lutz, T., Westermann, B., Neupert, W. and Herrmann, J.M. 2001. The mitochondrial protein Ssq1 and Jac1 are required for the assembly of iron sulfur clusters in mitochondria. J. Mol. Biol. **307**: 815-25

Magasanik, B. and Kaiser, C.A. 2002. Nitrogen regulation in *Saccharomyces cerevisiae*. Gene **290**: 1-18

Maillet, L. and Collart, M.A., 2002. Interaction between Not1p, a component of the Ccr4-not complex, a global regulator of transcription, and Dhh1p, a putative RNA helicase. J. Biol. Chem. **277**(4): 2835-42

Marini, A.M., Soussi-Boudekou, S., Vissers, S. and Andre, B. 1997. A Family of Ammonium Transporters in *Saccharomyces cerevisiae*. Mol. Cell Biol. **17**: 4282-4293

Marvin, M.E., Williams, P.H. and Cashmore, A.M. 2001. The isolation and characterization of a *Saccharomyces cerevisiae* gene (*LIP2*) involved in the attachment of lipoic acids groups to mitochondrial enzymes. FEMS Microbiol. Lett. **199**: 131-136

Mc Neil, J.B., McIntosh, E.M., Taylor, B.V., Zhang, F.R., Tang, S. and Bognar, A.L. 1994. Cloning and molecular characterization of three genes, including two genes encoding serine hydroxymethyltransferases, whose inactivation is required to render yeast auxotrophic for glycine. J. Biol. Chem. **269**(12):9155-65

Mewes, H.W., Frishman, D., Güldener,U., Mannhaupt, G., Mayer, K., Mokrejs, M., Morgenstern, B., Münsterkoetter, M., Rudd, S. and Weil, B. 2002. MIPS: a database for genomes and protein sequences. Nucleic Acids Res. **30**(1):31-4

Monschau, N., Stahmann, K.P., Sahm, H., McNeil, J.B. and Bognar, A.L. 1997. Identification of *Saccharomyces cerevisiae GLY1* as a threonine aldolase: a key enzyme in glycine biosynthesis. FEMS Microbiol. Lett. **150**(1): 55-60

Nagarajan, L. and Storms, R.K. 1997. Molecular Characterization of GCV3, the *Saccharomyces cerevisiae* Gene Coding for the Glycine Cleavage System Hydrogen Carrier Protein. J. Biol. Chem. **272**: 4444-50

Nickas, M.E. and Yaffe, M.P. 1996. *BRO1*, a novel gene that interacts with components of the Pck1p-mitogen-activated protein kinase pathway in *Saccharomyces cerevisiae*. Mol. Cell. Biol. **16**(6): 2585-93

Odorizzi, G., Katzmann, D.J., Babst, M., Audhya, A. and Emr, S.D. 2003. Bro1 is an endosome-associated protein that functions in the MVB pathway in Saccharomyces cerevisiae. J. Cell. Sci. **116**(10): 1893-903

Oliver, D.J. Neuburger, M., Bourguignon, J. and Douce, R. 1990. Glycine metabolism by plant mitochondria. Physiologia Plantarum **80**: 487-91

Ollagnier-De Choudens, S., Sanakis, Y., Hewitson, K.S., Roach, P., Baldwin, J.E., Munck, E. and Fontecave, M. 2000. Iron-sulfur center of biotin synthase and lipoate synthase. Biochemistry **39**(14): 4165-73

Pasternack, L.B., Laude, D.A. Jr. and Appling, D.R. 1994. C NMR Analysis of intercompartmental Flow of One-carbon Units into Choline and Purines in *Saccharomyces cerevisiae*. Biochemistry **33**: 74-82

Peterson, M.R. and Emr, S.D. 2001. The class C Vps Complex Functions at Multiple Stage of the vacuolar transport pathway. Traffic **2**: 476-486

Piper, M.D., Hong, S.P., Ball, G.E. and Dawes, I.W. 2000. Regulation of the Balance of One-carbon metabolism in *Saccharomyces cerevisiae*. J. Biol. Chem. **275**: 30987-95

Piper, M.D.W., Hong, S.P., Eißing, T., Sealey, P. and Dawes, I.W. 2002. Regulation of the yeast glycine cleavage genes is responsive to the availability of multiple nutrients. FEMS Yeast Res. **2**:59-71

Regenberg, B., Düring-Olsen, L., Kielland-Brandt, M.C. and Holmberg, S. 1999. Substrate specificity and gene expression of the amino-acid permeases in Saccharomyces cerevisiae. Curr. Genet. **36**: 317-28

Rolfes, R.J. and Hinnebusch, A.G. 1993. Translation of the yeast transcriptional activator GCN4 is stimulated by purine limitation: implications for activation of the protein kinase GCN2. Mol. Cell Biol. **13**: 5099-111

Rolfes, R.J., Zhang, F. and Hinnebusch, A.G. 1997. The Transcriptional Activators BAS1, BAS2, and ABF1 Bind Positively Regulatory Sites as the Critical Elements for Adenine Regulation of ADE5,7. J. Biol. Chem. **272**: 13343-54

Schilke, B., Voisine, C., Beinert, H. and Craig, E. 1999. Evidence for a conserved system for iron metabolism in the mitochondria of *Saccharomyces cerevisiae*. Proc. Natl. Acad. Sci. U.S.A. **96**(18): 10206-11

Schneider, R., Brors, B., Bürger, F., Camrath, S. and Weiss H. 1997. Two genes of the putative mitochondrial fatty acid synthase in the genome of *saccharomyces cerevisiae*. Curr. Genet. **32**: 384-88

Schmidt, S., Strub, A., Röttgers, K., Zufall, N. and Voos, W. 2001. The two mitochondrial heat shock proteins 70, Ssc1 and Ssq1, compete for the cochaperone Mge1. J. Mol. Biol. **313**: 13-26

Sinclair, D.A. and Dawes, I.W. 1995. Genetics of the Synthesis of Serine from Glycine and Utilisation of Glycine as Sole Nitrogen Source by *Saccharomyces cerevisiae*. Genetics **140**: 1213-1222

Sinclair, D.A., Hong, S.P. and Dawes, I.W. 1996. Specific induction by glycine of the gene for the P-subunit of glycine decarboxylase from *Saccharomyces cerevisiae*. Mol. Microbiol. **19**: 611-23

Springael, J.Y. and Andre, B. 1998. Nitrogen-regulated ubiquitination of the Gap1 permease of *Saccharomyces cerevisiae*. Mol. Biol. Cell. **9**(6): 1253-63

Springael, J.Y., De Craene, J.O. and Andre, B. 1999. The yeast Npi1/Rsp5 ubiquitin ligase lacking its N-terminal C2 domain is competent for ubiquitination but not for subsequent endocytosis of the gap1 permease. Biochem. Biophys. Res. Commun. **257**(2): 561-6

Springael, J.Y., Nikko, E., Andre, B. and Marini, A.M. 2002. Yeast Npi3/Bro1 is involved in ubiquitin-dependent control of permease trafficking. F.E.B.S. Lett. **517**(1-3): 103-9.

Soetens,O., De Craene, J.O. and Andre, B. 2001. Ubiquitin is required for sorting to the vacuole of the yeast general amino acid permease, Gap1. J. Biol. Chem. **276**(47): 43949-57

Stanbrough, M., Magasanik, B. 1995. Transcriptional and postrascriptional regulation of the general amino acid permease of *Saccharomyces cerevisiae*. J. Bacteriol. **177**(1): 94-102

Stauffer, L.T. and Stauffer, G.V. 1999. Role for the leucine-responsive regulatory protein (Lrp) as a structural protein in regulating the *Escherichia coli gcvTHP* operon. Microbiology **145**: 569-76

Stover, P. and Schirch, V. 1990. Serine hydroxymethyltransferase Catalyzes the hydrolysis of 5,10-Methyltetrahydrofolate to 5-Formyltetrahydrofolate. J. Biol. Chem. **265**: 14227-33

Strain, J., Lorenz, C.R., Bode, J., Garland, S., Smolen, G.A., Ta, D.T., Vickery, L.E. and Culotta, V.C. 1998. Suppressors of superoxide dismutase (SOD1) deficiency in *Saccharomyces cerevisiae*. Identification of proteins predicted to mediate iron-sulfur cluster assembly. J. Biol. Chem. **273**(47): 31138-44

Stuible, H.P., Meier, S., Wagner, C., Hannappel, E. and Schweizer, E. 1998. A novel phosphopantetheine:protein transferase activating yeast mitochondrial acyl carrier protein. J. Biol. Chem. **273**(35): 22334-22339

Sulo, P. and Martin, N.C. 1993. Isolation and characterization of LIP5. A lipoate biosynthetic locus of *Saccharomyces cerevisiae*. J. Biol. Chem. **268**(23): 17634-9

Tada, K. and Hayasaka, K. 1987. Non-ketotic hyperglycinaemia: clinical and biochemical aspects. Eur. J. Pediatr. **146**(3): 221-7

ter Schure, E.G., van Riel, N.A.W. and Verrips, T.C. 2000. The role of ammonia metabolism in nitrogen catabolite repression in *Saccharomyces cerevisiae*. FEMS Microbiol. Rev. **24**: 67-83

Tice-Baldwin, K., Fink, G.R. and Arndt, K.T. 1989. BAS1 Has a Myb Motif and Activates HIS4 Transcription Only in Combination with BAS2. Science **246**: 931-35

Tucker, M., Staples, R.R., Valencia-Sanchez, M.A., Muhlrad, D. and Parker, R. 2002. Ccr4p is the catalytic subunit of a Ccr4p/Pop2p/Notp mRNA deadenylase complex in *Saccharomyces cerevisiae*. EMBO J. **21**(6): 1427-36

Voisine, C., Cheng, Y.C., Ohlson, M., Schilke, B., Hoff, K., Beinert, H., Marszalek, J. and Craig, E.A. 2001. Jac1, a mitochondrial J-type chaperone, is involved in the biogenesis of Fe/S clusters in *Saccharomyces cerevisiae*. Proc. Natl. Acad. Sci. U.S.A. **98**(4): 1483-8

Wach, A., Brachat, A., Pohlmann, R. and Philippsen, P. 1994. New heterologous modules for classical or PCR-based gene disruptions in *Saccharomyces cerevisiae*. Yeast **10**(13): 1793-808

Wilson, R.L., Stauffer, L.T. and Stauffer, G.V. 1993. Roles of the GcvA and PurR Proteins in Negative regulation of the Escherichia coli Glycine Cleavage Enzyme System. J. of Bacteriol. **175**: 5129-5134

Winzeler, E.A., Shoemaker, D.D., Astromoff, A., Liang, H., Anderson, K., Andre, B., Bangham, R., Benito, R., Boeke, J.D., Bussey, H., Chu, A.M., Connelly, C., Davis, K., Dietrich, F., Dow, S.W., El Bakkoury, M., Foury, F., Friend, S.H., Gentalen, E., Giaever, G., Hegemann, J.H., Jones, T., Laub, M., Liao, H., Liebundguth, N., Lockhart, D.J., Lucau-Danila, A., Lussier, M., M'Rabet, N., Menard, P., Mittmann, M., Pai, C., Rebischung, C., Revualta, J.L., Riles, L., Roberts, C.J., Ross-MacDonald, P., Scherens, B., Snyder, M., Sookhai-Mahadeo, S., Storms, R.K., Véronneau, S., Voet, M., Volckaert, G., Ward, T.R., Wysocki, R., Yen, G.S., Yu, K., Zimmermann, K., Philippsen, P., Johnston, M. and Davis, R.W. 1999. Functional characterization of the *S. cerevisiae* genome by gene deletion and parallel analysis. Science 1999 **285**(5429): 901-6

Yeast Deletion Web Page:
http://sequence-www.stanford.edu/group/yeast_deletion_project/deletions3.html

Zaman, Z., Bowman, S.B., Kornfeld, G.D., Brown, A.J.P. and Dawes, I.W. 1999. Transcription factor Gcn4 for control of amino acid biosynthesis also regulates the expression of the gene for lipoamide dehydrogenase. Biochem. J. **340**: 855-862

Zelikson, R. and Luzzati, M. 1977. Mitochondrial and Cytoplasmic Distribution in *Saccharomyces cerevisiae* of Enzymes Involved in Folate-Coenzyme-Mediated One-Carbon-Group Transfer. Eur. J. Biochem. **79**: 285-92

Zhang, F., Kirouac, M., Zhu, N., Hinnebusch, A.G. and Rolfes, R.J. 1997. Evidence that Complex Formation by Bas1p and Bas2p (Pho2p) Unmasks the Activation Function of Bas1p in an Adenine-Repressible Step of ADE Gene Transcription. Mol. Cell. Biol. **17**: 3272-83

Zheng, Y. 1995. Regulation of the *GCV3* gene in *Saccharomyces cerevisiae*. M. Sc. Thesis, Concordia University.

ANNEXE 1 List of genes for strains with a G- Phenotype

plt	R	C	Relative growth on Gmin	Relative growth on Dmin	log2 (Gmin/Dmin)	ORF	Name	Function / Description (SGD)
334	A	10	0.86	1.86	-1.12	YAL054C	ACS1	Acetyl CoA synthetase
345	H	11	0.17	0.39	-1.25	YDR448W	ADA2	ADA and SAGA component, two transcriptional adaptor/HAT (histone acetyltransferase) complexes. Transcription factor
348	G	12	0.33	0.82	-1.33	YNL220W	ADE12	Adenylosuccinate synthetase
333	B	3	0.23	0.67	-1.51	YJR105W	ADO1	Adenosine kinase
327	A	7	0.17	0.45	-1.43	YDR264C	AKR1	Negative regulator of pheromone response pathway. required for endocytosis of pheromone receptors; involved in cell shape control.
315	E	1	0.84	1.71	-1.03	YCL050C	APA1	Diadenosine 5',5'''-P1,P4-tetraphosphate phosphorylase I
347	B	2	0.43	1.13	-1.39	YGL180W	APG1	Required for autophagy. protein kinase
301	H	11	0.56	1.13	-1.00	YLL042C	APG10	Involved in autophagy; protein-conjugating enzyme involved in the Apg12p-Apg5p conjugation pathway.protein-conjugating enzyme
333	E	1	0.43	0.97	-1.16	YLR423C	APG17	Required for activation of Apg1 protein kinase
314	A	2	0.32	0.66	-1.04	YHR018C	ARG4	Argininosuccinate lyase
321	C	2	0.17	0.35	-1.06	YDR173C	ARG82	Regulator of arginine-responsive genes with ARG80 and ARG81. dual specificity inositol 1,4,5-trisphosphate 6-kinase/inositol 1,4,5,6-tetrakisphosphate 3-kinase (IP3 6-/IP4 3-kinase)
346	H	3	0.01	0.04	-2.91	YGL148W	ARO2	Chorismate synthase
331	C	5	0.16	0.55	-1.79	YMR116C	ASC1	G-beta like protein
301	C	12	0.50	1.06	-1.09	YAL020C	ATS1	Protein with similarity to human RCC1 protein
340	C	3	0.10	0.79	-2.99	YBR068C	BAP2	Amino acid permease for leucine, valine, and isoleucine (putative)
332	C	2	0.15	0.77	-2.35	YJL095W	BCK1	Bypass requirement for protein kinase C homolog
311	B	11	0.12	0.37	-1.67	YDR375C	BCS1	
322	D	10	0.26	0.68	-1.39	YPL084W	BRO1	BCK1-like resistance to osmotic shock
372	D	5	0.14	0.58	-2.01	YGR262C	BUD32	Old format: Diploid mutants exhibit random budding
330	H	10	0.41	0.88	-1.12	YML111W	BUL2	Homologue of BUL1
370	B	2	0.36	0.87	-1.27	YDR197W	CBS2	Translational activator of COB mRNA; soluble protein. cytochrome b translational activator. Mitochondrial inner membrane
301	C	11	0.26	0.65	-1.33	YAL021C	CCR4	Carbon catabolite repression; transcriptional regulator for some glucose-repressed genes including ADH2
380	A	3	0.10	0.78	-2.98	YER061C	CEM1	Homology with beta-keto-acyl synthases
311	H	7	0.31	0.81	-1.39	YGR108W	CLB1	B-type cyclin

plt	R	C	Relative growth on Gmin	Relative growth on Dmin	log2 (Gmin/Dmin)	ORF	Name	Function / Description (SGD)
347	D	10	0.32	0.71	-1.17	YER141W	COX15	Cytochrome oxidase assembly factor
348	B	7	0.22	0.51	-1.19	YDL067C	COX9	Plays role in cytochrome c oxidase holoenzyme assembly or stability
302	F	8	0.23	0.58	-1.31	YLR087C	CSF1	
330	B	12	0.36	1.02	-1.50	YHR191C	CTF8	Kinetochore protein (putative)
370	F	7	0.27	1.82	-2.76	YPR124W	CTR1	High affinity copper transporter into the cell, probable integral membrane protein
380	F	6	0.47	1.38	-1.54	YAL012W	CYS3	Cystathionine gamma-lyase
343	A	1	0.14	0.72	-2.33	YGR155W	CYS4	Cystathionine beta-synthase
341	H	10	0.11	0.55	-2.40	YGR092W	DBF2	Kinase required for late nuclear division
326	E	9	0.20	0.46	-1.18	YKR024C	DBP7	RNA helicase (putative)
348	D	7	0.32	0.74	-1.21	YFL001W	DEG1	Similar to rRNA methyltransferase (Caenorhabditis elegans) and hypothetical 28K protein (alkaline endoglucanase gene 5' region) from Bacillus sp.
337	B	1	0.25	0.97	-1.98	YDL160C	DHH1	Putative RNA helicase of DEAD box family, required for Rap1p localization to telomeres
316	E	4	0.21	0.95	-2.17	YKL002W	DID4	Class E vacuolar-protein sorting and endocytosis factor
326	C	12	0.10	0.96	-3.28	YKL213C	DOA1	Required for normal intracellular ubiquitin metabolism and for normal rates of proteolysis of ubiquitin-dependent proteolytic substrates in vivo
310	C	12	0.04	0.56	-3.66	YDR069C	DOA4	Deubiquitinating enzyme; vacuole biogenesis gene
330	A	1	0.86	1.88	-1.13	YDR424C	DYN2	dynein light chain (putative)
310	G	5	0.52	1.31	-1.32	YDR125C	ECM18	ExtraCellular Mutant
330	E	4	0.53	1.23	-1.21	YMR312W	ELP6	RNA polymerase II Elongator protein subunit
303	E	2	0.16	0.56	-1.80	YML008C	ERG6	Ergosterol synthesis
344	C	4	0.09	0.42	-2.21	YFR019W	FAB1	1-phosphatidylinositol-3-phosphate 5-kinase
347	G	3	0.31	1.19	-1.94	YER183C	FAU1	Folinic Acid Utilization. 5,10-methenyltetrahydrofolate synthetase
335	G	12	0.63	1.37	-1.12	YCR034W	FEN1	1,3-beta-glucan synthase subunit (putative).ELO1 homolog
335	G	10	0.39	1.22	-1.63	YCR028C	FEN2	Protein with similarity to Dal5p and members of the allantoate permease family of the major facilitator superfamily (MFS)
301	C	1	0.52	1.38	-1.43	YAL035W	FUN12	
322	A	12	0.54	1.09	-1.00	YGL254W	FZF1	Involved in sulfite resistance. contains five zinc fingers. Transcription factor (putative)
342	H	11	0.36	0.77	-1.09	YER027C	GAL83	Glucose repression protein
335	**C**	**9**	**0.32**	**1.07**	**-1.74**	**YDR019C**	**GCV1**	**Glycine decarboxylase complex T subunit**
304	**C**	**10**	**0.18**	**0.90**	**-2.35**	**YMR189W**	**GCV2**	**Glycine cleavage system P subunit**
372	**A**	**12**	**0.79**	**1.65**	**-1.07**	**YAL044C**	**GCV3**	**H-protein subunit of the glycine cleavage system**
307	B	2	0.25	0.59	-1.26	YOR355W	GDS1	Involved in nuclear control of mitochondria
380	A	2	0.03	0.05	-1.07	YER054C	GIP2	Protein phosphatase regulatory activity
330	E	3	0.40	1.20	-1.59	YMR311C	GLC8	Protein phosphatase 1 (Glc7p) regulator
303	C	2	0.32	0.65	-1.02	YML048W	GSF2	Glucose Signaling Factor
343	H	5	0.34	0.88	-1.36	YJL101C	GSH1	Gamma-glutamylcysteine synthetase

plt	R	C	Relative growth on Gmin	Relative growth on Dmin	log2 (Gmin/Dmin)	ORF	Name	Function / Description (SGD)
335	A	11	0.54	1.10	-1.02	YDL234C	GYP7	GTPase-activating protein
321	H	12	0.48	1.00	-1.06	YGL237C	HAP2	Global regulator of respiratory genes. transcriptional activator protein of CYC1 (component of HAP2/HAP3 heteromer)
335	H	11	0.38	0.80	-1.07	YCR065W	HCM1	Dosage-dependent suppressor of cmd1-1 mutation; shows homology to fork head family of DNA-binding proteins
304	D	12	0.13	0.70	-2.42	YMR207C	HFA1	
343	E	1	0.36	0.98	-1.44	YJR055W	HIT1	Protein required for growth at high temperature
306	B	1	0.81	1.73	-1.10	YOR032C	HMS1	myc-family transcription factor homolog
303	G	11	0.17	0.41	-1.27	YMR032W	HOF1	SH3 domain containing-protein required for cytokinesis
380	A	1	0.03	0.10	-1.58	YER052C	HOM3	First step in common pathway for methionine and threonine biosynthesis. aspartate kinase (L-aspartate 4-P-transferase) (EC 2.7.2.4)
310	H	5	0.07	0.28	-2.10	YDR138W	HPR1	Hyperrecombination protein that suppresses intrachromosomal excision recombination
322	A	11	0.51	1.05	-1.03	YGL253W	HXK2	Glucose phosphorylation. hexokinase II (PII) (also called hexokinase B)
310	G	3	0.25	0.82	-1.70	YDR123C	INO2	Transcription factor required for derepression of inositol-choline-regulated genes involved in phospholipid synthesis
372	A	2	0.76	1.65	-1.13	YOL081W	IRA2	Negatively regulates cAPK by antagonizing CDC25. GTPase activating protein highly homologous to Ira1p neurofibromin homolog
371	C	8	0.02	0.11	-2.69	YLL027W	ISA1	Iron transport, mitochondrial matrix. Iron Sulfur Assembly -- IscA/NifA homolog
346	C	7	0.37	0.91	-1.29	YDR497C	ITR1	Member of sugar transporter superfamily. myo-inositol transporter
305	A	9	0.51	1.04	-1.01	YMR294W	JNM1	Coiled-coil domain protein required for proper nuclear migration during mitosis (but not during conjugation)
335	C	7	0.14	0.42	-1.57	YDR017C	KCS1	Shows homology to basic leucine zipper family of transcription factors
334	A	11	0.65	1.43	-1.14	YAL058C-A	KRE20	
372	F	2	0.70	2.08	-1.57	YDR532C	KRE28	
301	A	11	0.67	1.51	-1.17	YAL056W	KRH1	Krh1 binds in the two-hybrid system with Gpa2 but probably does not act as effector of Gpa2
341	D	8	0.34	0.77	-1.19	YNL071W	LAT1	Pyruvate dehydrogenase complex dihydrolipoamide acetyltransferase component (E2)
308	E	8	0.28	0.66	-1.25	YPL213W	LEA1	Old format: Null mutant is viable but grows slowly and is temperature sensitive. Null mutant also exhibits defects in spliceosome formation.
370	**E**	**9**	**0.59**	**1.20**	**-1.03**	**YLR239C**	**LIP2**	**LIPoyl ligase 2**
318	**E**	**2**	**0.15**	**0.44**	**-1.58**	**YOR196C**	**LIP5**	**Involved in lipoic acid metabolism.**
332	B	11	0.36	0.77	-1.08	YJL100W	LSB6	LAs17 Binding protein

plt	R	C	Relative growth on Gmin	Relative growth on Dmin	log2 (Gmin/Dmin)	ORF	Name	Function / Description (SGD)
332	A	7	0.25	0.79	-1.67	YJL124C	LSM1	
311	B	12	0.17	0.62	-1.86	YDR378C	LSM6	snRNP protein
371	A	7	0.22	0.94	-2.09	YMR021C	MAC1	Metal-binding transcriptional activator
335	B	11	0.27	0.90	-1.76	YDR005C	MAF1	Mod5 protein sorting
372	F	5	0.58	1.66	-1.51	YFL016C	MDJ1	Involved in protection against heat-induced protein aggregation but not necessary for protein import into the mitochondrion. DnaJ homolog involved in mitochondrial biogenesis and protein folding
331	G	9	0.40	1.20	-1.58	YPR070W	MED1	Essential for transcriptional regulation, mediator complex subunit
341	D	11	0.39	0.90	-1.21	YNL076W	MKS1	Negative transctiptional regulator
302	B	2	0.56	1.17	-1.07	YLL061W	MMP1	High affinity S-methylmethionine permease
372	B	10	0.04	0.29	-2.71	YPL050C	MNN9	Protein required for complex glycosylation
346	F	9	0.36	1.23	-1.76	YGL124C	MON1	
372	B	1	0.49	1.25	-1.37	YNL297C	MON2	Protein with similarity to N-terminal region of the human protein BIG1
372	B	4	0.14	0.59	-2.12	YER068W	MOT2	Negative regulator of gene expression. zinc finger protein (putative)
348	H	3	0.03	0.28	-3.23	YNL284C	MRPL10	Mitochondrial ribosomal protein MRPL10 (YmL10)
346	A	9	0.15	0.68	-2.19	YDR462W	MRPL28	Mitochondrial ribosomal protein MRPL28 (YmL28)
344	A	2	0.27	0.76	-1.48	YLR439W	MRPL4	Ribosomal protein 60S L4
370	B	1	0.77	1.58	-1.04	YDR194C	MSS116	Mitochondrial RNA helicase of the DEAD box family. RNA helicase DEAD box. Mitochondrial matrix
345	E	1	0.60	1.29	-1.11	YDL040C	NAT1	N-terminal acetyltransferase
321	B	8	0.48	1.14	-1.25	YDR162C	NBP2	
332	G	3	0.42	0.89	-1.09	YHR004C	NEM1	Nuclear Envelope Morphology
316	G	1	0.47	1.50	-1.67	YKL040C	NFU1	Nifu-like protein. Localisation in mitochondrial matrix
321	C	3	0.20	0.49	-1.26	YDR176W	NGG1	Involved in glucose repression of GAL4p-regulated transcription.
372	D	1	0.06	0.38	-2.56	YPR072W	NOT5	Member of the NOT complex, a global negative regulator of transcription
311	E	12	0.19	0.61	-1.69	YDR432W	NPL3	involved as a protein carrier in mRNA export, involved in mitochondrial protein targeting
326	A	12	0.42	0.88	-1.06	YNL183C	NPR1	Protein kinase homolog
336	G	8	0.38	0.79	-1.06	YDL116W	NUP84	Structural protein. component of nuclear pores; Part of complex with Nup120p, Nup85p, Sec13p, and a Sec13p homolog
316	G	12	0.18	0.75	-2.03	YKL055C	OAR1	3-oxoacyl-[acyl-carrier-protein] reductase
372	C	5	0.08	0.22	-1.51	YGL038C	OCH1	Membrane-bound alpha-1,6-mannosyltransferase
343	F	5	0.45	0.96	-1.10	YOR269W	PAC1	Required for viability in the absence of the kinesin-related Cin8p mitotic motor.
335	F	1	0.43	1.30	-1.61	YBR279W	PAF1	RNA polymerase II-associated, nuclear protein that may serve as both a positive and negative regulator of a subset of genes, perhaps operating in parallel with Gal11p

plt	R	C	Relative growth on Gmin	Relative growth on Dmin	log2 (Gmin/Dmin)	ORF	Name	Function / Description (SGD)
338	C	12	0.54	1.11	-1.03	YGL094C	PAN2	Poly(A) ribonuclease 135 kDa subunit
306	B	5	0.11	0.60	-2.40	YOR036W	PEP12	Integral membrane protein; c-terminal TMD; located in endosome
327	E	1	0.15	0.67	-2.12	YDR323C	PEP7	Vacuolar segregation protein required for vacuole inheritance and vacuole protein sorting. three zinc fingers; cysteine rich regions of amino acids are essential for function
347	E	7	0.32	0.77	-1.26	YER153C	PET122	Translational activator of cytochrome c oxidase subunit III
338	D	8	0.19	0.42	-1.18	YOR158W	PET123	Mitochondrial ribosomal protein of small subunit
339	E	6	0.21	0.44	-1.07	YNR045W	PET494	Translational activator of cytochrome C oxidase
371	E	9	0.36	1.28	-1.83	YPL031C	PHO85	Involved in phosphate and glycogen metabolism and cell cycle progression. cyclin-dependent protein kinase
338	B	8	0.55	1.28	-1.23	YGL023C	PIB2	Phosphatidylinositol 3-phosphate binding
344	E	10	0.15	0.32	-1.15	YPL268W	PLC1	Phosphoinositide-specific phospholipase C
344	A	7	0.47	0.94	-1.01	YNR052C	POP2	Putative transcription factor
380	B	4	0.24	0.57	-1.28	YPL188W	POS5	Involved in oxidative stress
310	D	4	0.36	1.16	-1.69	YDR075W	PPH3	Protein phosphatase type 2A
343	C	8	0.18	0.54	-1.58	YPL148C	PPT2	Phosphopantetheine:protein transferase (PPTase)
310	G	6	0.26	0.77	-1.54	YDR126W	PSL10	
302	C	5	0.40	0.92	-1.20	YLR019W	PSR2	Plasma membrane Sodium Response 2
310	C	3	0.77	1.52	-0.98	YDR055W	PST1	Protoplasts-secreted
345	C	5	0.27	0.89	-1.73	YDL006W	PTC1	Serine-threonine protein phosphatase
346	E	5	0.36	0.80	-1.15	YDR529C	QCR7	Ubiquinol-cytochrome c oxidoreductase subunit 7 (14 kDa)
316	C	8	0.28	0.67	-1.24	YLR204W	QRI5	
330	A	8	0.33	0.96	-1.56	YER095W	RAD51	Involved in processing ds breaks, synaptonemal complex formation, meiotic gene conversion and reciprocal recombination.
310	D	5	0.59	1.27	-1.11	YDR076W	RAD55	RecA homolog. interacts with Rad51p and Rad57p by two-hybrid analysis. similar to DMC1, RAD51, RAD57
342	G	1	0.24	0.83	-1.78	YCR028C-A	RIM1	Required for mitochondrial DNA replication
343	C	2	0.29	0.84	-1.54	YMR139W	RIM11	Required for Ime1p phosphorylation, association of the Ime1p-Ume6p meiotic activator, early meiotic gene expression, and sporulation
370	A	9	0.01	0.30	-5.18	YBL093C	ROX3	RNA polymerase II holoenzyme/mediator subunit
332	A	11	0.10	0.55	-2.49	YJL121C	RPE1	D-ribulose-5-Phosphate 3-epimerase
315	A	8	0.43	0.89	-1.05	YHR200W	RPN10	Homolog of the mammalian S5a protein, component of 26S proteasome
338	A	9	0.38	1.02	-1.41	YOR182C	RPS30B	Ribosomal protein S30B
315	F	6	0.17	0.79	-2.24	YCR009C	RVS161	Protein required for viability after N, C, or S starvation
311	C	9	0.11	0.42	-1.97	YDR388W	RVS167	Involved in endocytosis. cytoskeletal protein (putative)

plt	R	C	Relative growth on Gmin	Relative growth on Dmin	log2 (Gmin/Dmin)	ORF	Name	Function / Description (SGD)
326	C	11	0.10	0.22	-1.06	YKL212W	SAC1	Integral membrane protein localizing to the ER and Golgi
340	A	1	0.45	1.33	-1.57	YBR037C	SCO1	Inner mitochondrial membrane protein
318	B	12	0.15	0.47	-1.65	YOR140W	SFL1	Transcription factor with domains homologous to myc oncoprotein and yeast Hsf1p required for normal cell surface assembly and flocculence
315	B	11	0.32	0.69	-1.11	YCL010C	SGF29	Probable 29kKDa Subunit of SAGA histone acetyltransferase complex
310	B	4	0.77	1.72	-1.16	YBR258C	SHG1	
310	B	9	0.39	1.15	-1.56	YBR263W	SHM1	
324	H	6	0.06	0.32	-2.52	YBL058W	SHP1	Isolated as a suppressor of the lethality caused by overexpression of the phosphoprotein phosphatase 1 catalytic subuniut encoded by GLC7
302	F	1	0.33	1.25	-1.93	YLR079W	SIC1	P40 inhibitor of Cdc28p-Clb5 protein kinase complex
370	A	4	0.15	0.33	-1.16	YBL007C	SLA1	Involved in assembly of cortical actin cytoskeleton, contains 3 SH3 domains, interacts with Bee1p. Cytoskeletal protein binding protein
314	A	7	0.46	1.45	-1.67	YHR030C	SLT2	Suppressor of lyt2
306	F	6	0.20	0.64	-1.69	YOR290C	SNF2	Involved in the coordinate regulation of phospholipid synthesis. transcriptional regulator
346	F	5	0.09	0.70	-2.97	YGL115W	SNF4	Involved in release from glucose repression, invertase expression, and sporulation. associates with Snf1p
330	B	3	0.13	0.71	-2.48	YHL025W	SNF6	Chromatin remodeling Snf/Swi complex subunit
302	C	10	0.30	0.77	-1.36	YLR025W	SNF7	Involved in derepression of SUC2 in response to glucose limitation
332	F	2	0.53	1.18	-1.15	YJL036W	SNX4	Sorting NeXin
380	F	7	0.09	0.39	-2.04	YJR104C	SOD1	Cu, Zn superoxide dismutase
332	G	5	0.20	0.62	-1.62	YHR008C	SOD2	Manganese-containing superoxide dismutase
303	F	8	0.52	1.08	-1.05	YMR016C	SOK2	Protein that can when overexpressed suppress mutants of cAMP-dependent protein kinase
334	A	9	0.51	1.04	-1.02	YAL047C	SPC72	Spc72p interacts with Stu2p in the two-hybrid assay; Spc72p localizes to the spindle pole bodies. Molecular weight is 72 kD
301	D	9	0.29	1.08	-1.89	YAL009W	SPO7	Dispensable for mitosis, but required for a normal mutation rate, required for premeiotic DNA synthesis, recombination, meiosis I, meiosis II, glycogen degradation and spores
338	D	1	0.22	0.83	-1.88	YGR104C	SRB5	RNA polymerase II holoenzyme/mediator subunit
345	H	8	0.12	0.50	-2.04	YDR443C	SSN2	Non-specific RNA polymerase II transcription factor

plt	R	C	Relative growth on Gmin	Relative growth on Dmin	log2 (Gmin/Dmin)	ORF	Name	Function / Description (SGD)
372	B	9	0.34	0.81	-1.24	YPL042C	SSN3	Component of RNA polymerase II holoenzyme, involved in RNA pol II carboxy-terminal domain phosphorylation.
370	F	1	0.58	2.12	-1.87	YLR369W	SSQ1	Stress seventy Q. HSP70 family chaperone
315	B	9	0.24	0.64	-1.44	YCL008C	STP22	protein membrane targeting
319	C	10	0.07	0.15	-1.05	YJL176C	SWI3	Transcription factor
337	C	9	0.27	0.65	-1.27	YDL185W	TFP1	Hydrogen-transporting ATPase activity, rotational mecanism.
310	A	6	0.74	1.53	-1.04	YBR240C	THI2	Transcriptional activator of thiamine biosynthetic genes
343	A	3	0.60	1.44	-1.27	YLR237W	THI7	Thiamine transporter
308	A	2	0.51	1.03	-1.01	YOL072W	THP1	
344	H	10	0.29	0.83	-1.50	YBR126C	TPS1	Trehalose-6-phosphate synthase/phosphatase complex 56 kDa synthase subunit
310	F	12	0.46	1.28	-1.48	YDR120C	TRM1	N2,N2-dimethylguanosine-specific tRNA methyltransferase
331	G	6	0.49	1.31	-1.43	YPR066W	UBA3	Ubiquitin-like protein activating enzyme
310	E	2	0.75	1.69	-1.16	YDR092W	UBC13	Ubiquitin-conjugating enzyme
301	H	8	0.13	1.17	-3.18	YLL039C	UBI4	Involved in stress response system. Ubiquitin
340	B	7	0.46	1.22	-1.39	YBR058C	UBP14	Ubiquitin-specific protease
328	D	6	0.14	0.76	-2.43	YFR010W	UBP6	Deubiquitinating enzyme (putative)
346	B	3	0.45	1.04	-1.20	YDR470C	UGO1	Outer membrane protein required for for mitochondrial fusion
321	D	9	0.35	0.88	-1.33	YDR207C	UME6	C6 zinc finger URS1-binding protein. Regulator of both repression and induction of early meiotic genes.
325	G	6	0.37	0.81	-1.14	YNL229C	URE2	Nitrogen catabolite repression regulator that acts by inhibition of GLN3 in good nitrogen source.
338	B	2	0.32	1.17	-1.88	YNL054W	VAC7	Integral vacuolar membrane protein
345	F	10	0.32	0.93	-1.53	YDL077C	VAM6	Required for the vacuolar morphogenesis in yeast
311	B	1	0.19	0.66	-1.78	YDR359C	VID21	Vacuolar import degradation
316	G	11	0.20	0.63	-1.67	YKL054C	VID31	Vacuole import and degradation. Uk molecular fonction
320	C	6	0.43	0.92	-1.09	YLR410W	VIP1	Homologous to S. pombe asp1+
337	F	6	0.51	1.08	-1.07	YGR105W	VMA21	Protein involved in vacuolar H-ATPase assembly or function
372	C	12	0.25	1.58	-2.65	YPL045W	VPS16	Vacuolar sorting protein
316	G	2	0.18	0.69	-1.98	YKL041W	VPS24	Involved in secretion
333	B	1	0.35	0.86	-1.28	YJR102C	VPS25	
339	C	2	0.10	0.85	-3.08	YNR006W	VPS27	Cysteine rich putative zinc finger
346	C	5	0.12	0.70	-2.57	YDR495C	VPS3	Vacuolar sorting protein
372	D	8	0.16	0.95	-2.56	YLR396C	VPS33	Vacuolar sorting protein essential for vacuolar morphogenesis and function
372	B	8	0.05	0.30	-2.56	YLR240W	VPS34	Phosphatidylinositol 3-kinase
320	C	11	0.40	1.01	-1.32	YLR417W	VPS36	Defective in vacuolar protein sorting

plt	R	C	Relative growth on Gmin	Relative growth on Dmin	log2 (Gmin/Dmin)	ORF	Name	Function / Description (SGD)
323	E	9	0.31	0.93	-1.58	YPR173C	VPS4	AAA ATPase. Defective in vacuolar protein sorting; homologous to mouse SKD1 and to human hVPS4
310	D	8	0.64	1.27	-0.98	YDR080W	VPS41	Vacuolar protein sorting
372	C	3	0.38	1.06	-1.47	YGL095C	VPS45	Protein of the Sec1p family essential for vacuolar protein sorting
301	E	2	0.29	1.30	-2.18	YAL002W	VPS8	Involved in vacuolar protein sorting; required for localization and trafficking of the CPY sorting receptor
330	G	7	0.55	1.15	-1.08	YML097C	VPS9	Required for Golgi to vacuole trafficking, shares similarity to mammalian ras inhibitors
372	B	6	0.06	0.14	-1.38	YLR337C	VRP1	Involved in cytoskeletal organization and cellular growth. proline-rich protein verprolin
326	A	4	0.29	0.83	-1.50	YNL197C	WHI3	Protein involved in regulation of cell size. RNA binding protein (putative)
301	B	5	0.37	0.98	-1.40	YAL046C	YAL046C	
310	A	3	0.63	1.55	-1.29	YBR235W	YBR235W	
310	A	5	0.65	1.54	-1.24	YBR239C	YBR239C	
310	B	2	0.64	1.52	-1.24	YBR250W	YBR250W	
310	B	3	0.77	1.64	-1.09	YBR255W	YBR255W	
310	B	5	0.70	1.74	-1.30	YBR259W	YBR259W	
310	B	12	0.62	1.43	-1.21	YBR267W	YBR267W	
310	H	3	0.59	1.63	-1.46	YDR135C	YCF1	Metal resistance protein with similarity to human cystic fibrosis protein CFTR and multidrug resistance proteins
315	E	12	0.54	1.10	-1.02	YCR001W	YCR001W	
348	A	10	0.26	0.61	-1.24	YCR024C	YCR024C	Mitochondrion asparagine-tRNA ligase
380	D	2	0.35	1.31	-1.90	YDL119C	YDL119C	
336	H	9	0.21	0.87	-2.09	YDL133W	YDL133W	
341	C	8	0.32	1.07	-1.74	YDR048C	YDR048C	
310	C	1	0.18	1.61	-3.19	YDR049W	YDR049W	
310	C	5	0.49	1.24	-1.35	YDR057W	YDR057W	
310	D	1	0.97	2.16	-1.16	YDR070C	YDR070C	
310	D	12	0.68	1.37	-1.01	YDR089W	YDR089W	
310	E	1	0.19	1.96	-3.35	YDR090C	YDR090C	
310	E	5	0.61	1.42	-1.22	YDR095C	YDR095C	
310	F	5	0.75	1.53	-1.03	YDR109C	YDR109C	
310	G	7	0.84	1.71	-1.01	YDR128W	YDR128W	
321	A	9	0.37	0.78	-1.08	YDR149C	YDR149C	
321	B	1	0.88	1.81	-1.04	YDR153C	YDR153C	
345	H	7	0.06	0.51	-3.21	YDR442W	YDR442W	
322	A	9	0.30	0.71	-1.26	YGL250W	YGL250W	
313	G	2	0.15	0.45	-1.55	YHL023C	YHL023C	
370	C	2	0.21	0.43	-1.04	YDL198C	YHM1	High copy suppressor of abf2 lacking the HMG1-like mitochondrial HM protein; putative mitochondrial carrier protein
332	G	10	0.13	0.32	-1.26	YHR067W	YHR067W	
371	C	4	0.35	1.10	-1.67	YJL046W	YJL046W	
332	C	6	0.33	0.77	-1.22	YJL084C	YJL084C	
332	A	10	0.22	0.46	-1.07	YJL120W	YJL120W	

plt	R	C	Relative growth on Gmin	Relative growth on Dmin	log2 (Gmin/Dmin)	ORF	Name	Function / Description (SGD)
326	F	3	0.36	1.00	-1.46	YKR035C	YKR035C	
330	C	5	0.36	1.43	-2.01	YLL049W	YLL049W	
320	A	10	0.45	1.15	-1.35	YLR386W	YLR386W	
333	E	11	0.24	0.55	-1.17	YLR435W	YLR435W	
344	B	4	0.54	1.14	-1.09	YPR024W	YME1	Mitochondrial protein of the CDC48/PAS1/SEC18 family of ATPases
343	B	2	0.38	0.79	-1.05	YML036W	YML036W	
303	G	9	0.42	0.91	-1.12	YMR031W-A	YMR031W-A	
303	H	11	0.53	1.26	-1.26	YMR144W	YMR144W	
341	E	8	0.46	1.01	-1.15	YNL091W	YNL091W	
339	D	4	0.44	0.92	-1.05	YNR025C	YNR025C	
318	B	11	0.07	0.22	-1.57	YOR139C	YOR139C	
307	B	9	0.23	1.13	-2.28	YOR364W	YOR364W	
370	A	2	0.19	0.42	-1.14	YPL005W	YPL005W	
370	A	1	0.43	0.85	-1.00	YPL013C	YPL013C	
308	H	10	0.52	1.15	-1.15	YPL162C	YPL162C	
344	B	2	0.48	1.13	-1.22	YPR022C	YPR022C	
370	F	6	0.27	1.94	-2.84	YPR123C	YPR123C	
310	B	10	0.46	1.14	-1.30	YBR264C	YPT10	Similar to Rab proteins and other small GTP-binding proteins
303	E	9	0.48	1.12	-1.21	YML001W	YPT7	Gtp-binding protein of the rab family; required for homotypic fusion event in vacuole inheritance, for endosome-endosome fusion, and for fusion of endosomes to vacuoles when expressed from high copy plasmid

ANNEXE 2 List of genes for strains with a G+ Phenotype

plt	R	C	Relative growth on Gmin	Relative growth on Dmin	log2 (Gmin/Dmin)	ORF	Name	Function / Description (SGD)
312	E	2	1.51	0.71	1.08	YER045C	ACA1	
301	E	6	0.04	0.02	1.18	YAR015W	ADE1	phosphoribosylaminoimidazole-succinocarboxamide synthase
345	B	2	1.28	0.64	1.01	YBR149W	ARA1	D-arabinose dehydrogenase
380	E	7	0.11	0.05	1.21	YPR060C	ARO7	chorismate mutase
320	D	11	0.46	0.16	1.51	YLR242C	ARV1	Protein involved in sterol distribution
312	G	11	1.63	0.81	1.00	YGR124W	ASN2	Asparagine synthase (glutamine-hydrolyzing)
305	F	5	1.28	0.60	1.09	YNL271C	BNI1	cytoskeletal regulatory protein binding
342	G	5	0.75	0.30	1.30	YCR047C	BUD23	random budding in diploid null mutants
372	A	4	0.80	0.32	1.32	YER014C-A	BUD25	involved in bipolar budding
311	B	4	0.04	0.01	1.32	YDR364C	CDC40	DNA replication S-phase of miktotic cell cycle mRNA slicing
370	H	4	0.13	0.07	1.00	YPL132W	COX11	Mitochondrial membrane protein required for insertion of Cu(B) and magnesium during assembly of cytochrome c oxidase
370	H	5	0.10	0.01	3.88	YML129C	COX14	mitochondrial membrane
380	B	5	0.90	0.40	1.17	YJL201W	ECM25	
329	B	3	1.09	0.47	1.21	YKR076W	ECM4	
372	B	2	0.72	0.33	1.11	YNL280C	ERG24	C-14 sterol reductase
320	D	5	0.28	0.06	2.11	YLR233C	EST1	Telomere elongation protein (ever shorter telomeres)
312	F	3	2.06	0.78	1.41	YER060W-A	FCY22	purine-cytosine permease
313	B	4	0.94	0.29	1.71	YGR160W	FYV13	
332	G	9	1.26	0.63	1.01	YHR059W	FYV4	
311	F	11	0.53	0.16	1.71	YEL009C	GCN4	transcriptional activator of amino acid biosynthetic genes
312	**A**	**5**	**1.11**	**0.25**	**2.17**	**YEL046C**	**GLY1**	**threonine aldolase**
312	F	5	1.85	0.79	1.22	YER065C	ICL1	isocitrate lyase
312	A	3	0.86	0.33	1.40	YEL044W	IES6	
380	A	7	0.46	0.17	1.41	YER086W	ILV1	threonine deaminase
372	E	5	1.91	0.77	1.31	YIL094C	LYS12	lysine biosynthesis
316	E	3	0.48	0.22	1.09	YKL001C	MET14	methionine metabolism
370	H	3	0.09	0.03	1.62	YNL252C	MRPL17	mitochondrial large ribosomal subunit
329	G	4	1.17	0.36	1.69	YOL112W	MSB4	incipient bud site
313	B	3	1.06	0.29	1.88	YGR159C	NSR1	nuclear localization sequence binding protein
312	C	8	1.69	0.83	1.03	YER007W	PAC2	Tubulin folding cofactor E
319	C	8	1.89	0.88	1.11	YJL179W	PFD1	protein folding
316	G	3	1.23	0.53	1.22	YKL043W	PHD1	pseudohyphal growth
322	C	2	0.07	0.03	1.56	YGR006W	PRP18	RNA splicing factor associated with U5 snRNP
312	G	2	1.88	0.79	1.25	YER075C	PTP3	protein tyrosine phosphatase
345	G	9	0.30	0.13	1.24	YDL090C	RAM1	farnesyltransferase beta subunit essential for processing of ras proteins
346	A	11	1.99	0.91	1.13	YDR465C	RMT2	arginine metabolism
325	E	9	0.16	0.08	1.04	YGL070C	RPB9	RNA polymerase II subunit
313	H	9	0.99	0.37	1.43	YHR010W	RPL27A	ribosomal protein L27A

plt	R	C	Relative growth on Gmin	Relative growth on Dmin	log2 (Gmin/Dmin)	ORF	Name	Function / Description (SGD)
305	G	7	1.09	0.49	1.15	YOR001W	RRP6	35S primary transcript processing
370	H	12	0.15	0.06	1.29	YJR113C	RSM7	mitochondrial small ribosomal subunit
312	E	4	1.78	0.81	1.13	YER047C	SAP1	interacts with Sin1p
312	G	9	1.71	0.76	1.17	YER087C-A	SBH1	protein transporter
380	**C**	**6**	**2.78**	**0.17**	**3.99**	**YOR184W**	**SER1**	**phosphoserine aminotransferase**
313	E	1	0.96	0.04	4.51	YGR208W	SER2	phosphoserine phosphatase
348	H	6	1.03	0.27	1.93	YOL148C	SPT20	histone acetyltransferase SAGA complex member. transcription factor
380	D	5	1.34	0.65	1.04	YLR182W	SWI6	Involved in cell cycle dependent gene expression
380	B	6	0.82	0.37	1.14	YJL138C	TIF2	translation initiation factor eIF4A subunit
342	A	7	1.36	0.28	2.28	YJL129C	TRK1	potassium transporter
381	A	3	3.03	1.46	1.06	YOR187W	TUF1	Translation elongation factor Tu, mitochondrial
336	B	12	1.39	0.68	1.03	YJL029C	VPS53	Required for Vacuolar Protein Sorting. hydrophilic protein that is peripherally associated with the late Golgi and forms a stable complex with Vps52p and Vps54p
336	A	4	1.75	0.81	1.12	YCR076C	YCR076C	
336	A	6	1.59	0.66	1.28	YCR079W	YCR079W	proteine phosphatase
336	A	8	2.23	1.01	1.15	YCR082W	YCR082W	
348	B	2	1.73	0.74	1.22	YDL038C	YDL038C	
311	H	6	1.11	0.52	1.10	YEL033W	YEL033W	
312	A	4	1.21	0.27	2.17	YEL045C	YEL045C	
312	E	3	1.39	0.68	1.04	YER046W-A	YER046W-A	questionable
312	F	7	1.74	0.85	1.03	YER067W	YER067W	
312	G	3	1.93	0.74	1.39	YER079W	YER079W	
328	B	7	1.40	0.70	1.01	YFL034W	YFL034W	
347	A	8	1.06	0.48	1.13	YGL168W	YGL168W	
328	A	3	1.05	0.47	1.15	YIL090W	YIL090W	
336	B	6	1.50	0.73	1.05	YJL017W	YJL017W	
329	B	4	1.20	0.42	1.52	YKR077W	YKR077W	
302	C	2	1.19	0.55	1.12	YLR016C	YLR016C	
329	C	2	1.32	0.56	1.24	YMR069W	YMR069W	
370	H	7	0.08	0.02	1.79	YMR098C	YMR098C	
370	H	2	0.08	0.03	1.47	YMR158W	YMR158W	
333	A	1	1.81	0.52	1.81	YOL160W	YOL160W	
348	H	9	1.88	0.69	1.45	YPL158C	YPL158C	
348	H	10	1.44	0.58	1.32	YPL183W-A	YPL183W-A	structural constituent of ribosome